Upscaling the TetraSpar

Large-scale floating wind turbines design methodology and modelling

G. T. J. Verbeeten

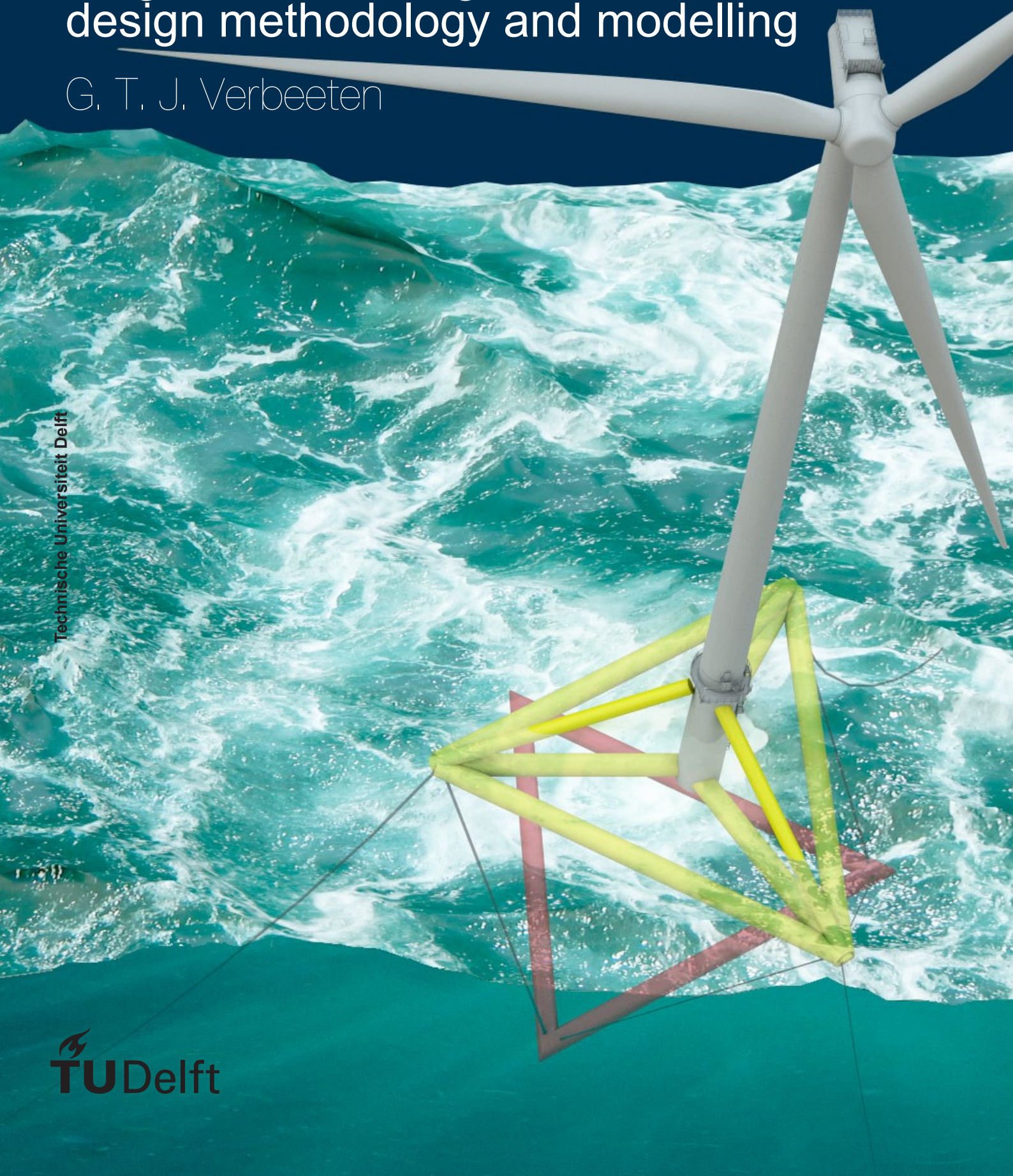

Technische Universiteit Delft

TU Delft

Upscaling the TetraSpar

Large-scale floating wind turbines design methodology and modelling

by

G. T. J. Verbeeten

to obtain the degree of Master of Science
at the Delft University of Technology,
to be defended on Friday 11 September 2020 at 14:00.

Student number:	4213343	
Project duration:	6 December 2019 – 11 September 2020	
Thesis committee:	Ir. A. C. M. van der Stap,	TU Delft, chair
	Dr. ir. B. C. Ummels,	TU Delft, supervisor
	Ir. J. Maris,	Royal Dutch Shell, supervisor

TU Delft

Abstract

During the past decade, the offshore wind energy industry evolved to bigger turbines, going into deeper waters and farther offshore. As bottom-fixed wind turbines are limited to shallow water depths, floating wind structures are the next frontier to unlock the vast potential of wind energy. Despite many techno-economic challenges, several full-scale floating wind structures have been successfully deployed and have shown the potential for floating offshore wind. One project near completion is the 3.6 MW TetraSpar demonstrator developed by Stiesdal Offshore Technologies, Shell and Innogy. With its tetrahedral shaped base and suspended counterweight keel, developed with the focus on ease of fabrication and installation, this spar concept is expected to offer a competitive package for floating wind using future, larger (10 MW+) wind turbines.

The goal of this research is to investigate the capability of the TetraSpar platform to accommodate significantly larger wind turbines and to identify challenges in an early stage of development. Since technology upscaling of floating wind substructures has not been done before, this thesis first develops a novel design methodology for upscaling and then is applies it to the TetraSpar as case study. This work builds on academic efforts thus far but focusses on the key design drivers in for upscaling of floating wind, namely the fundamental equilibria in vertical and rotational direction: the structure's weight is equal to its buoyancy, and the restoring moment equals the maximum overturning moment by wind. Specific emphasis is put on correctly capturing these equilibria, as they generally apply for floating wind substructure technologies, including the TetraSpar.

First a design basis is created with functional requirements and design criteria for floating wind structures in general, and specifics to the TetraSpar. Also, key specifications of future 10 MW, 15 MW and 20 MW wind turbine types are explored. Secondly, a model is developed for upscaling based on physical modelling of hydrodynamic stability (water and waves) and aerodynamic thrust (wind). Based on these inputs, the substructure is upscaled using the future turbine type wind thrusts. The model employs an algorithm to find a new equilibrium design point and computes key properties for upscaled substructures. The resulting design concepts are then evaluated for first order wave-structure interactions using a diffraction/radiation solver (WAMIT). Key evaluation aspects are free-floating hydrodynamics, including hydrodynamic coefficients, wave forces and response amplitude operators. Fourth, selected structural elements of the upscaled design concepts are evaluated for structural strength. The fifth and final step assesses the extent to which the now evaluated upscaled design concepts still meet on the functional requirements and design criteria.

The thesis concludes that the developed, first-order design methodology is suitable to explore upscaled design concepts of floating offshore wind turbines. By computing an estimation of the physical dimensions and behaviour of the substructure, this allows for the evaluation of the technical and economic feasibility. Key findings of the physical modelling are the linear trends for structure mass over power rating of the wind turbine, sensitivities in design choices for maximum allowable heel angle due to wind, and keel draught for the TetraSpar specifically. Compared to other technologies, it is found that found that the TetraSpar concept offers a relatively lightweight platform for future wind turbines up to 15 MW to 20 MW. No fundamental technical showstoppers are identified for upscaling, but it is found that as the structure progresses to larger wind turbines, aspects like in-port water depth, physical dimensions of structural elements, and installability of the TetraSpar at sea will become more challenging. It is expected that at some stage in the development towards large-scale floating wind structures, trade-offs will have to be made to arrive at an improved design. For this, the methodology developed for this thesis can be applied, for example by exploring a lighter, wider TetraSpar design with more slender structural elements. Furthermore, it is recommended to further investigate the mooring design, fabrication capacity and deployment procedures of larger floating wind substructures in general, and upscaled TetraSpar designs in particular

Preface

Who would have thought that our world is able to change and adjust to a new reality within such a short time frame? I am amazed by the resilience and adaptability of everyone, and that we are able to achieve ambitious goals while facing difficult times. This thesis report forms my final tasks towards completing the study programme in Offshore & Dredging Engineering, and marks my last endeavours as student at the Delft University of Technology. This project encapsulates my drive towards multidisciplinary project and challenges, and while we have not been able to achieve all bold plans we thought of at the beginning of the project, I am proud of the work and results presented given the challenging circumstances and 'the new normal' during the COVID-19 pandemic.

I am thankful of both the TU Delft and Shell for providing the opportunities to complete my academic career with this interesting project. It introduced me to the dynamic and interesting world of offshore energy, and the enormous challenges this field is facing for the upcoming decades. I want to thank all who have contributed to the project in many different ways, without your support I would not have been able to complete this works. In particular I would like to thank:

André van der Stap. I vividly remember our first meeting to discuss potential thesis topics, where you drew a rough sketch of an innovative floating turbine concept. I was not convinced by your drawing skill, but you said it might be an interesting and challenging topic to pursue.

You were more than right. Thank you for your lively lectures in my first year of Offshore and Dredging Engineering, sharing your decades of experience in the offshore industry, opening the opportunities within the TetraSpar, and for you guidance and counselling throughout the past months.

Bart Ummels. For introducing me to the wider offshore wind industry, your sharp mind and critical eye, and your endless enthusiasm towards this project. I thoroughly enjoyed our lengthy discussions and brainstorming sessions. And thank you for keeping me on track and ensuring that we all kept the focus towards an academic thesis work.

Jan Maris. I am grateful for you to be my daily supervisor on this project. Your combination of knowledge, experience, interest and enthusiasm is fundamental to the results of this thesis. You challenged me and pushed me to improve myself and this project, which lead to significant improvements and progress within the project.

Steven Zijp. It was great to see you in action as project manager within the TetraSpar. Thank you for your trust and confidence to set my own project scope, while ensuring it stays relevant to the TetraSpar, as well as your input and feedback and for your openness to me. And for being my project manager when I needed it, guiding me back into control over the project when I lost it.

The TetraSpar project team. It was amazing to see such a feat of engineering unfold in real time, and capture the learnings from successes and challenges within the project. I am still astonished on the importance of a team and its individual team members towards the complete project, truly people are key. Unfortunately my project finishes too early to see the TetraSpar be finished and installed, but given the high quality and ambition within the team I foresee a bright future for the concept. All the best!

My family and friends. For their input and feedback, for sharing your own ups and downs in these difficult times, offering your support at the times I needed, and for all the valuable distractions. Your encouragements over the past months helped me tremendously.

Gijs Verbeeten
Delft, September 2020

There are no solutions. There are only trade-offs. - *Thomas Sowell*

Cover image by DTU (2019).

Contents

Nomenclature

Greek symbols

η	wave amplitude
θ	angle of rotation
λ	wave length
ρ	material density
ϕ	velocity potential
ω	angular wave frequency
∇	submerged volume or displacement

Latin symbols

D	diameter
d	water depth
g	gravitational acceleration
F	force
H_s	significant wave height
k	wave number
m	mass
q_i	generalised coordinate for i direction
T	wave period
t	time, wall thickness
U_z	wind velocity at z m height
v	water particle velocity

Abbreviations

CAD	computer-aided design
COB	centre of buoyancy
COG	centre of gravity
FOWT	floating offshore wind turbine
RNA	rotor-nacelle assembly
RAO	response amplitude operator
SOT	Stiesdal Offshore Technologies
SWL	still water level
TLP	tension-leg platform
VIO	vortex induced oscillations
WTG	wind turbine generator

List of Figures

List of Tables

1 Introduction

As the world's population and welfare continues to grow, the demand for energy around the world is still increasing and there are no expectations that this will level off in the foreseeable future (IEA, 2019). At the same time the demand for renewable energy is growing at a faster pace to combat global climate change, and to meet the ambitious goals of the 2015 Paris Agreement on sustainable energy to limit the global temperature rise.

In the past two decades, offshore wind energy has proven itself to be able to provide renewable electricity to society successfully. Even though in 2018 offshore wind provided just 0.3% of the global electricity supply (Cozzi et al., 2019), the prospects on offshore wind energy are that it will be a significant portion of the future's energy mix. Simultaneously, individual offshore wind turbines have significantly grown in physical dimensions and power rating, as bigger wind turbine generators (WTG) are better in terms of power production, energy reliability and total levelised costs of energy. Currently, there is no reason to believe that the physical growth and evolution of WTGs will slow down.

Up until now almost all developments of offshore wind farms have been based on bottom fixed structures, but as the industry ventures into deeper waters floating foundations to offshore wind turbines are becoming more interesting for commercial development. Many different concepts for floating wind turbines have been proposed, some have even been materialized and deployed offshore. One of the floating support structure concepts currently in development is the TetraSpar by Stiesdal Offshore Technologies (SOT).

This chapter starts with a short overview of offshore wind and floating wind structures and introduces the TetraSpar concept, followed by the design considerations regarding floating wind structures, and the theory and analysis of the growth of floating structures. Then the problem statement and research objectives of the thesis are discussed, to conclude with the methodology of this thesis.

1.1. Offshore wind energy, floating wind turbines and the TetraSpar

Since the first offshore wind park was commissioned in 1991, the offshore wind industry is defined by going bigger, farther and deeper. Ever growing wind turbines in larger wind parks, placed farther offshore in deeper waters have pushed the exponential growth of offshore wind energy. In past decade, global installed capacity has increased eight fold to over 23 GW, annual deployment increases by 30% per year, whereas individual wind turbine capacity tripled to over 9 MW and tip height doubled to 200 m (Cozzi et al., 2019). As of right now, there are no signs that the exponential growth will slow down.

While the numbers seem impressive, the success of offshore wind energy is still relatively small on a global scale. The vast majority of the completed wind projects are located in the North Sea and Baltic sea region, and a handful of wind parks in the East China Sea. Many projects with gigawatts of production capacity are in the pipeline in new countries like Australia, India and the USA, but remain for the (far) future. The main reason that offshore wind is not more widespread at this moment is due to water depth. Fixed support structures currently limit the large-scale deployment of offshore wind to water depths of approximate 50 m. Also, in the largest offshore markets in Europe and mainland China, there is currently still sufficient space for large fixed foundation wind farms, while floating support structures are currently still expensive to develop and operate.

Figure 1.1: Classifications for three floating wind foundations. Left a spar, middle a semi-submersible and right a tension-leg platform (Bauer, 2017).

Shallow water basins like in North-Western Europe are perfect grounds for the development of offshore wind energy, but are an anomaly on a global scale. The majority of nearshore coastal areas have a unfavourable bathymetry, where waterdepth quickly exceeds the limit for viable bottom fixed offshore wind turbines. In addition, the technical wind energy potential in deeper waters far greater than in shallow waters. According to Cozzi et al. (2019) waters deeper than 60 m have a technical wind potential of more than 330 000 TW h per year, over three times that of shallow water offshore wind. To tap into that vast resource of renewable energy, floating offshore wind turbines (FOWT) might pose the solution. However, the costs of floating offshore wind must become comparable to currents costs of bottom-founded offshore wind energy, which is increasingly competitive with fossil energy sources.

1.1.1. Outline of offshore floating wind foundations

The idea of floating wind turbines has been around for a long time; since the 1970s over 30 different design concepts in Europe, Japan and the USA have been proposed and developed (Atcheson and Garrad, 2016). However, many of these concepts have never been fully developed, as only 73 MW of cumulative floating wind capacity has been installed to date (Spearman and Strivens, 2020).

All floating wind support structure concepts can be classified into one of the three main categories of offshore floating platforms as depicted in Figure 1.1:

- Spars: ballast stabilised structure with a large mass located towards the keel of the structure to lower the centre of gravity.
- Semi-submersibles and barges: buoyancy stabilised structures with a large water plane area to stabilise the platform.
- Tension leg platforms (TLP): mooring stabilised structure type through taut tendons connected securely to the sea bed.

It should be noted that these categories are not mutually exclusive, most floating wind support structures use a combination of traits from different classes.

The three categories originate from the traditional offshore sector, the oil & gas industry has decades of experience with developing and operating floating platforms. Still, the development of viable floating foundations for offshore wind applications are the next frontier in the offshore industry, largely due to the different requirements of FOWT comparte do to conventional floating platforms. According to Atcheson and Garrad (2016), the fundamental differences for FOWTs are based on the design and scale for continuous un-manned operations; significantly lower risks posed to the environment in case of failure; installation in relative shallow waters compared to oil & gas platforms; and the mass production of wind platforms versus one-off designs.

There are a few important benefits for the utilisation of floating support structures compared to bottom fixed foundations in the context of offshore wind energy. According to Henderson et al. (2016) these are:

- “greater choice of sites and countries, as well as reduced penalty for variability in water depth and ground conditions across a site;
- wide and flexible choice of concepts; as evidence view the wide variety of technology solutions proposed and being demonstrated;
- the most cost optimal foundation concept for deeper water; the future will show where the transition water depth is;
- good flexibility of construction and installation procedures;
- easier removal, relocation and decommissioning.”

Challenges for FOWTs compared to bottom-fixed WTGs can be found in the development of the foundation itself which often more complex than bottom-fixed monopiles or jackets; on the power export cable, both on dynamics of the cable between floater and seabed, and a likely increase in distance to shore; and the necessity of a mooring system. In general, a FOWT structure is highly dynamic system compared to bottom-fixed counterparts, which has major implication on terms of costs, installation and serviceability to the structure.

Even though these challenges are significant to overcome for large-scale deployment for floating offshore wind projects, Spearman and Strivens (2020) expect that by 2040 the worldwide market for floating wind will increase by a factor thousand, with up to 70 GW of installed capacity. Innovations on subsystems like wind turbines and exports cables, lessons learned from current pilot and demonstration projects, and the favourable upscaling of floating foundations may unlock the vast potential of deep water wind energy.

1.1.2. The TetraSpar concept explained

Originally conceived by Henrik Stiesdal (2017) and SOT, the TetraSpar is a unique floating foundation design for offshore wind turbines based on a conventional spar stability mechanism. Depicted in Figure 1.2, the floating platform consists of two bodies: a tetrahedral shaped space frame structure in yellow, and a ballasted keel in red suspended by flexible lines. The keel acts as a counterweight against overturning actions by environmental loading, while the floater generates the required buoyancy to keep the structure afloat. At the time of writing a full-scale 3.6 MW demonstrator model is in the final stages of development by SOT in collaboration with Shell and Innogy, and is expected to be installed offshore by 2021.

According to Stiesdal (2019), the TetraSpar is designed to prioritise the industrialisation of the concept, with a focus on costs, and ease of fabrication, construction and installation. The modular braces are fabricated using standardized manufacturing techniques commonly used for wind turbine support towers. The substructure is assembled quayside by joining the braces with pin connections. The structure then is completed in-port, with the keel lifted close to the floater. The limited draught allows the TetraSpar to be towed to production site by conventional tugs, after which the structure transforms to the operational spar configuration with the keel lowered.

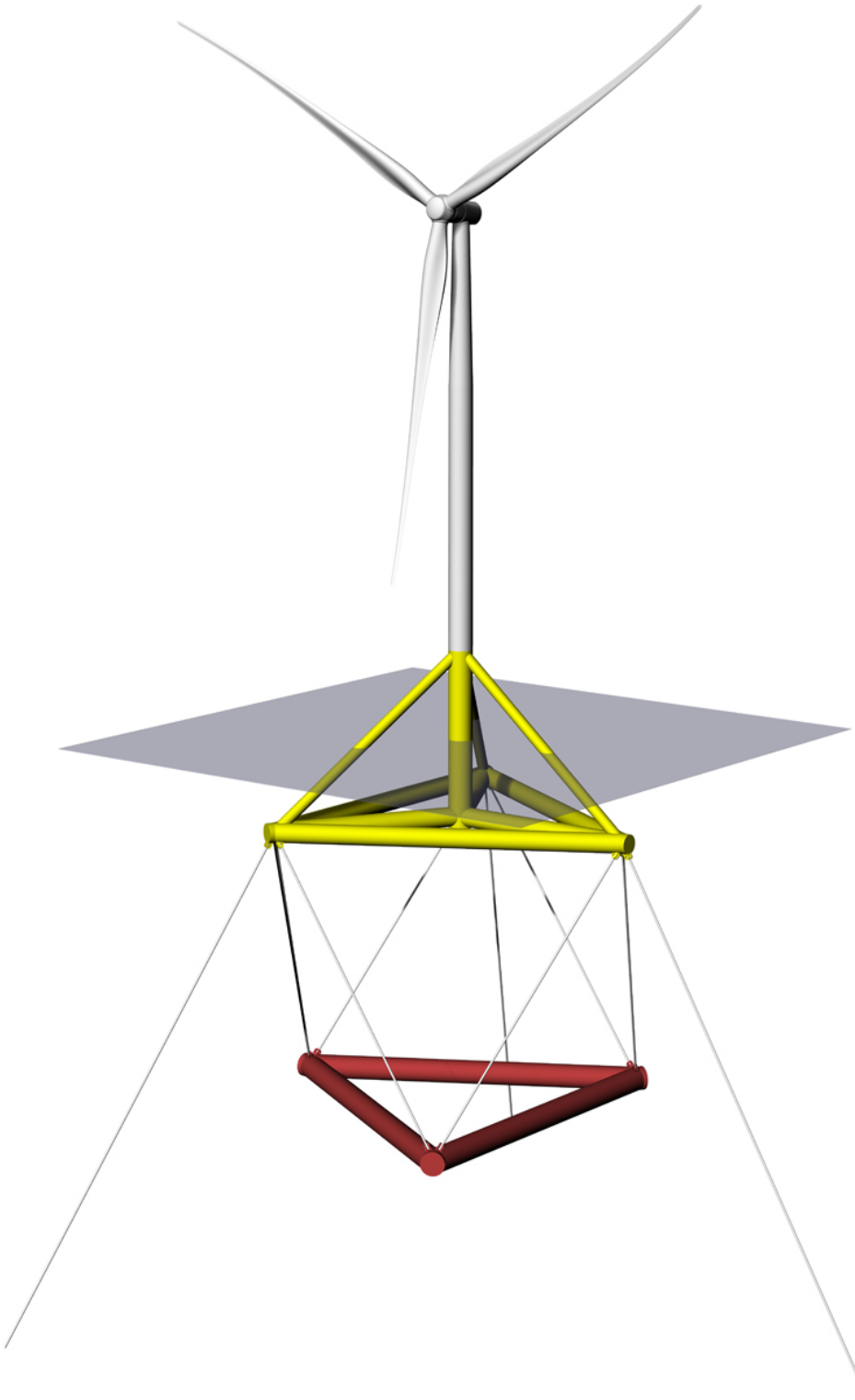

Figure 1.2: Concept drawing of the TetraSpar 3.6 MW design by SOT.

1.2. Design considerations for floating wind turbines

The development of floating wind foundation involves a complex design process with many aspects to be taken into consideration. It is only a decade ago that the first-scale scale megawatt sized floating offshore wind turbine was deployed. The primary purpose of a floating offshore foundation is to provide a safe and stable platform to its payload. The substructure is designed with the aspects on site conditions, load induced motions, complexity of design process, and the construction, installation and operations and maintenance processes. According to Henderson et al. (2016), the floater can be broken down into four subsystems: structure, mooring, anchoring and electrical cable. With these subsystems in mind, the following design considerations are key to the development of FOWTs:

- Motion response and station keeping. Motions of the floater must be within an envelope to ensure the integrity of structure and other subsystems in the full envelope of offshore environmental events. The mooring system should allow for a limited amount of excursion, while being as light and cheap as possible.
- Structural loading. The structure must be able to withstand decades of countless loadings by waves, wind, currents and other environmental actions in multiple limit states.
- Maturity of design. Lessons learned from bottom-fixed offshore wind projects and oil and gas platforms may accelerate the development of FOWTs. Developers must strike a balance between an innovative floating foundation, and proven technology and practices from the offshore industry.
- Fabrication and installation. Standardised fabrication processes are key for reliable and effective deployment of floating offshore wind. Installation should be an integral design aspect of the floater, and may prove to be a primary success factor in the future.
- Safety is key and should be the number one priority. A successful floater design that poses any unsafe situation during fabrication, installation, operation or decommissioning is considered a failed project.

In addition to these selection criteria, there are a number of functional requirements that a floating wind turbine must fulfil in order to be regarded a success. These functional requirements are linked to a number of design requirements that can be defined by clear figures or specifications. A number of these functional requirements are:

- Lifetime: the structure should be able to operate for a set amount of time.
- Environmental: given the metocean conditions at the specified site, the structure should be able to withstand the full weather and sea envelope.
- Stability: to provide a stable foundation to its payload, the structure should limit its (rotational) motions to a workable maximum.
- Dynamics: motions and derived velocities and accelerations should be low enough to protect the payload. Natural periods of the structure should well outside the excitation periods. For marine structures pitch and heave can be often be considered to be most critical.
- Excursion: the floater is able to travel within a defined region in which mobility is allowed.
- Fabrication and installation: fabrication to be done by established or proven techniques, installation scope is done with a limited offshore campaign.

From an offshore engineering perspective, these criteria are analysed in this report against a background of relevant phenomena as represented in Figure 1.3. Next to these elements of environment, weight, buoyancy and mooring, other items like marine growth, icing and corrosion may be included in future studies.

Different floating wind substructures deal with these design considerations in different ways, inherent to its foundation class. Due to its unique design and the focus on industrialisation, the TetraSpar borrows many elements from these classes and combines it into one concept to deal with the aforementioned considerations.

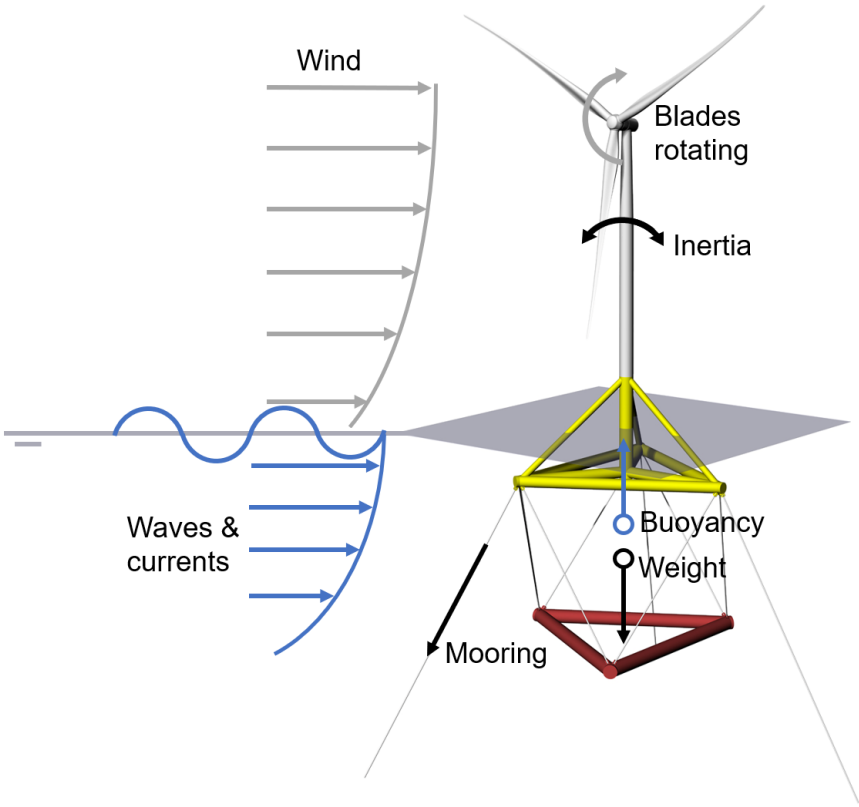

Figure 1.3: A selection of the key phenomena to include in the development and analysis of floating offshore wind turbines.

When the TetraSpar is assembled in port and during tow-out to site, it floatation and stability behaviour resembles a semi-submersible design. When the structure reaches the site, the structure transforms to a spar classification, by lowering and ballasting the keel. This transformation decreases the exposed area of the structure near the water line, and lowers the overall centre of gravity. Advantages to this transition is the limited draught during construction and installation compared to a conventional spar, and lower structural loading while in operations compared to a semi-submersible.

1.3. Upscaling of floating wind turbines

To keep up with the growth in size and power rating of wind turbine generators, the interest in the development of large floating wind support structures has accelerated after the first megawatt scale floating wind turbine was commissioned in 2009. But the question remains how an existing foundation design can be upscaled to support the ever growing wind turbines. This section provides a brief overview of the literature and materialized projects on the upscaling of FOWTs.

1.3.1. Rational scaling laws

A well defined and proven approach to scale existing geometries is with the use of so-called rational scaling laws. Common application of scaling laws is in small scale model testing, like ships in wave tanks and aeroplanes in wind tunnels. The main goal of these small-scale tests is to accurately describe loads and motion behaviours of a full-scale model.

Arguably it was Galileo Galilei who in 1638 discussed the concept of geometric scaling and dimensional analysis (Peterson, 2002):

> I said that the surface of a small solid is comparatively greater than that of a large one. - *Galileo Galilei*

Imagine two cubes, one with edges twice as long as the other. The bigger cube has a surface area four times that of the smaller cube and an internal volume of eight times larger. In other words, the

surface of a body increases by a length squared, while the volume increases by a length cubed. By dimensional analysis, i.e. by breaking down the problem into a base physical quantity of length, Galilei was able to study multiple phenomena of a scaled cody, and introduced the so-called square-cube law.

Scaling laws and dimensional analysis allow researchers to dissect an issue into a systematic approach, and are able to find effects and consequences to the total system by changing one characteristic. In engineering applications dimensional analysis is mostly based on the three base quantities of mass, length and time.

In the research on wind energy technology scaling laws are common practice to anticipate loads, dimensions and other characteristics of future, bigger wind turbines (Sieros et al., 2012). By introducing a scaling factor, and assuming geometric self-similarity of the subject, it is relatively easy to scale a design and derive the scaled properties.

It is often said that the increase in size of wind turbines generators adhere to Galilei's square-cube law (Jamieson and Hassan, 2011; Sieros et al., 2012). The leading indicator for wind turbines is the power rating, which is a direct function of the swept area of the rotor. Following Galilei's example of two cubes, it can be derived that for an increase in power rating by a factor squared, the mass of the WTG should increase by a factor cubed. This poses a major challenge to future development of WTGs, as the ratio of power output over mass, i.e. the revenue over costs, decreases unfavourable as turbines grow in size.

1.3.2. Upscaling of floating platforms for oil and gas production

Even though floating offshore wind turbines are a relatively young technology, a lot of the underlying knowledge and experience is found in the traditional offshore industry. Already in the 1980s full sized floating oil and gas substructures were deployed (Ramboll, 2018), and can be a valuable source of knowledge and experience to accelerate the maturity of a floating wind foundation concept. By analysing the scaling trends among conventional oil and gas platforms lessons might be learned for applications in floating wind.

A study by Ramboll (2018) researches the relationship between the substructure hull weight or structure displacement to topsides weight for the three main classifications of foundations for spars, semi-submersibles and TLPs. Overall, smaller topsides require a relatively bigger substructure compared to larger superstructures, and tension-leg platforms have a significantly better ratio of topside mass to substructure weight than the other two classes, which underlines the advantage of a TLP as lightweight structure. However due to a large spread of data points no clear scaling or sizing trends are to be identified in the data. As an example, in the data for spars it was found that for similar sized topsides, the substructure weight could vary by a factor three.

According to the report, 'the designs vary significantly which means that the same type of substructure has not been directly scaled to suit a different both topside mass or environmental conditions. There are some general arrangements, respectively families of designs sharing similar features [...], however each design is individually developed for a specific site and project.' Each oil and gas floating substructure is a unique concept, specifically designed for the site and project. These structures are not engineered as standardized units, and it seems that both project or site-specific requirements, and technological advancements define the size and scale of the substructure. Therefore, for offshore wind projects, similar aspects such as the design, costs, speeds of manufacturing and installation must be specifically considered as well.

1.3.3. Academic research on upscaling of floating offshore wind turbines

At the time of writing only a handful of representative academic, open-access studies are available on the topic of upscaling of floating wind support structures, most notably by George (2014), Leimeister (2016), Islam (2016) and Kikuchi and Ishihara (2019). All but one are master theses and all base their approach on the square-cube law and apply scaling to semi-submersible floaters.

The study by George (2014) initiates with the OC4 DeepCwind semi-submersible design, and derives a scaling factor based on the ratio of the increased mass of a larger payload, over the base case. The payload is defined as the complete WTG superstructure of RNA and support tower. The resulting scaling factor is applied to the length dimensions of the base-case design to scale-up accordingly. In addition, George develops a second approach based on a constant draught of the structure, and

adjusts the floater's displacement to account for the increased mass of a larger WTG. This second approach is focused on the fabrication and installation of the concept with existing infrastructure.

Research by Leimeister (2016) starts with the same OC4 DeepCwind semi-submersible floater, and derives a scaling factor based on the ratio of power rating of the upscaled wind turbine to base case. This scaling factor is applied to all length dimensions of the foundation. Furthermore, Leimeister also applies the scaling factor based on mass ratios like George, and proposes a hybrid upscaling approach to account for a difference in scaling between the floater in general, and the interface between the support tower and foundation.

Also Islam (2016) applies a scaling factor based on the ratio of power output to a fictional design of a 5 MW WindFloat substructure. One of the main recommendations of that study is that the application of a global scaling factor based on the ratio of power output results to an over-dimensioned substructure. The upscaled structure's displacement is too large, and is adjusted accordingly by hydrostatic calculations afterwards.

The article by Kikuchi and Ishihara (2019) researches upscaling for the Fukushima FORWARD semi-submersible design from the 2 MW demonstrator, to 5 MW and 10 MW designs, with the lessons learned from George (2014) and Leimeister (2016). Kikuchi and Ishihara scale the structure's mass according to the square-cube law, but the floater dimensions are determined according to other (practical) constraints like draught scaled to dock size, freeboard scaled to designed wave height and main column scaled to tower bottom diameter. They do not use a scaling factor to the length dimensions of the floater.

All academic studies discussed above start the upscaling methodologies based on the square-cube law, and all but one derive a main scaling based on either mass or power ratios, and apply this factor to the floater length dimensions. This scaling factor then is applied to the length dimensions of the structure to increase the overall size of the floater.

These studies advise that a upscaling methodology based on one single scaling factor for the entire structure is not enough to arrive at a completed design. Other design considerations have to be taken into account, not dictated by a main scaling factor. Overlap between the studies is found in acknowledgement on boundary condition on maximum draught, the interface between substructure and turbine support tower and other practical aspects. In addition, all studies are limited to a WTG power rating of 10 MW maximum, while currently OEMs are developing commercial wind turbine models up to 15 MW which are expected to be launched in a couple of years.

One driver to the upscaling of FOWT is the anticipated advantage for larger scale structure; the relative mass of a floating wind platform per power rating decreases for larger wind turbines. One of the main capital expenditure items for floating marine structures is the amount of primary steel mass required for the structural strength and design. A recent study by Spearman and Strivens (2020) endorses the economic benefits of larger wind turbine generators, but for floating offshore wind structures. Figure 1.4 shows normalised trends of primary steel mass over power rating, averaged by a set of generic FOWT designs in all floating structure categories, for a power output range of 6 MW to 15 MW. Spearman and Strivens state "when doubling the WTG rating from 6 MW to 12 MW (i.e. an increase of power by 100%), the primary steel mass of floating substructures on average only increases by 55%" and "that for floating substructures, larger WTGs are very favourable regarding mass and thus procurement cost per MW of the substructure."

1.3.4. Review of materialized upscaled floating wind foundations

In addition to a couple of theoretical studies, there are a few FOWT projects that have been upscaled to a larger wind turbine. A detailed comparison of the upscaled substructures to the initial designs is difficult, open access data on these commercial projects is limited. However, the data that is available does give some insight into the process of upscaling for materialized floating wind concepts. At the time of writing, a few of the most notable projects are the Hywind spar by Equinor, the WindFloat semi-submersible by Principle Power and the Ideol Floatgen barge with damping pool.

In 2009, the first megawatt scale floating offshore wind turbine was installed: the Hywind demo spar by Equinor. A 2.3 MW wind turbine was mated to a slender cylindrical substructure and commissioned off the coast of Norway (Roddier et al., 2016). Like other spar foundations, the Hywind stabilised by adding ballast to the bottom of the foundation. This lowers the centre of gravity of the structure, and acts as a counterweight to overturning moments by environmental forces. A few years later in 2016,

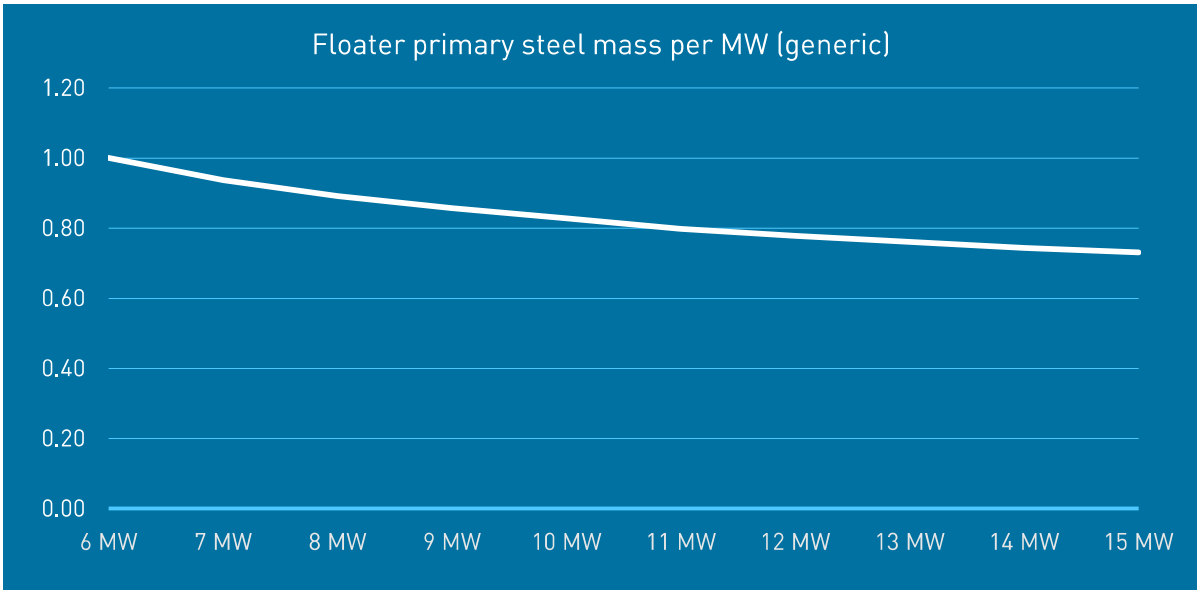

Figure 1.4: Normalised trends of substructure primary steel mass over power rating for generic FOWT designs, adapted from Spearman and Strivens (2020).

the spar concept was upscaled to accommodate a 6 MW wind turbine in the Hywind Scotland pilot for the world's first floating wind farm.

The first megawatt scale semi-submersible floating offshore wind turbine is the 2 MW WindFloat by Principle Power, commissioned in 2010. This design consists of three large diameter columns arranged in a triangular frame, with the wind turbine placed on top of a column. The second iteration is the recent WindFloat Atlantic, supporting an 8.3 MW turbine which makes it currently the largest floating offshore wind turbine structure. Images of both materialized upscaled FOWT designs are depicted in Figure 1.5, data on the main dimensions of both are presented in Table 1.1. No respresentative data was found on the Ideol barge concepts.

Both upscaled iterations of the Hywind Scotland spar and WindFloat Atlantic semi-submersible show that there is more to the design and development of upscaling a floating foundation than only applying a theoretical scaling factor to the length dimensions of the substructure. Developers of these structures have accounted for other important designed considerations, like local water depth for the upscaled Hywind Scotland with a reduced draught, or installation and fabrication capabilities like the limited increase in width for the WindFloat Atlantic.

Table 1.1: Main dimensions of initial and upscaled FOWT designs for Hywind spar and WindFloat semi-submersible. Data by Roddier et al. (2016); Principle Power (2014, 2020).

Design	Parameter		Initial	Upscaled
Hywind	Year		2009	2016
	Power rating	MW	2.3	6.0
	Displacement	m^3	5300	12000
	Draught	m	100	80
	Diameter	m	8.3	14.5
WindFloat	Year		2010	2019
	Power rating	MW	2.0	8.3
	Displacement	m^3	2800	-
	Column diameter	m	8.2	-
	Distance columns	m	38	50
	Column length	m	23	30

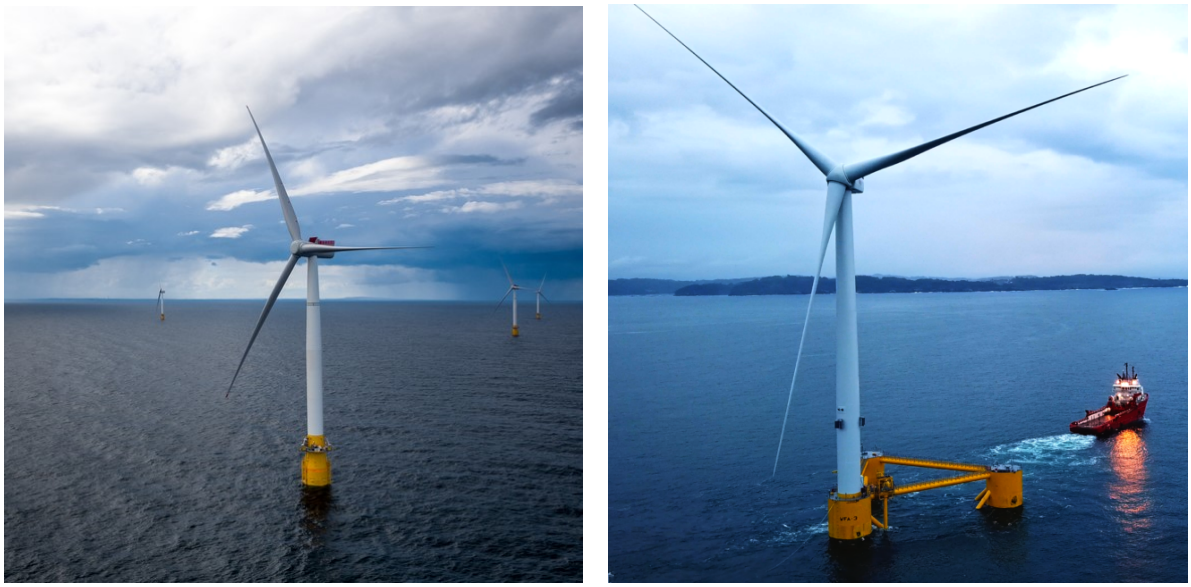

Figure 1.5: Upscaled FOWTs, left the 6 MW Hywind Scotland spar by Equinor (2017) and right the 8.3 MW WindFloat Atlantic semi-submersible by Principle Power (2019).

1.4. Thesis problem statement

It is evident that large floating wind turbines will be part of the future's energy mix, with more power generated per unit installed and a higher capacity factor for larger wind turbine generators it makes both technical and economic sense. However, critically analysing the previous pieces of text on the upscaling of floating offshore foundations show that there is no clear, predefined approach towards the upscaling of floating (wind turbine) structures. Theoretical upscaling by use of scaling factors require manual adjustments afterwards, and it is debatable if the chosen parameters are design driving. Furthermore, materialized upscaled floating offshore wind foundations do not show to adhere to any of these rational scaling laws.

At the time of writing, a full-scale 3.6 MW demonstrator of the TetraSpar concept is near completion. The main goal of this demonstrator is to prove the technical feasibility of the innovative TetraSpar concept on terms of motions, fabrication, structural strength and other aspects that make a safe and stable platform to wind turbines. However it is unexpected that the relative small wind turbine generator will be economically viable for commercial deployment, as current developments in wind turbines are for power outputs over 10 MW. On paper the TetraSpar looks to be strong concept for a FOWT; it ticks many of the boxes on the design considerations in section 1.2. However, as wind turbines grow into the double digit megawatts it is a question if the TetraSpar is suitable to be scaled up to support these large turbines.

An important factor of this problem to take into consideration is time. While other FOWT concepts have been upscaled in relative small iterative steps which already took at least 7 years to develop, the TetraSpar demonstrator currently trails behind these concepts in terms of power rating. To be commercially of interest in the near future for Shell as project stakeholder, the next TetraSpar design has to skip a medium sized iteration, and should be able to support a wind turbine of at least 10 MW to keep up with floating wind developments.

The problem this thesis tackles comes in twofold and combines both statements of above: to develop an upscaling design methodology suitable for floating wind support structures, and to test that design methodology to the TetraSpar concept as a case-study. The upscaled TetraSpar design concepts will be designed for hypothetical, generic wind turbines with a power rating of 10 MW for short term deployment, a 15 MW for a medium time horizon and a 20 MW wind turbine for a long term future.

The design methodology is simplified process to upscale an existing design of a floating wind support structure, in which no major aspects concerning the design of FOWTs are overlooked. The resulting structures by this upscaling design methodology shall not be detailed designs, but it will result global

concept designs of a floating platform for offshore wind. This should allow developers to make big steps in the upscaling of floating wind platforms, and identify potential challenges to the upscaled structure early on.

1.5. Research objective and questions

Combining the research on a design methodology for the upscaling of floating offshore wind turbines, and the case-study into the TetraSpar concept the overarching project objective of this research is:

To determine the critical design parameters for a TetraSpar scale-up and investigate its technical feasibility.

This objective is developed by the use of scaling laws or other scaling methods, incorporating functional requirements and design criteria on floating wind substructures, adhere to the TetraSpar's unique selling points and take into account the scale-up limits on practical aspects like construction and installation. The main research question associated to the project's objective reads:

Can the TetraSpar substructure be scaled-up to accommodate for larger wind turbines, while maintaining the TetraSpar's unique selling points?

Considering the strong points of the TetraSpar concepts, which will be further eleborated in chapter 2, the hypothesis to the main research question is that indeed the TetraSpar is a suitable platform to accommodate larger wind turbines, but that at a certain points some (practical) aspects become limiting in further upscaling.

Subquestions supporting the main research question are divided into the two-part problem statement. For the generalized design methodology the subquestions are:

- What are the key design drivers for floating wind turbine foundations?
- What existing upscaling methods have been applied to (floating) offshore support structures?
- What is the impact of upscaling on the design, development and other practical implications of larger floating wind foundations?

For the TetraSpar case-study the supporting subquestions are:

- What are critical functional requirements, design parameters and the unique selling points to the TetraSpar? And how will these be affected by adapting the design to a larger wind turbine?
- How does the TetraSpar increase in dimensions to accommodate larger wind turbines?
- Which trade-offs can be made for the upscaling of the substructure if one or more constraints are met?

1.6. Methodology and thesis outline

The developed upscaling design methodology is the guide through this thesis. The process consists of five steps, the outline of this report follows these steps one by one in the chapters of this thesis report.

1. Introduction to the concept floating offshore wind turbines, an overview of previous attempts at upscaling of floating substructures and the main challenges to overcome for a successful FOWT development, discussed in chapter 1.
2. Design basis. It starts with laying down the ground work for the floating offshore wind turbine. Gather defining characteristics of an existing design of the floating foundation, and its builds a framework of key input data like wind turbine generator, site conditions, functional requirements and design criteria, as described in chapter 2.
3. Hydrostatic analysis of the structure in chapter 3. The first requirement to all floating structures is hydrostatically stable. In this step the upscaling process is performed to the case-study, and checked if it is stable in a quasi-hydrostatic analysis

4. Hydrodynamic analysis of the resulting upscaled structure in chapter 4. In this step the resulting upscaled structure is analysed on the dynamics and motions, and checked if the results meet the requirements.

5. Structural design of the upscaled structure is discussed in chapter 5. It is outside the scope of this thesis to deliver a detailed design and strength analysis of the structural design of the resulting upscaled platform. This chapter deals offers a framework on the structural design, and analysis some of the most important challenges that may arise when the foundation is upscaled.

6. Resulting upscaled structures. When all steps in hydrostatics, hydrodynamics and structural design are passed the resulting upscaled design concept is discussed in chapter 6, and it is critically analysed if the outcome is a feasible platform to accommodate larger wind turbines. Furthermore some sensitivity studies are analysed and discussed, to see which changes have the most impact on the resulting design.

7. In the final chapter 7, the complete process and methodology will be evaluated, and recommendations and suggestions for further research on both the general upscaling methodology and the TetraSpar case study will be given.

2

Design basis, input and assumptions

Before any design for an upscaled FOWT can be initiated, a set of ground rules or a design basis has to be defined to which the resulting structure is assessed on performance, safety and other criteria. Starting with the general design considerations for floating wind, functional requirements are derived for upscaled designs of the TetraSpar case study. Then other input parameters on metocean conditions and properties of upscaled wind turbines are gathered, which are combined to a detailed description of the generalised upscaling design methodology.

The main goal of the generalised upscaling design methodology is to be able to quickly generate a first draft design concept for an upscaled iteration of an existing FOWT support structure, assess its feasibility and identify potential challenges regarding the functional requirement and design criteria. Because many (engineering) factors of the upscaled design are unknown from the start of the process, assumptions and approximations are needed to overcome these uncertainties. The final section of this chapter will discuss these assumptions to the upscaling design methodology.

2.1. TetraSpar description, functional requirements and design criteria

The following section introduced the TetraSpar design in more detail and describes concept defining properties. Furthermore, the key functional requirements and design criteria are listed for an upscaled concept design should to fulfil.

2.1.1. TetraSpar description

The driving force behind the TetraSpar design is the focus on economics and industrialisation of FOWTs. The starting point of the concept is at the fabrication and assembly of the foundation. Similar to wind turbine support towers the main elements of the TetraSpar are slender, thin-walled cylinders, which enable the braces to be manufactured by well developed manufacturing processes for support towers, and lowers the learning curve for construction of the concept. Another benefit to the open design with slender cylinders is the decreased hydromechanic forces acting onto the structure, and lowers the (steel) weight of the platform.

The individual braces are joined together by pin connections and nodes, allowing the TetraSpar to be assembled in a time-efficient manner. The floater and substructure are assembled onshore and quayside in the sheltered waters of a harbour by land-based crane, and is mated to the keel by connecting the suspension lines. These flexible suspension lines allow for a minimised draught during the installation phase, and enables the TetraSpar to be towed-out to site using conventional tug boats, which is significantly cheaper for installation than specialized crane vessels.

Depicted in Figure 2.1, the main components to the TetraSpar structure are the wind turbine generator, floater and suspended keel. The superstructure (or payload) is the combination of the WTG rotor and nacelle, and support tower. The tetrahedral shaped floater consists of one centre column, and three radial, diagonal and lateral braces.

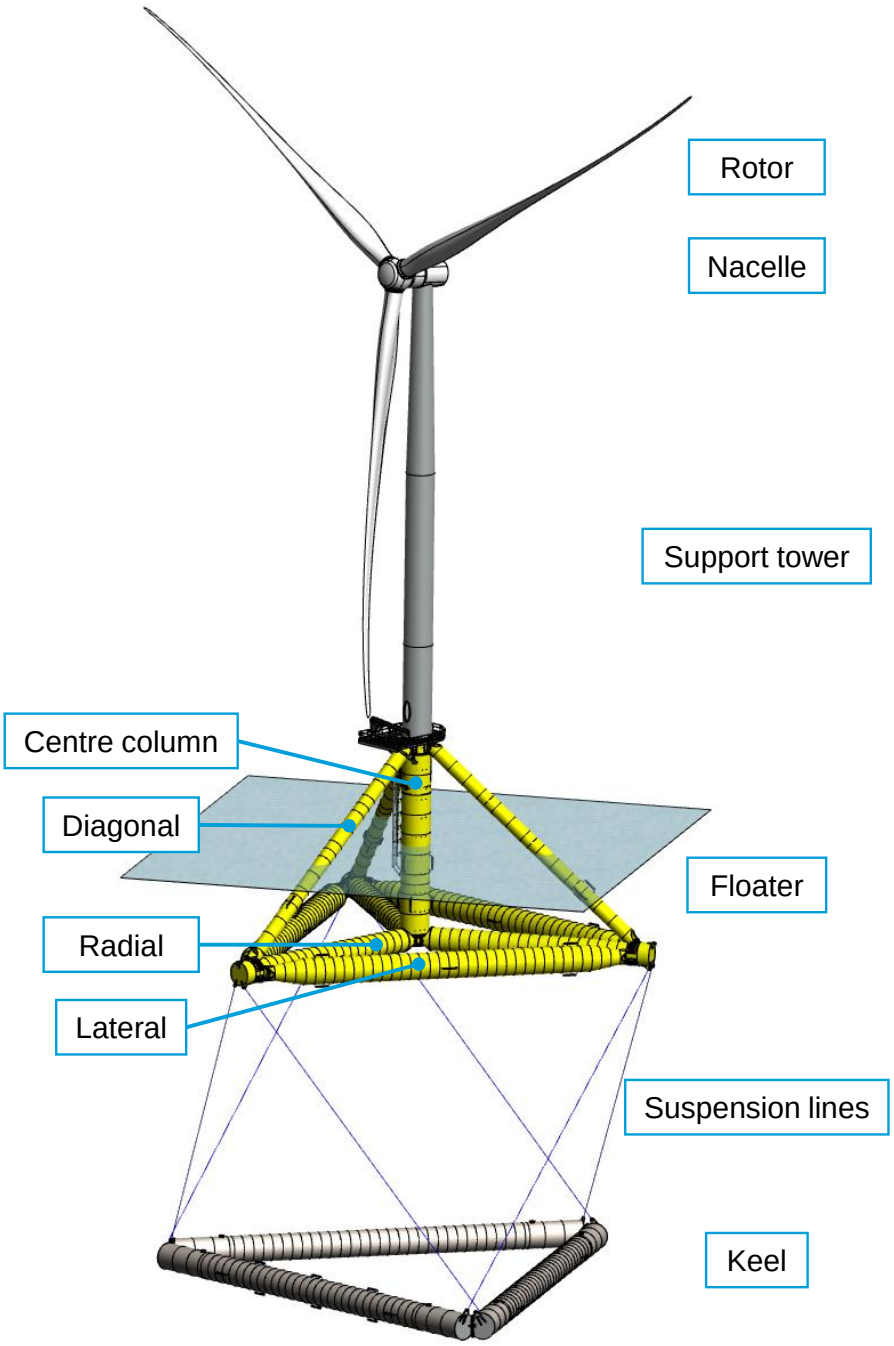

Figure 2.1: Description of TetaSpar's main components and naming convention of elements.

From the fairleads at the radial ends run six suspension lines down to the triangular shaped keel. The ballasted keel lowers the centre of gravity of the structure. The keel structure is fabricated using the same production techniques, and is partially ballasted by concrete to achieve neutral buoyancy during installation. When the structure reaches its intended site, the keel is lowered and is further ballasted by seawater, which lowers the complete structure until the floater is partially submerged.

The design of the 3.6 MW demonstrator defines the initial design for all upscaled design concepts. The main properties and dimensions of the structure are listed in Table 2.1, dimensions of the individual braces are found in Table 2.2. Properties and characteristics of the TetraSpar demonstrator, e.g. substructure frame shape and concept defining suspended keel, are considered a given fact to the upscaled designs.

Table 2.1: Properties of TetraSpar 3.6 MW demonstrator.

Parameter	Value	
Power rating	3.6	MW
Rotor diameter	130	m
Hub height above SWL	85	m
Floater draught	15	m
Keel draught	65	m
Structure mass	5600	ton
Substructure steel mass	1600	ton
Payload mass	440	ton

Table 2.2: Approximate dimensions of TetraSpar 3.6 MW substructure elements.

		Centre column	Diagonal	Radial	Lateral	Keel
Diameter	m	4.30	2.15	3.50	4.00	4.10
Length	m	31	38	34	51	64
Volume	m^3	440	140	315	620	820
Steel mass	ton	160	55	105	135	205

2.1.2. Functional requirements

As described in section 1.2, there are many design considerations for a floating offshore wind turbine to be taken into account for a feasible design concept. The following text outlines the functional requirements and consequential key design criteria to demonstrate technical feasibility of a concept design for the TetraSpar scale-ups.

The following the functional requirements for the upscaled design concept are described as fundamental necessities of fabrication and operating a TetraSpar platform, while considering the concept defining characteristics.

Even though this list is incomplete, a selection of key functional requirements for this thesis work are:

- The floating platforms are designed for and are evaluated to accommodate generic wind turbine generator models with rated power outputs of 10 MW, 15 MW or 20 MW.
- The design concepts are designed for metocean conditions representative for offshore Norway at the Metcentre (see section 2.2), while considering both site location and tow route.
- The substructure provides a safe and stable platform to the wind turbine generator for the full envelope of offshore conditions, including:
  - Operations. Allow for continuous operations of the wind turbine generator and power export in the operational window with wind velocities at hub height between $3\,m\,s^{-1}$ to $25\,m\,s^{-1}$.
  - Survival. The structure is able to withstand extreme metocean conditions for a storm with a 50-year return period.
- The structure is complete and independently stable during installation and during operations.
- Substructure should be able to access and leave standard industrial harbours.
- Fabrication and manufacturing of individual elements of the structure are done by proven and standardized production processes. Substructure is a modular design to allow for time-efficient assembly.

2.1.3. Design criteria

From the design fundamentals and considerations, and from the aforementioned functional requirements the following key design criteria are set for the upscaled TetraSpar. Overall, the standard by DNV GL (2018) ST-0119 Floating offshore wind turbines is the main guidance for the FOWT structures,

including all other references standards in the document. In addition, the following design criteria specificically to the TetraSpar are in place:

- Stability requirements:
  - Static heeling angle of wind turbine in operational wind speeds is limited to 5°.
  - Structure must be intact stable at all times.
- Motion requirements:
  - The natural periods of the structure shall not interfere with force excitation frequencies, including those from hydrodynamic and wind turbine generator loading.
  - Wind turbine RNA accelerations may not exceed $5\,\mathrm{m\,s^{-2}}$.
  - Horizontal offsets are limited to 25% distance between the substructure foundation keel and seabed in ultimate conditions.
- Structural requirements:
  - No snatch loads to occur in any line.
  - Fatigue life shall be in accordance with design standard for a design life of 20 years.
- Fabrication requirements:
  - Diameters of the substructure braces cannot be larger than the diameter of the support tower. This ensures that the main braces can be fabricated using the same manufacturing processes.
  - The centre column is set equal to the base diameter of the support tower.
  - Distance from centre column to quayside must be smaller than 40 m (assumed reach of land-based crane).
- Installation and operation requirements
  - Interface between super- and substructure must always be above highest wave crest.
  - Tip clearance shall be at least 30 m from still water line to lowest tip elevation.
  - No specialized crane vessels should be needed during assembly or installation of the structure.
  - Tow-out of the completed structure to be done by conventional tug-boats.
  - Floater shall be accessible for operations and maintenance in sea states according to design load cases 1.2 and 1.6 by DNV GL (2016) ST-0437 Loads and site conditions for wind turbines.

2.2. Offshore site conditions

To lay a foundation for the TetraSpar case-study, a representative offshore site must be selected to which the upscaled design concepts can be tested on performance. For practical purposes the Marine Energy Test Centre is chosen as offshore site, the same site as where the 3.6 MW TetraSpar demonstrator will be put to the test. It is located in North Sea, near the South-Westerns coastal area of Norway, approximately 10 km from shore, depicted in Figure 2.2.

There are two main advantages of selecting this location as representative offshore site. The Marine Energy Test Centre (Metcentre) is home to the world's first full-scale FOWT, the Hywind spar demonstrator. This has the benefit that a lot of metocean data has been captured over the years, available to the development team of the TetraSpar, and through an article by Onstad et al. (2016). The other advantage of the Marine Energy Test Centre is that this area of the North Sea is notoriously harsh to offshore structures. The general notion is when the structure able to withhold itself in these challenging conditions, it can be assumed that it will suffice for most locations worldwide.

An overview of the most relevant metocean conditions of the Marine Energy Test Centre is presented in Table 2.3. Note that contrary to bottom-fixed structures, information on tides and surges is not essential to FOWTs as floating structures follow the slow variation of the still water level.

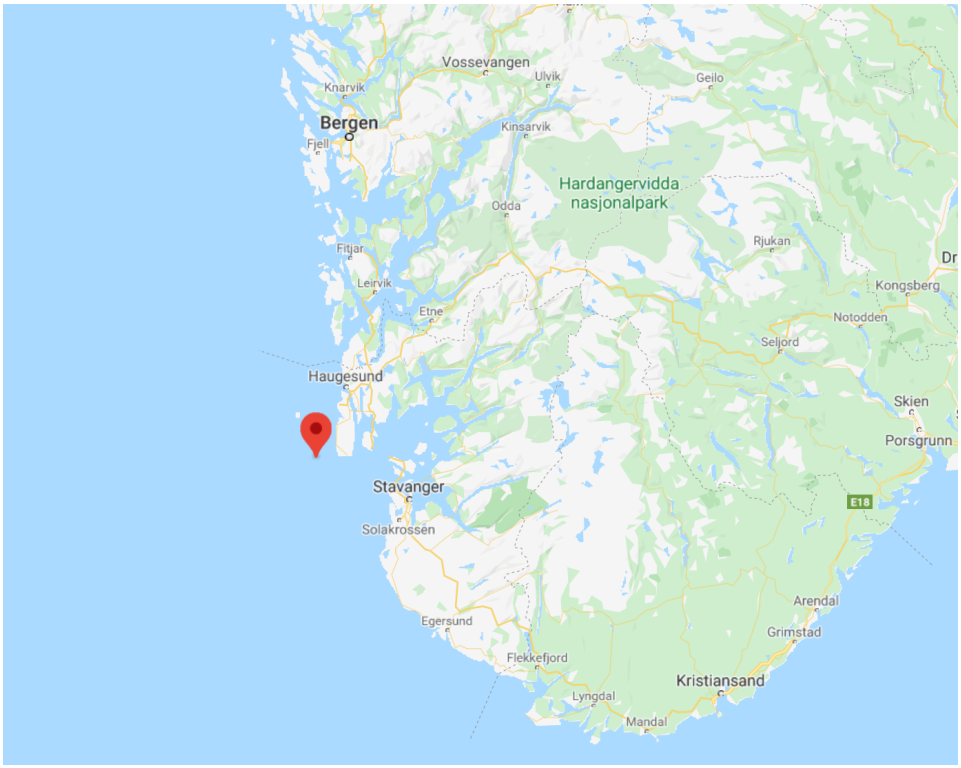

Figure 2.2: Offshore site in South-West of Norway. Marker indicates Marine Energy Test Centre site at approximate 59°09'N 5°01'E (Google Maps, n.d.).

Table 2.3: Summary of metocean conditions at the Metcentre site. Wind gusts, significant wave heights and ocean currents by Onstad et al. (2016), spectral peak wave periods estimated by Nygaard and Mathiesen (2008).

Parameter		Mean value		50 year extreme	
Water depth	m	d	220		
Wind gust speed at 3.5 m height	$m\,s^{-1}$	$U_{3.5,m}$	9.0	$U_{3.5,50-yr}$	30.5
Significant wave height	m	$H_{s,m}$	1.5	$H_{s,50-yr}$	13.3
Spectral peak wave period	s	$T_{P,m}$	8.7	$T_{P,50-yr}$	16.3
Current speed at 20 m depth	$m\,s^{-1}$	$v_{c,m}$	0.3	$v_{c,50-yr}$	1.4

2.3. Future offshore wind turbine generators

Upscaling of wind turbines is a hot topic in the industry. The past decade has seen a tremendous growth wind turbines both in amount of installed units, and increase in size and power output per unit. According to IRENA (2019), the weighted average power output of installed wind turbines has more than doubled to approximate 9 MW since 2010, and it is expected that this will double again in 10 years, as seen in Figure 2.3. But the question rises if this growth is sustainable, and to what size wind turbines will grow in the future. According to Jensen et al. (2017) there are no technological show stoppers to the development of wind turbines up to 20 MW in power rating.

The drive towards larger wind turbines is mainly powered by a more viable business case; larger wind turbines are able to provide energy more reliably with a higher capacity factor (Cozzi et al., 2019), and provide a lower levelised cost of energy, estimated to be around 85 €/MWh for 10 MW turbines, and 80 €/MWh for 20 MW wind turbines (Jensen et al., 2017).

Combining both findings on lower levelised costs of energy for large scale offshore wind turbines, and a decrease of primary steel mass for FOWTs per power rating discussed in subsection 1.3.3, a complete package of both WTG and floating wind platform should become economically more interesting as power ratings increase.

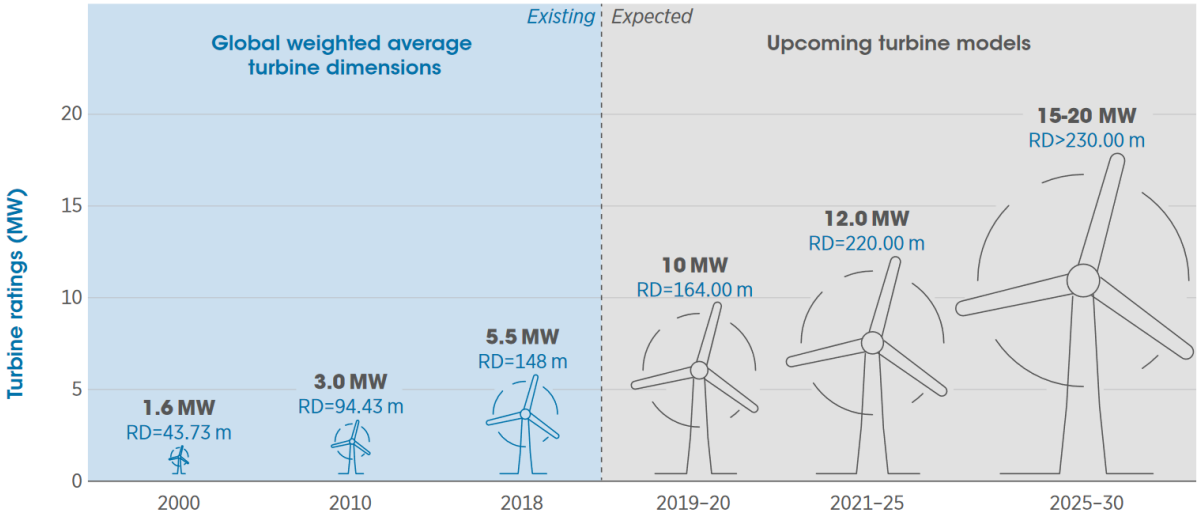

Figure 2.3: Rotor diameter and power rating of installed wind turbines from 2000 up to 2030 by IRENA (2019).

2.3.1. Wind turbine scaling laws

As introduced in subsection 1.3.1, researchers commonly use rational scaling laws and dimensional analysis to forecast dimensions and properties of future wind turbines. Based on scaling laws and dimensions analysis, scaling factors are derive which can be applied to an initial design. Important in the upscaling procedure for wind turbines are geometric self-similarity and aerodynamic similarity, a wind turbine cannot change its shape significantly while being scaled by scaling factors.

A scaling factor is a free to chose parameter, and is usually derived as a ratio between a scaled concept over the base case design. A scaling factor is often an expression of a difference in length between the scaled and reference design, and relates other properties of a wind turbine as a function of this difference (Gasch and Twele, 2011; Sieros et al., 2012). In wind turbine research, a common characteristic length L is chosen based on the rotor diameter. From this starting point many other WTG parameters are derived using dimensional analysis, some of which are presented in Table 2.4.

Based on dimensional analysis, and using the rotor diameter as a characteristic length of the wind turbine generate, the square-cube law predicts that the power generation is proportional to the rotor diameter squared, while mass should scale by a cubed factor. These relations form the basis for most of the previous academic research into the upscaling of FOWTs. Studies by George (2014), Leimeister (2016) and Islam (2016) derive a length scaling factor s based on either mass or power rating as the inverse of the relations presented in Table 2.4:

$$\text{Mass: } s_m = \left(\frac{m_{WTG,upscaled}}{m_{WTG,inital}}\right)^{\frac{1}{3}} \qquad \text{Power: } s_P = \left(\frac{P_{upscaled}}{P_{inital}}\right)^{\frac{1}{2}} \tag{2.1}$$

This scaling factor s is then applied to length dimensions of the substructure in aforementioned studies. However, as discussed in subsection 1.3.3, these studies advise against the application of a single scaling factor to the entire structure.

Assuming that costs of the use of (structural) materials in a WTG is one of the leading cost indicators, the square-cube law predicts that total costs of a turbine increase with a faster rate than power rating. However, studies like Jensen et al. (2017) show that it is still economically beneficial to construct and operate larger wind turbines, which indicates that the theoretical square-cube law might not be valid.

2.3.2. Sizing trends of offshore wind turbines

By researching historic data of wind turbine dimensions, it should be possible to investigate the trends in increase of dimensions for current and future wind turbine models. If the square-cube law holds, the data should show that trend lines of power rating and RNA mass as function of the rotor diameter should describe a power law trend line of s^2 and s^3 respectively.

Data is gathered for commercially developed wind turbines over a range from 3 MW to 11 MW, provided by industry experts on anonymous basis, and for academic reference turbines from 5 MW up

Table 2.4: Overview of common parameters used for scaling of wind turbine generators (Gasch and Twele, 2011; Sieros et al., 2012).

Parameter	Expression	Scaling factor
Mass	$m = \rho V = \rho L^3$	s^3
Power	$P = \frac{1}{2}\rho C_p \frac{\pi}{4} L^2 v_{air}^3$	s^2
Acceleration	a	s^0
Aerodynamic thrust	$F = \frac{1}{2}\rho C_T \frac{\pi}{4} L^2 v_{air}^2$	s^2
Aerodynamic moment	$M = FL$	s^3
Area moment of inertia	$I_t = \int x^2 dA$	s^4
Mass moment of inertia	$I_{xx} = mL^2$	s^5

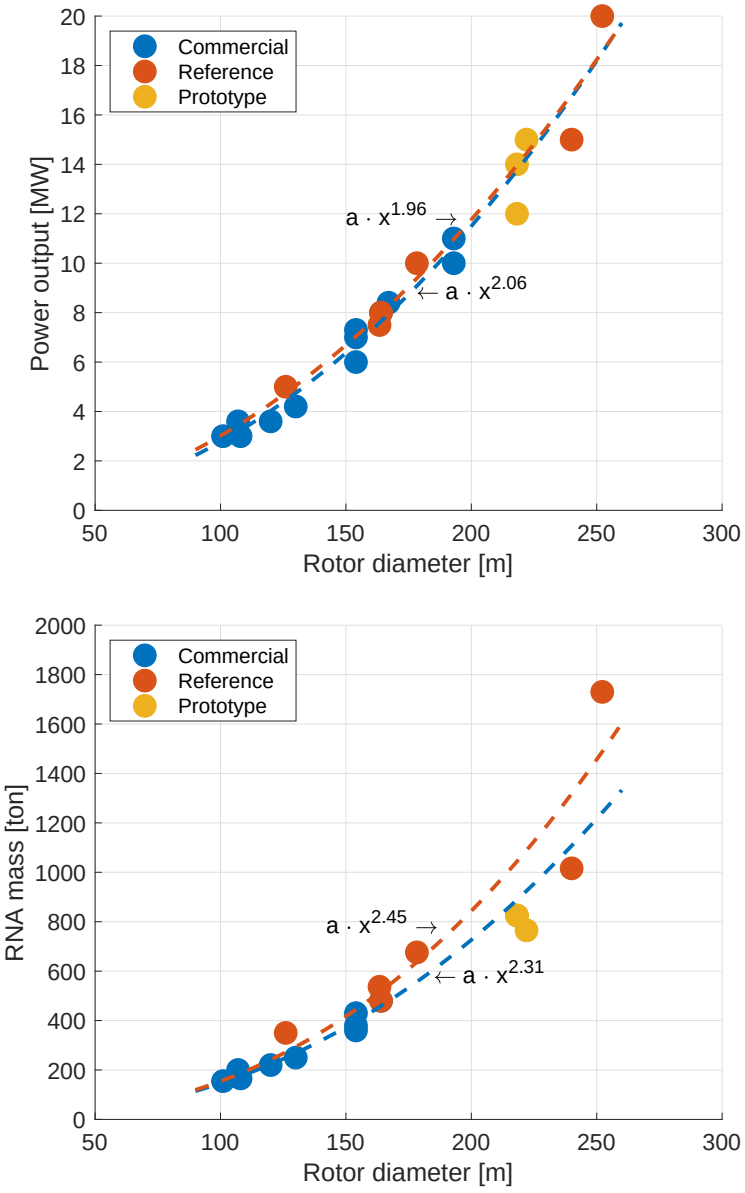

Figure 2.4: On top data points and trend lines of WTG rated power output as function of rotor diameter, below data points and trend lines of RNA mass as function of rotor diameter.

Table 2.5: Resulting dimensions of wind turbines according to the curve fitted power laws, and compared to existing wind turbine desings in italics of NREL (Jonkman et al., 2009), LEANWIND (Desmond et al., 2016), DTU (Bak et al., 2013), GE (de Vries, 2019), IEA (Gaertner et al., 2020) and INNWind (Jensen et al., 2017). Dimensions for the SG 14-222D are estimated by industry experts.

Power rating	Rotor diameter [m]	RNA mass [ton]	Power density [W m^{-2}]
5 MW	133	285	361
NREL 5 MW	*126*	*350*	*401*
8 MW	168	483	361
LEANWIND 8 MW	*164*	*480*	*379*
10 MW	187	621	364
DTU 10 MW	*178*	*677*	*401*
12 MW	204	762	367
GE Haliade-X 12-14 MW	*218*	*825*	*321 - 374*
SG 14 MW 222 DD	*222*	*765*	*361*
15 MW	228	979	367
IEA 15 MW	*240*	*1016*	*332*
20 MW	262	1354	371
INNWind 20 MW	*252*	*1730*	*400*

to 20 MW. Reference turbines are, according to Jonkman et al. (2009), “to be used as a reference by research teams throughout the world to standardize baseline offshore wind turbine specifications”. Even though reference turbines are not optimised like commercial wind turbine designs, they provide a good basis for further research purposes. In addition a few recently published prototype models in the range of 12 MW to 14 MW are included to see where the future is heading to according to OEMs.

In Figure 2.4, the gathered data points and resulting trend lines based on a power law are plotted. Even though this study is not ideal due to the limited sample size and available data, there are clear trends to identify in both graphs. In general, wind turbines do follow the s^2 scaling factor accurately on power rating, as predicted by scaling laws. However, trends of mass as function of a characteristic length follow a more nuanced scaling factor of $s^{2.3}$ to $s^{2.4}$, compared to a s^3 curve the square-cube law predicts. This implies that mass scales more closely relative to power rating than the square-cube law implies. According to experts involved with this project, the discrepancy can be contributed to technological advancements in materials engineering and generator design of wind turbines.

Next step is to generate theoretical wind turbine models based on the curve fits, and compare the resulting properties to existing WTG designs. The results are presented in Table 2.5, the derived properties are based on the trend lines for commercial designs (the blue lines in Figure 2.4). The reason for choosing trend lines for commercial turbines is that the academic reference turbines are designed with a significantly higher power density number up to 400 W m^{-2}, whereas commercial turbines in general have a more realistic power density in the order of 360 W m^{-2}. The required rotor diameters for most reference turbines is relatively optimistic and small, compared to the commercial designs.

On the other hand, the academic reference turbines generally overestimate the RNA mass of the wind turbine generators, which is a disadvantage to the support structure. Therefore it is assumed that the trend lines for commercial turbines represent a more realistic progression for the future.

The latest published reference turbine, the IEA 15 MW by Gaertner et al. (2020), does fall more in line with the trends of recent commercial wind turbine generators, as well as the most recent prototype models by GE and SG. It is designed with a larger diameter rotor for a lower power density figure, and a lighter RNA mass than trends based on previous reference wind turbines.

2.3.3. Definition of theoretical offshore wind turbines for case-study

For the TetraSpar case-study, three theoretical and generic upscaled turbines of 10 MW, 15 MW and 20 MW are defined based on the literature research, common requirements for offshore wind turbines and in collaboration with industry experts. The resulting generic WTG designs and specifications are listed in Table 2.6, next to the current WTG used for the 3.6 MW demonstrator.

Rotor diameter, hub height and RNA mass are based on the scaling trends identified in Figure 2.4,

Table 2.6: Specifications of generic WTG designs for the TetraSpar case-study.

Power rating	MW	3.6	10	15	20
Rotor diameter	m	130	187	228	262
Hub height	m	85	124	144	161
RNA mass	ton	200	621	1079	1354
Tower base diameter	m	4.3	8.0	10.0	12.0
Tower mass	ton	240	574	860	1170

the tower dimensions are generated based on reference turbines by Bak et al. (2013) and Gaertner et al. (2020). Appendix A explains in detail how these dimensions of the generic upscaled WTG designs are generated.

2.4. Upscaling design methodology based on overturning moment

Based on literature review on academic research and materialized efforts (section 1.3), it is concluded that there is no definitive approach to the upscaling of FOWTs. It seems that theoretical scaling factors based on power rating or payload mass ratios show a general direction for the substructure to be upscaled, but the academic research based on upsizing by scaling factors recommend many adjustments to be made for a feasible upscaled design concept.

Even though the power output rating of a WTG is a fair indicator for the dimensions and loads of the superstructure, it cannot be a direct input parameter to size the support structure. Leimeister (2016) and Islam (2016) show that scaling based on power rating s_P (Equation 2.1) requires manual adjustments or other scaling factors to be used after the initial upscaling effort by that scaling factor. Scaling based on payload mass is debatable as well. George (2014) and Leimeister (2016) recommend scaling based on mass of the superstructure s_m (Equation 2.1) and state that this factor delivers feasible and representative designs.

This conclusion does not align with data on floating structures for oil and gas. Ramboll (2018) shows that there is a wide spread of the ratio between topsides to support foundation in terms of weight. Building on that experience of decades of floating platforms, it does not seem likely that the mass of the wind turbine generator directly translates to sizing of the substructure. In addition, even though wind turbines are relatively large superstructures in length dimensions, these structures are relatively lightweight to size. Typically, wind turbine generators including support tower, only account up to 10% of the total mass of the floating structure; the primary steel and ballast of the floating foundation are the leading weight items.

Reflecting on the two examples of commissioned upscaled floating wind substructures it does not seem that these structures follow any of the theoretical scaling factors, and adapt the design to accommodate to other design considerations.

As former academic upscaling approaches do not converge to a single uniform methodology, do require manual adjustments after applying scaling factors, and do not correspond with trends observed in traditional floating offshore structures, a new upscale design methodology is proposed.

According to Henderson et al. (2016) the "*mean wind turbine thrust overturning moment* can be considered primary design driver." The wind creating thrust onto the wind turbine rotor combined with a long lever arm from the rotor to the substructure create a large overturning moment, which must be counteracted and stabilised by the substructure as restoring moment. The underlying stability mechanism to counteract the wind overturning moment is dependent on the classification of substructure as outlined in section 1.1.

The proposed new upscaling method is based on the maximum wind overturning moment a wind turbine generator experiences, combined with a limited amount of allowable heel angle the structure may experience. The latter parameter results from the requirements for a stable platform, and is further explained in subsection 2.4.1. In general, wind thrust is maximum at or near the rated wind speed of a wind turbine of approximately 11 $\mathrm{m\,s^{-1}}$, depicted in Figure 2.5. By estimating the maximum wind thrust for any size of wind turbine generator based on rotor diameter, per Figure 2.4, and a required hub height it is possible to define a wind overturning moment for a given wind turbine power rating. Through statics engineering it follows that the substructure must generate enough counteracting restoring moment to

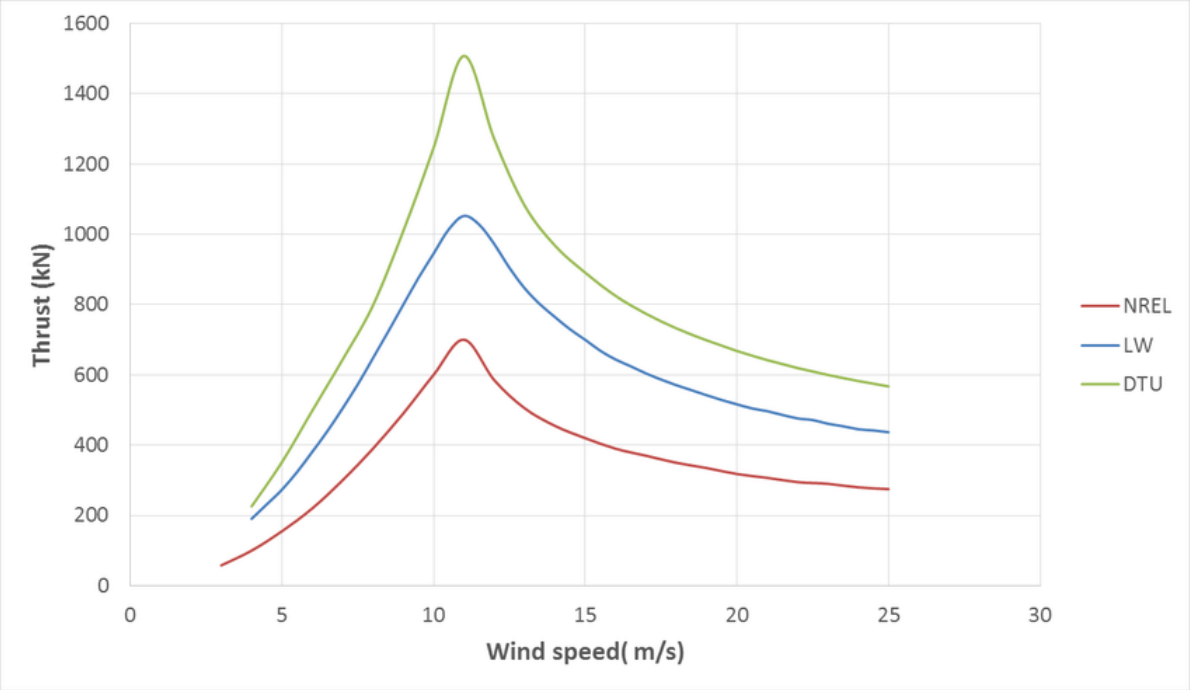

Figure 2.5: Thrust curves of NREL 5 MW, Leanwind 8 MW and DTU 10 MW reference wind turbines by Desmond et al. (2016). Maximum aerodynamic thrust occurs near rated wind speeds of approximately 11 m s^{-1}.

balance the thrust.

In Figure 2.6, a flowchart of the proposed design methodology is presented. Starting form an initial design for a floating substructure, and gathering input data on an upscaled wind turbine data, site conditions, and functional requirements and design criteria, the following steps are to be taken:

1. Hydrostatic analysis. Here the fundamental equilibria for vertical and rotational directions are considered. The upscaling design methodology starts by developing a substructure with enough restoring moment to counteract the increase wind overturning moment, and by creating enough additional buoyancy in the floating foundation to support the increased weight of the payload and substructure. For this step a maximum static heeling angle due to wind thrust must be determined, generally below 10°.

2. Hydrodynamic analysis. The upscaled design that has been iterated through the hydrostatic process now must be analysed on the motions and loadings of the structure for the intended metocean environment. Items like maximum excursions, structural accelerations and other criteria shall be considered during this step. If adjustments must be made to accommodate improvements to the structure's dynamics, then first it must be rechecked on the hydrostatic requirements.

3. Structural analysis. After passing the hydrodynamic analysis, an analysis on the structural design is required on the limit states of ultimate, fatigue, serviceability and accidental. Main goal is to determine the structural integrity of the floater on the loads and dynamics it may experience over a lifetime.

The order of these steps is crucial to determine the technical feasibility of the FOWT structure. Before anything else, a floating structure must be inherently (statically) stable to provide a safe platform to its payload. This static stability is independent to the environmental setting.

Only after the statics of the structure are determined, it is effective to continue to the dynamic component of the structure. Here, loads, motions and accelerations for the complete structure and internal components are assessed to the local metocean design conditions, and to be used as input to the structural analysis. This step considers if the structure's strength is sufficient to survive the offshore climate for decades to come. If the upscaled FOWT design passes all checks, the resultant floating structure then can evaluated if it meets requirements and demands set at the beginning of the project.

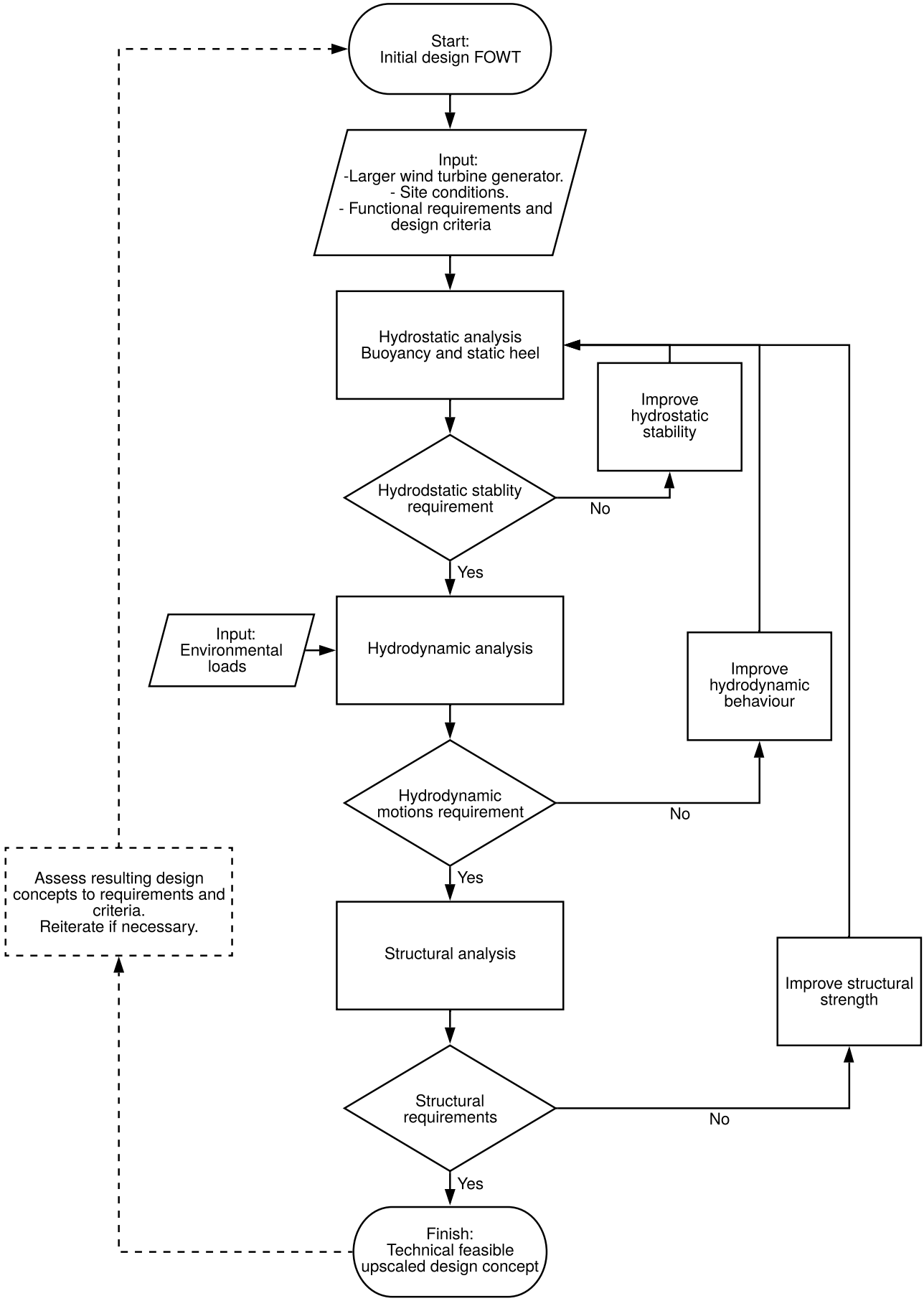

Figure 2.6: Flowchart of the general design methodology for floating offshore wind turbines developed for this thesis work.

As depicted in Figure 2.6, each step requires a moment of evaluation and potential reiteration if requirements and criteria are not met, and may have impact on every aspect. Hence that after every iteration and improvement the process starts again at first analysing the hydrostatics, then the hydrodynamics and structural analysis described earlier.

2.4.1. Comments on rotational stability design driver

Defined in section 2.4, the generalised upscaling design methodology is based on the stability of the structure, with the notion that the structure will rotate when exposed to external loads. There are many factors that contribute to the heel of the structure, classified into two categories of external and internal actors. On the external factors the key factors are:

- Aerodynamic loads. The wind interacting with the rotor and rest of the superstructure cause thrust and drag, causing a horizontal force and resulting overturning moment.
- Hydromechanic loads. Waves and currents induce hydromechanic forces in all directions, which in turn rotate the structure. These loads are directly related to the shape and size of the submerged structure.

For internal factors, that are directly a result of the design of the structure, are the following of importance:

- Centre of gravity. As weighted average of all mass in the structure, the centre of gravity can be seen as the centre around which the structure rotates (assuming a rigid body). The position is greatly depended on the design of the structure, and affects the amount of overturning moment that external loads induce. Key to the centre of gravity is the relative position of lightweight structural elements versus location of ballast.
- Centre of buoyancy. As counterpart of the centre of gravity, the centre of buoyancy (weighted average of all submerged elements) acts in the opposite direction to weight, but with an equal magnitude. If the structure starts heeling, the centre of buoyancy and centre of gravity will act as a couple.
- Water plane area. A structure with more area piercing the waterline is able to withstand higher overturning moments for a same amount of rotation.
- Mass and inertia. Especially in dynamic analysis the amount of mass or inertia the structure has influences the amount of heel of the structure. In a situation with fast changing forces, a structure with a large amount of mass or inertia will be slower to respond to the loads.
- Mooring system. From the fairlead the mooring lines pull the floater back to its resting position. The amount of force the mooring system imposes is not only dependent on external forces that push the floater away from initial position, but also through the design of the mooring system itself with properties on mooring type, configuration and line weight.
- Control system. Contemporary wind turbines are equipped with advanced systems to control the blades and nacelle to optimise power production. This control system could affect the aerodynamic load onto the rotor, and therefore be able to control the rotational stability.

All these factors may influence the stability of the floating structure, are deeply intertwined with each other and are highly variant over the full weather envelope offshore. As an example, an increase in mass directly affects the total submerged volume, which in turn influences the hydromechanic loads acting onto the structure and the restoring forces by the mooring system. A change in the shape of the floating substructure may change the water plane area, but also has effect on the exposed structure area in terms of loads by environmental forcing.

There is no single answer on how one of these factors affect the rotational stability of a floating structure, while omitting the effects of the other phenomena. There are many variables involved, with at least an equal amount of unknowns. Similar to the development of many other complex systems, the detailed design of a FOWT structure requires iterative design approaches and intricate descriptions of the model, and must strike an acceptable balance between all aspects.

For the upscaling design methodology developed for this report, with the goal to generate first-order draft concepts of FOWT designs, it is chosen to reduce all contributing factors to only the wind overturning moment by maximum rotor thrust. Arguments for deciding on this key design parameter are:

- It allows for a well defined input parameter, directly linked to WTG rotor diameter and power rating.
- It separates the (quasi-)static wind action from the relatively high dynamic wave action. The aerodynamic thrust creates a constant rotational offset, wave action induces oscillations relative to the constant heel angle by wind.
- It provides a distinct and generic design input variable for any FOWT concept, indifferent to local metocean conditions, as all WTGs are designed to operate at rated wind speeds.
- It is a direct design parameter affecting the (quasi-)static equilibria of the structure.

Fundamental to the design methodology is the principle stability mechanism of the floating platform. Design choices, parameters and criteria are highly dependent on the classification of floating structure, and affects how a platform achieves both buoyancy and stability for overturning moment. subsection 2.4.2 discusses the main design choices and consequences for generic spar, semi-submersible and TLP platforms when designing for stability.

For a floating platform to be stable and create enough restoring moment to counteract an external overturning moment, a small angle of rotation or heel, is required. One of the criteria chosen for this upscaling design methodology is to allow the structure to rotate 5.0° by the wind overturning moment, assuming that aerodynamic thrust is static relative to other dynamic actions. This value is chosen by the example of Matha et al. (2015), but there is no consensus among academic literature what the allowable angle should be. Some advice a maximum heel angle of 10°, like Leimeister et al. (2016); Kolios et al. (2015) for FOWTs, whereas Halkyard (2015) states that conventional oil and gas spar platforms are designed for a maximum of 5.0° of rotation.

By assuming a relative small static wind heel angle as design basis, the upscaled design concept can rotate and oscillate by other dynamic forces like waves, currents and turbine winds. Beneficial to a small maximum static heel angle are, among others, a limited reduction in energy production due to decrease of projected area by the rotor, and the decrease of bending moments in the structure when the top mass is out of plumb. In addition, one can imagine that a large heel angle may have negative effects on the rotating equipment and other subsystems inside the WTG. On the other hand, a larger static wind heel angle requires a smaller substructure to generate enough restoring moment.

2.4.2. Expected design concepts for floating wind platform classifications

Part of this thesis work is to develop a generalised upscaling design methodology for floating wind structures, regardless of the type of structure. This section outlines the expectations and implications of the previously described design methodology based on overturning moment for the three floating platform classifications. For each category of floater two main design points or choices are discussed. It should be noted that for all three classifications, the platform should allow for a small angle of rotation, to be able to counteract the wind overturning moment.

Ballast stabilised platforms, or spars, gain their stability by a large structural weight and a low centre of gravity. The substructure acts as a counter weight to the overturning moments applied to the structure.

To accommodate larger wind turbines with increased wind overturning moments, spar structures have two options according to the upscaling design methodology: increase the total structural weight or lower the centre of gravity. The former option requires that for every unit of additional weight added to the structure, an equal amount of buoyancy has to be created. This increases the displacement and volume of the structure, which in turn increases the hydrodynamic loads onto the substructure. The second option may be resolved by placing denser ballast lower into the substructure, or increase the draught of the structure. As seen with the Equinor Hywind concepts, the second option could be less favourable as local water depths cannot support deeper draught structures.

Buoyancy stabilised platforms like semi-submersibles and barges remain stable by a large water plane area moment of inertia. Increased stability for these substructures is created by increasing the water plane area and/or increasing the distance of the water piercing elements farther away from the centre of the structure.

The second option is more favourable in terms of hydrodynamic forcing, as it limits the increase in substructure submerged volume. However, Principle Power's WindFloat design shows that an increase in outer dimensions of the structure hampers the installability and manufacturing capabilities of the floating structure. For larger wind turbines, semi-submersibles and bargers employ a combination of a larger water plane area, designed at a strategic distance farther away while adhering to practical limits like maximum width.

Mooring stabilised platforms, or tension-leg platforms, are stable due to stiff tendons secured to the sea bed and permanently under tension. TLPs must follow the strict condition that under no circumstances a tendon goes slack. The TLP substructure ensures this by a net positive buoyancy, such that any overturning moment and resulting force acting onto a tendon fairlead, is less than the tensile force carried through the tendon to the sea bed.

For larger wind turbines with increased overturning moments, the submerged volume will increase to fulfil the no slack condition. As TLP's buoyancy increase, the maximum tensile forces in the tendons will increase. To avoid the maximum tendon breaking strength the distance between tendon fairlead and structure centre is increased to create a larger lever arm between tendon and structure. This in turn increases the width of the structure, and the footprint of the tendons at the seabed. At the time of writing, no representable upscaled FOWT TLP structures are deployed.

3

Hydrostatic analysis

For any floating structure its most fundamental condition to fulfil is to be able to float and do this stable, a small perturbation should not result in the capsizing of the structure. This first requirement can be assessed through a hydrostatic analysis of the floating structure, in essence a study of an equilibrium of forces and moments in a (quasi)static manner.

Because of this core principle, the actual upscaling of a FOWT design is based on the hydrostatic premise before any other analysis is executed. The following chapter discusses the principles of hydrostatics, performs the upscaling of the TetraSpar case-study, and compares the resulting upscaled design concepts to other upscaling methodologies.

3.1. Statics and stability of floating structures

As stated by Journée and Massie (2008), the "static stability of a floating structure encompasses the up-righting properties of the structure when it is brought out of equilibrium or balance by a disturbance in the form of a force and/or moment." For a hydrostatic analysis the most important equilibria to consider are in the vertical and rotational directions, in which the sum of resulting forces or moments are equal to zero. Equilibrium in horizontal direction is not of interest for now, there are no hydrostatic forces acting onto a floating structure.

Hydrostatic stability in vertical direction is found in Archimedes' law. It states that a submerged body experiences an upwards buoyancy force F_B proportional to the submerged volume ∇ and the density of the fluid ρ:

$$F_B = \rho \cdot g \cdot \nabla \tag{3.1}$$

For a body afloat in vertical equilibrium, the upward buoyancy force must be equal to the downward force of weight of the body, or the submerged volume is equal to the mass of the displaced fluid. The buoyancy force can also be interpreted as the integral of the vertical component of the hydrostatic pressure $p = \rho \cdot g \cdot z$ over the body's surface.

For a floating structure to be in equilibrium in rotational direction, the sum of the moments acting on that structure is equal to zero. For a body at rest and no external moment applied, the centre of buoyancy will be vertically aligned with the centre of gravity. Because the buoyant force is equal and opposite to the weight of the structure, the body is in equilibrium only when the lever arm of the pair of forces is zero.

When a floating body is rotated by an external heeling moment, the centre of buoyancy will shift to a new position due to a change in shape of the submerged volume of the structure. This translation of centre of buoyancy leads to a lever arm $\overline{GZ}$, defined by the distance between the centre of gravity G and the vertical line of the new centre of buoyancy B_1, indicated in Figure 3.1. As the weight and buoyant force act as a pair of forces, and with a non-zero lever arm, an internal restoring moment M_S is generated and defined by:

$$M_S = \rho \cdot g \cdot \nabla \cdot \overline{GZ} \tag{3.2}$$

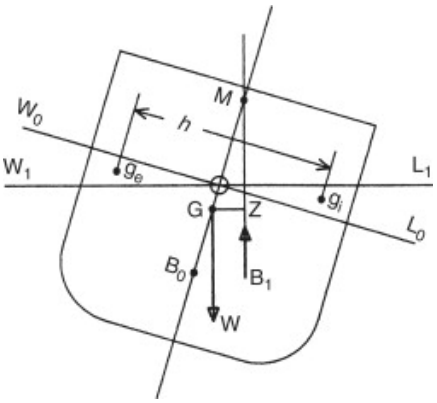

Figure 3.1: Definition of the metacentre M, on the line of the centre of gravity G and the initial centre of buoyancy B_0, and at the intersection with the vertical line of the new centre of buoyancy B_1 after a small rotation (Molland, 2011).

The structure will find a new equilibrium when the internal restoring moment M_S is equal and opposite to the external heeling moment. Through trigonometry, the lever arm is found as the distance between the body's centre of gravity and metacentre as $\overline{GZ} = \overline{GM} \cdot \sin\theta$, given a rotation of θ amount.

For structures designed for a range of relative small angles of rotation, up to 10° according to Journée and Massie (2008), and to which the water plane remains similar in shape when rotated, the initial metacentric height of a floating structure is expressed by:

$$\overline{GM} = \overline{KB} + \overline{BM} - \overline{KG} \tag{3.3}$$

This three part definition is composed of the distance between the keel and centre of buoyancy $\overline{KB}$, the distance between the keel and the centre of gravity $\overline{KG}$, and the distance between the centre of buoyancy and the metacentre $\overline{BM}$. This last term is the ratio of the area moment of inertia of the water plane over the submerged volume of the body, $\overline{BM} = I_T/\nabla$.

One of the fundamental requirements to any floating platform is to provide a stable and safe foundation to its payload. On the basics of hydrostatics, the platform must possess positive stability, i.e. if the structure is subjected to small disturbance from an equilibrium position, the structure should tend to return to the equilibrium position.

For an equilibrium in vertical direction, Equation 3.1 shows that when a structure's submerged volume is increase, by forcing it downwards into the fluid, the buoyant force F_B will increase by equal amounts and resists any further increase of submerged volume. When the downward force is no longer applied, the buoyant force will push the structure upwards until an equilibrium between the amount of submerged volume (or weight) and buoyancy is found.

Positive stability in rotation found when the value of $\overline{GZ}$ is larger than zero. For small rotations by an external moment generates an amount of restoring moment M_S by a factor of $\sin\theta$, a larger rotation will result to proportionately more restoring moment. Therefore a floating body structure with a positive value of $\overline{GZ}$ will tend to return to its initial equilibrium position.

The condition for a positive value of $\overline{GZ}$ implies that the metacentric height must always be greater than zero, or that the metacentre should always be above the centre of gravity. Rewriting Equation 3.3 to these conditions leads to:

$$\overline{KB} + \frac{I_T}{\nabla} > \overline{KG} \tag{3.4}$$

To put into words, the distance of keel to centre of buoyancy plus the contribution of the water plane area must be greater than the distance of keel to centre of gravity for a structure to be positively stable in rotation directions.

As stated in the introduction of this report, different classes of floating platforms achieve stability in different manners. While vertical floating stability for all floating structures is achieved in similar manner, allow enough additional structure body to be able to submerge in case of vertical forcing, the rotational stability is approach in fundamental different ways.

A spar platform is stable because of its location of the centre of gravity being lower than its centre of buoyancy, and Equation 3.4 holds. The water plane contribution is significantly smaller than the other terms, due to the relative small water plane area moment of inertia I_T divided by a large amount of submerged volume. The drawback to this type of structure is the relative large mass needed to offset the high centre of gravity of the payload, and the large draught to increase the distance between the centres of gravity and buoyancy.

A semi-submersible class floater is stable because of the large water plane area moment of inertia relative to the submerged volume. This type of platform should be designed in such way that the sum of the two terms on the left of Equation 3.4 is larger than the distance between keel and centre of gravity. This does allow a semi-submersible to have a relative high centre of gravity, usually near or above the water line, and limit the required draught of the structure. However this does come at the disadvantage of a relative large amount of exposed structure near the waterline.

3.2. Approach and delineations to hydrostatic analysis

The initial hydrostatic design and analysis of a FOWT is based on the floating stability of the structure. According to DNV GL (2018), “floating stability implies a stable equilibrium and reflects a total integrity against downflooding and capsizing”.

By means of simplified analytic calculation, an initial design concept of an upscaled FOWT is developed based on these floating stability requirements. As discussed in the previous section, these hydrostatic properties of the floating platform are focused on equilibria in vertical and rotational directions.

For the analysis in vertical direction, Archimedes’ law is leading and dictates that the amount of submerged volume should be equal to the mass of the structure divided by the fluid density. When a structure’s mass increases, e.g. by installing a larger payload or adding more ballast, it must be balanced out by adding more buoyancy to the structure until a new equilibrium is found This can be achieved by adding elements with positive buoyant properties; the self-weight of the element is smaller than the weight of the displaced fluid when submerged.

According to Vugts (2016) a thin-walled cylindrical steel element, a common building block in the offshore industry, is neutrally buoyant for a diameter over wall thickness ratio $D/t \approx 30$. For steel tubular braces with a higher ratio of D/t the member is positive buoyant, and an increase of this ratio results to an approximate linear increase in buoyant capacity. However, some elements require a higher D/t-ratio for strength, braces near the waterline are characterised by a relatively thick wall compared to other braces far away from wave action. The benefit of using a constant D/t-ratio as rule of thumb in the upscaling process is that the density of the cylinder remains constant regardless of dimensions.

For stability in rotation direction the codes by DNV GL (2018) differentiate requirements for different classes of substructures. For spar-type platforms it states that “the metacentric height $\overline{GM}$ should be equal to or greater than 1.0 m”, with $\overline{GM}$ defined by Equation 3.3.

In the case of semi-submersibles, the rotational stability requirement is more complex to design and check for. Not only should a semi-submersible have a positive initial metacentric height value, but “the area under the righting moment curve to the second intercept or downflooding angle, whichever is less, shall be equal to or greater than 130% of the area under the wind heeling moment curve to the same limiting angle”, DNV GL (2018). This difference to the requirement for spar structures is due to the large water plane area of a semi-submersible, and the significant change of the $\overline{BM}$ when the structure rotates. Therefore the codes require a full analysis of the restoring moment of the structure, and compare it to the (extreme) external heeling moment is may experience.

For the TetraSpar case-study, the upscaled design concepts will be checked on stability for the following conditions, defined by DNV GL (2018):

- “operation, i.e. a normal working condition with the wind turbine operating
- temporary conditions, i.e. transient conditions such as installation and changing of draught
- survival condition, i.e. conditions during extreme storms
- transit, in particular tow-out”

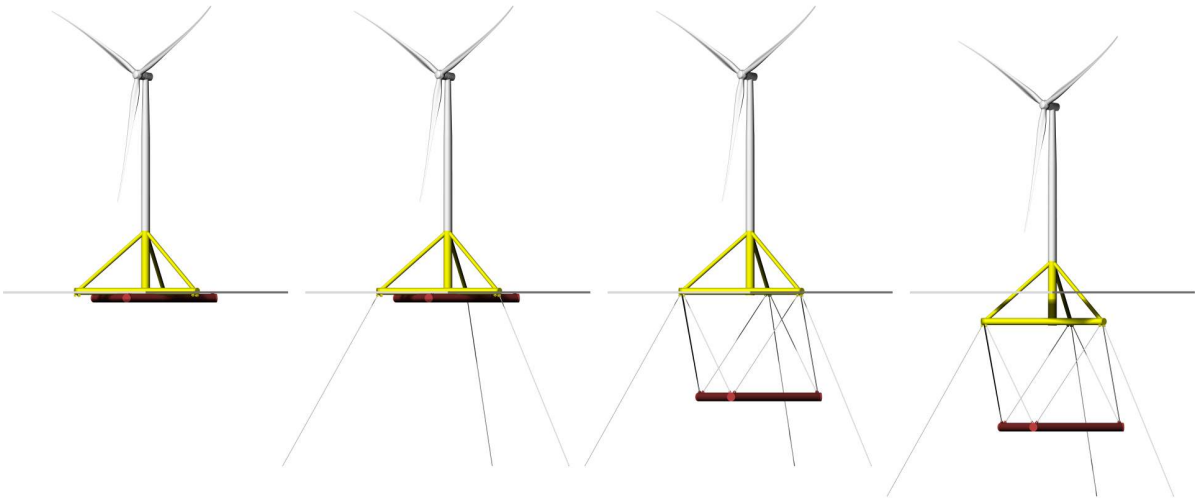

Figure 3.2: Transformation of the TetraSpar during installation. From left to right: tow-out configuration as semi-submersible with, hook-up, lowering of the keel and ballasting to operational configuration.

Due to the suspended keel design of the TetraSpar, and the transformation of the structure from a semi-submersible class during tow-out to the spar configuration for operations as depicted in Figure 3.2, each condition should be checked on (hydrostatic) stability given the platform's configuration.

In the upscaling method for the TetraSpar, the tetrahedral shape of the floater and triangular shape of the keel will remain intact and and the outer dimensions of the the structure will remain equal to the 3.6 MW demonstrator. Furthermore, the specific densities of all braces will remain the equal and are based on the existing mass and volume of the 3.6 MW demonstrator, as presented in Table 2.2. The equivalent density figures include elements cylinder stiffeners, joint connections and other structural components. Then these densities are converted to simplified straight cylinders with a constant equivalent D/t-ratio.

If during upscaling more weight or buoyancy is required to stabilise the structure, diameters of strategically selected braces will be increased. Special care will be taken for the dimensioning of the keel braces, as these should be neutrally buoyant when deballasted. This is achieved by combining thin-walled cylinders for the keel structure, and additional weight by adding just enough cement to the cylinders to equalize the weight of the keel to the displaced volume. Other upscaling guidelines are found in Appendix A.

For the stability calculations on the restoring moment M_S when the TetraSpar is in its operational configuration, the contribution of the water plane area is neglected. For the 3.6 MW demonstrator, the value for $\overline{BM} = 0.40$ m in operational configuration, while the values for centres of gravity and buoyancy are $\overline{KG} = 22$ m and $\overline{KB} = 32$ m respectively. The metacentric height is $\overline{GM} \approx 10$ m to which the water plane contribution is less than 5% to the total stability.

The upscaled TetraSpar concepts are designed based on the requirements for the spar operations configuration. The resutling design concept will be checked for other conditions and configurations as well, especially for the semi-submersible tow-out configuration. For simplicity, only the initial metacentric height is be checked for a value of $\overline{GM}$ of larger than zero in tow-out configuration with a deballasted

keel lifted close to the floater, as depicted in Figure 3.2 on the left.

3.3. Hydrostatic upscaling by overturning moment

Reflecting back to section 2.4, it is said that the overturning moment can be considered to be one of the key design drivers. This statement is further underlined by DNV GL (2018) standards on the general intact stability of FOWTs: "The floating structure shall be capable of maintaining stability during operation of the wind turbine at the wind speed that produces the largest rotor thrust." The review on scaling laws and factors show that previous studies into the upscaling of FOWTs have missed this key design criterion, and that the derived scaling factors are not always found in the design of wind turbine generators, nor for floating platforms in general.

Upscaling based on overturning moment provides a different method that is based on the stability of the floating platform. It combines the two fundamental equilibria of hydrostatics in vertical and rotational directions into one method, by anticipating the physical dimensions and masses of future wind turbines, and the wind forcing onto the wind turbine rotor and resulting overturning moment, making it suitable to generate an upscaled design concept based on an initial floating foundation.

The superstructure's dimensions and masses are based on the (historical) trends as discussed in section 2.4. In addition to a minimum of required additional buoyancy due to an increase of payload mass, the rotor diameter also indicate a required minimum hub height for that turbine. This is the start of the second step on overturning moment is taken. By estimating the maximum thrust a WTG may experience, usually near or at rated wind speeds, and combining it with the hub height, a maximum wind overturning moment can be derived. This external moment then is used in the equations for restoring moment, to which the floating structure must have a high enough metacentric height, combined with enough structural weight to counteract the external heeling moment by wind.

Recall that the aerodynamic thrust on a WTG rotor is defined as:

$$F_T = \frac{\pi}{8} \cdot \rho_{air} \cdot C_T \cdot D_{rotor}^2 \cdot u_{air}^2 \tag{3.5}$$

By assuming that maximum thrust is at a rated wind speed of 11 m s^{-1}, air has a density of 1.225 kg m^{-3}, and a generic coefficient of thrust at rated wind speed of approximate 0.65 (Frohboese et al., 2010), a reasonable estimate for maximum aerodynamic thrust on a wind turbine as a function of rotor diameter only is:

$$F_{T,max} \approx 38 \cdot D_{rotor}^2 \tag{3.6}$$

Then the maximum overturning moment must be determined based on the maximum rotor thrust. For bottom-fixed wind turbines the lever arm is taken from rotor hub to mud line, but for the design of floating wind structures the determination of the lever arm is not so evident. Commonly rotations and moments are calculated around the centre of gravity of the structure. However, the location of the centre of gravity is yet to be determined by the upscaling design methodology. For two reasons is the lever arm for overturning wind moment chosen to be from rotor hub height to still water level (SWL). One reason is because this distance is known beforehand when selecting a wind turbine, based on the air gap requirement for lowest tip elevation. The other reason is that only the submerged volume contributes to the restoring moment, similar to the embedded body of a monopile in soil for bottom-fixed WTGs. Any volume not submerged does not create any additional restoring moment for the structure, this stops at the water line.

Reflecting to the equations for hydrostatic stability in vertical and rotational direction, and incorporating simplifications for the upscaling of the TetraSpar, the governing equations for the hydrostatic upscaling are:

$$m_{structure} = \rho_w \cdot \nabla \tag{3.7}$$

$$M_{O,wind} = M_S$$

$$F_{T,max} \cdot z_{hub} = \rho_w \cdot g \cdot \nabla \cdot \overline{GZ} \tag{3.8}$$

$$\overline{GZ} \approx (z_{COG} - z_{COB}) \cdot \sin\theta$$

Equation 3.7 represents the vertical equilibrium of structural mass equals the mass of the displaced fluid, whereas Equation 3.8 is rotational equilibrium, and the key design equation for the upscaling procedure. The latter equations include the assumption that the water plane contribution $\overline{BM}$ in the equation for $\overline{GM}$ (Equation 3.3) is negligible due to the small water plane of a spar platform compared to its displacement. This reduced $\overline{GM}$ to only the distance between the centre of buoyancy (COB) and centre of gravity (COG). A free body diagram of the hydrostatic equilibria in vertical and rotational direction is presented in Figure 3.3.

As the governing equations have been set, the next step is to execute the upscaling design procedure for the TetraSpar. Starting with the current design, the existing braces are converted to an equivalent density parameter with corresponding thin-walled steel cylinder, see Table A.1 for an overview. As the length dimensions are set according to the upscaling guidelines in see Appendix A, any additional buoyancy or weight to balance the structure must come from an increase in diameter of strategic chosen braces.

For the TetraSpar the different braces each have their own distinct function; the keel is to lower the COG and increase the weight, while the submerged braces of the floater create the required buoyancy and raise the COB. As the centre column and diagonals are dimensioned according to the interface diameter of the WTG support tower (see Appendix A for guidelines), only radial, lateral and keel braces are variable parameters to balance the system.

An algorithm is developed to automate the process of the upscaling of the TetraSpar platform. Starting with the initial 3.6 MW demonstrator design, the first step taken is to increase the floater buoyancy by enlarging the horizontal brace diameters to even out the increased payload mass of the larger wind turbine. Furthermore, for the base-case upscaling concept designs the keel draught is fixed to 65 m below SWL, a keel depth equal to the demonstrator.

The algorithm starts an iterative search by slowly increasing the diameter and mass of the keel, compensating the increased keel weight by enlarging the volume of radial and lateral braces, and calculate the resulting centres of buoyancy and gravity for each iteration. The structure's draught is calculated to check if it is still in the desired range. The resultant value of $\overline{GM}$ is combined with the total displacement and a small inclination of 5.0° to calculate the structure's restoring moment M_S. When the restoring moment is equal to the external overturning moment by wind the iteration stops and final values are saved.

The last step is to check the upscaled structure for intact stability in installation configuration, when the structure behaves more like a semi-submersible, as depicted in Figure 3.2 on the left. The distance between keel and floater is diminished and the keel is de-ballasted to neutral buoyancy. Then a new floater draught is calculated based on the de-ballasted structural weight, and the value for metacentric height is computed for this configuration. In contrast tothe spar configuration, the water plane area moment of inertia will have a significant contribution to the stabilit, as indicated in Figure 3.4. When the value of $\overline{GM}$ is positive for this installation stability the algorithm stops and the upscaled concept design is saved.

A flowchart of the process and algorithm described above for the upscaling of the TetraSpar is presented in Figure 3.5. The calculation method is based on analytic equations for hydrostatic stability, developed in Matlab, and the results are compared to stability calculations for the 3.6 MW demonstrator design by an external engineering consultancy.

3.4. Analysis and evaluation

The resulting upscaled TetraSpar design concepts are summarised in Table 3.1. These results follow the methodology as described in Figure 3.5, the upscaling guidelines of Appendix A, a keel depth of 65 m, and a maximum inclination by wind overturning moment of 5.0°.

The first thing to note of these results is the relative change between the wind overturning moment and the resultant structural mass. The amount of mass required to stabilise the increased wind overturning moment decreases comparatively towards larger power ratings, i.e. the ratio of mass over overturning moment $m_{structure}/M_{O,wind}$ is more favourable for the larger floating wind support structures. Similar trends are identified for the steel mass of the substructure, where the amount of steel required decreases relatively to the increase in overturning moment.

Table 3.1: Properties of upscaled TetraSpar design concepts based on the methodology for overturning moment by wind, with a keep draught of 65 m and a maximum static inclination by wind of 5.0°.

Power rating		MW	10	15	20
$F_{T,max}$		N	1.3×10^6	2.0×10^6	2.6×10^6
$M_{O,wind}$		Nm	1.6×10^8	2.8×10^8	4.2×10^8
$m_{structure}$		kg	1.8×10^7	3.0×10^7	4.2×10^7
$\overline{GM}$ operations		m	11.5	11.7	12.4
$\overline{GM}$ installation		m	19.7	11.2	7.1
Substructure steel mass		kg	5.1×10^6	8.6×10^6	1.2×10^7
Floater steel mass		kg	3.1×10^6	5.2×10^6	7.2×10^6
Keel mass ballasted		kg	1.3×10^7	2.3×10^7	3.2×10^7
	centre column	m	8.0	10	12
	diagonal	m	4.0	5.0	6.0
Brace diameter	radial	m	5.9	7.8	9.2
	lateral	m	6.8	8.9	10.5
	keel	m	7.3	9.6	11.5

Second item is the values for metacentric height. There is a slight trend towards larger values of $\overline{GM}$ for larger substructures in operational configurations, meaning the rotational stability of the structure increases while a larger wind turbine is present. This is partially due to the increase of the water plane stability contribution $\overline{BM}$, which is neglected in the upscaling methodology for the TetraSpar. For the 3.6 MW demonstrator this value approximate 0.40 m. However for the 20 MW design concept, the value of $\overline{BM}$ increases to 0.82 m due to significant larger braces at the water line.

The effect of neglecting the $\overline{BM}$ factor that the upscaled structures have a metacentric height that is too high compared to the upscaling algorithm based on only centres of buoyancy and gravity to balance the overturning wind moment. The resulting upscaled structures with the value of $\overline{GM}$ tend to rotate slightly less than the 5.0° assumed at the beginning of the upscaling methodology.

On the topic of metacentric height, the $\overline{GM}$ value for the installation configuration decreases for larger substructures. While the 10 MW upscaled design concept still has a larger metacentric height for the installation configuration than in operations, which makes the semi-submersible configuration more stable the spar, the 20 MW concept design is less stable comparatively. Compared to a value of $\overline{GM} =$ 55 m for the 3.6 MW demonstrator, all upscaled designs are statically less stable as semi-submersible. An free body diagram of the TetraSpar in semi-submersible configuration, with indicative locations for locations of centre of gravity, centre of buoyancy and additional restoring moment by a large water plane area moment of inertia is presented in Figure 3.4.

This decrease in metacentric height largely due to the significant increased height of the centre of gravity during installation, wheras the floater's footprint and derived water plane area of inertia remain similar in magnitude. This relative decrease in static stability during the installation phases of the structure might pose the need for additional or temporary stability devices while the TetraSpar is constructed in port or during tow-out to site.

Similarities between the designs are found in the contributions of different features to the full structure. For all four designs, the payload of WTG and support tower are approximately 5% of the total mass, while the ballasted keel accounts up to about 75% of the structural mass. Similarly the substructure steel mass, that is the combined mass of all steel elements of floater and unballasted keel, account to roughly 25% of the total mass for four FOWTs.

The concept of self-similarity is valid for all upscaled designs, as the mass ratios to the structure's total mass are in general kept equal for all design concepts compared to the 3.6 MW demonstrator.

Lastly an evaluation on the resulting brace diameters. One criteria to the upscaling process is the limit to brace diameter; no brace may be larger than the tower base diameter. The thought is that TetraSpar's braces are constructed by the same production techniques as support towers, thus are bounded to the same (physical) limits of manufacturing. As the centre columns are equal in diameter to the tower base, and all other braces are smaller in diameter, this criteria is met for all upscaled designs

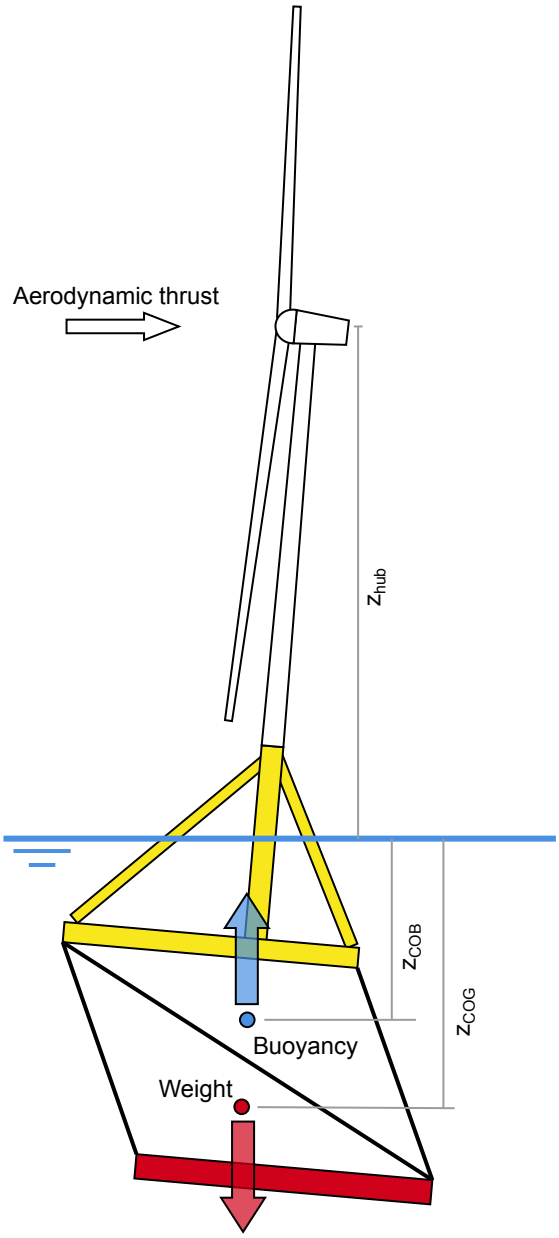

Figure 3.3: Free body diagram for hydrostatic analysis and upscaling of TetraSpar while in operational spar configuration.

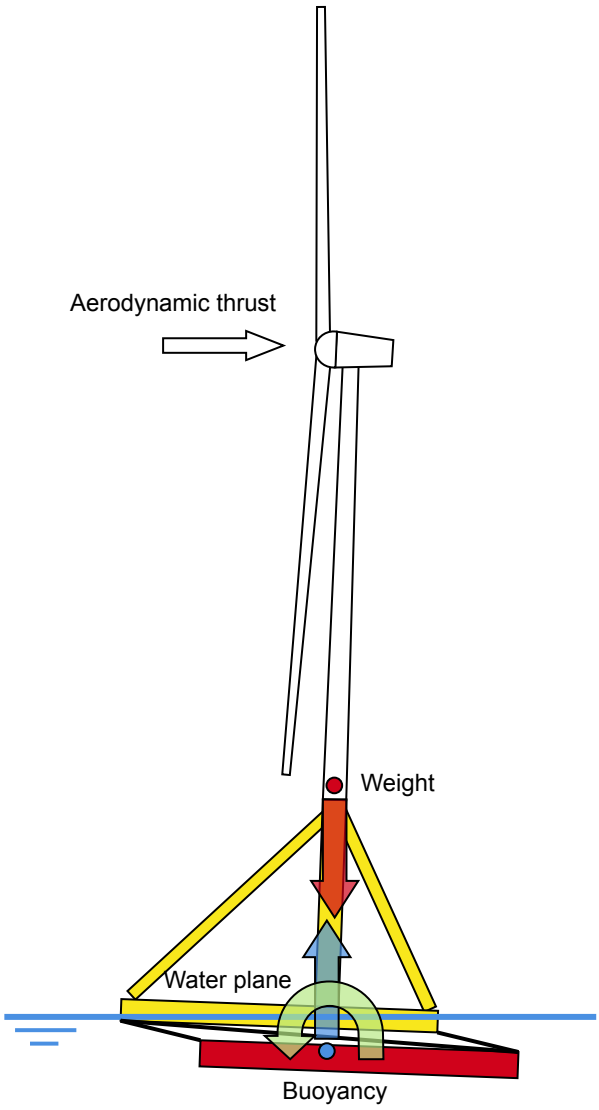

Figure 3.4: Indicative free body diagram of TetraSpar during installation configuration. Contrary to operational configuration as a spar, the contribution towards stability by the water plane is substantial.

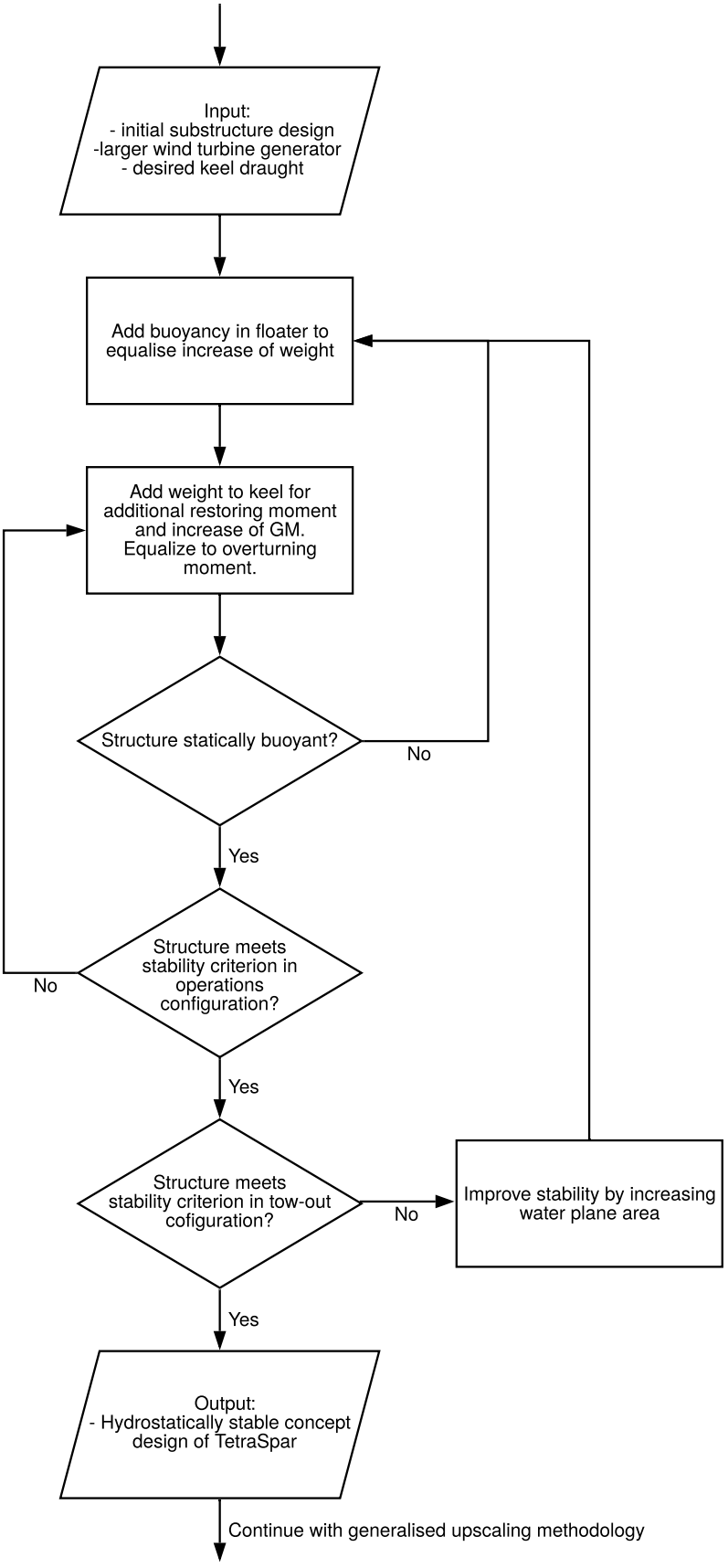

Figure 3.5: Flowchart for the upscaling algorithm of the TetraSpar based on wind overturning moment in a hydrostatic analysis.

4

Hydrodynamic analysis

Introduced in the first chapters of this thesis, it is made clear what the importance is to a FOWT to provide a stable dynamic platform. In contrast to bottom-fixed wind turbines, where all structure actions are transferred to the soil, floating wind foundations will experience more dynamic motions due to environmental forcing by wind, waves and currents. Because it is not feasible to design a passive floating structure that minimises all motions in all directions, the design of the floating platform should be such that it allows for some motions in all direction without endangering the integrity of the system.

This chapter explores the general dynamics of floating structures, then explains the action by and relevance of water waves onto the structure, and develops a frequency domain method to analyse the resulting upscaled structures from the hydrostatic analysis on the dynamic behaviour.

4.1. Dynamics of structures

Compared to the hydrostatic analysis of chapter 3, a dynamic problem involves an action that does vary with time. The result of a action varying in time is a response of the structure varying in time. According to Vugts (2013), the modelling process of the dynamics of a structure is divided into mass, damping and stiffness properties. From Newton's second law, the acceleration of a body with mass m in a general direction q is fully defined by the applied action of a excitation force $F_E(t)$, a restraining spring force $F_S = c \cdot q(t)$ and a damping force $F_D = b \cdot \dot{q}(t)$. Rearranged this leads to the main equation of dynamics:

$$F_E(t) = m \cdot \ddot{q}(t) + b \cdot \dot{q}(t) + c \cdot q(t) \tag{4.1}$$

A classical example to visualise this equation is by a single degree of freedom system of a body with mass m moving in direction of q, connected to a fixed base by a damper and a spring with parameters b and c respectively. The system is excited by a force which can usually be described is a sinusoidal form $F_E(t) = F_0 \cdot \cos \omega t$. This equation functions as the building block for all further derivations on the hydrodynamic analysis of upscaled floating structures.

For simplicity for this thesis, the floater system and its motions are assumed to be linear and of first order. This assumption allows for the superposition of the induced loads by hydrodynamics. Journée and Massie (2008) describe the two loads for superposition as:

- "The so-called hydromechanic forces and moments are induced by the harmonic oscillations of the rigid body, moving in the undisturbed surface of the fluid.
- The so-called wave exciting forces and moments are produced by waves coming in on the restrained body."

The hydromechanic forces will be discussed in subsection 4.1.1, along with other directly linked characteristics of floating structures. The second point on wave exciting is discussed in subsection 4.1.2.

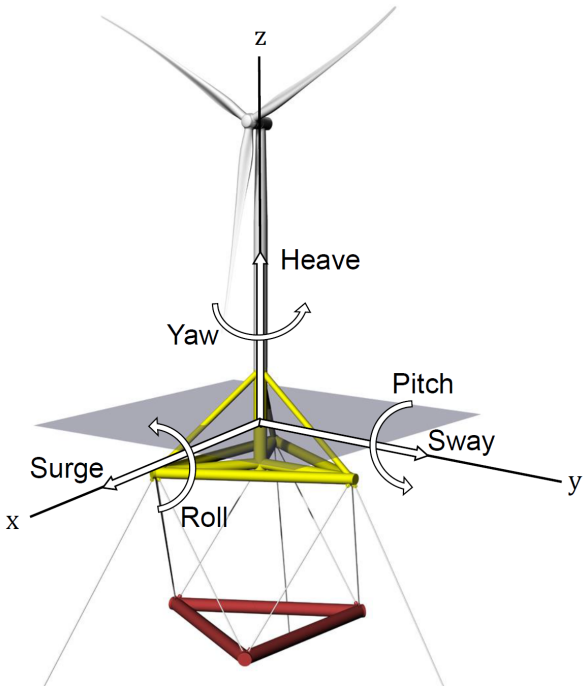

Figure 4.1: Convention of motion directions in translation and rotation for a floating structure.

4.1.1. Characteristics of floating structure dynamics

To further analyse the dynamics of a floating structure, first a few definitions have to be explained. Like any object in a three dimensional space, the motions of a rigid body has six degrees of freedom; three translations and three rotations. According to marine engineering convention these six degrees of freedom are defined as surge, sway and heave for translations along, and roll, pitch and yaw for rotations around the x-, y-, and z-axis respectively. This convention is depicted in Figure 4.1.

The dynamics of offshore structures are governed by actions of different external excitation forces and moments like wind, waves and currents, as well by body inertia and other characteristics of the structural design. For this chapter the induced motions due to waves are assumed to be the most important to the hydrodynamic response of offshore structures, forces by wind and currents are characterised by a longer period compared to waves. Furthermore, it is assumed that for extreme metocean conditions the wave action is the most dominant dynamic force compared to currents and winds.

Due to the harmonic nature of the external excitation forces, the structure's motions in displacement, and for time derivatives for velocity and acceleration, can be expressed as a harmonic function, assuming no relative phase angles:

$$\text{Displacement: } q_i(t) = q_i \cdot \cos(\omega t) \tag{4.2}$$

$$\text{Velocity: } \frac{\partial q_i(t)}{\partial t} = -\omega \cdot q_i \cdot \sin(\omega t) \tag{4.3}$$

$$\text{Acceleration: } \frac{\partial^2 q_i(t)}{\partial t^2} = -\omega^2 \cdot q_i \cdot \cos(\omega t) \tag{4.4}$$

For the rest of the thesis, the general directions of q_i are defined for the subscript $i = 1\ldots6$ according to the marine engineering conventions of surge, sway, heave, roll, pitch and yaw respectively.

Starting with the fundamental equation of motion of Equation 4.1, there are three parameters on the right side of the equation describing the system. The first to discuss is the mass term m. For conventional 'dry' structures this term is fairly straightforward defined as the mass or moment of inertia terms for an acceleration in translation or rotation respectively. In analysis for marine structures the mass term has to be expanded by a term of added mass or moment of inertia, denoted by the term a. Added mass is the result of the deflection of the surrounding fluid when the body accelerates through the fluid. This increases the total inertia of the system, hence the expansion of the mass term. As the mass of the

body is equal to the displacement and fluid density (from hydrostatics), the new mass term becomes $m = \rho\nabla + a$. The added mass term is correlated to the shape of the body, can be different for each direction of motion, and can be a function of motion's frequency.

The second term to consider is the wave damping term. The motions of a body are damped by the induced waves which withdraw and transport energy away from the body. This wave damping is proportional to the body velocity and expressed as the coefficient b. The main assumption for the wave damping coefficient is that the fluid surrounding the body is ideal (behaves as a potential flow). In real fluids there are other damping terms like skin friction and separation phenomena which are generally non-linear and relatively small for large marine structures (Journée and Massie, 2008). The damping term is highly influenced by the motion's frequency and dependent on the shape of the body.

The third term is the restoring coefficient c. For motions in the direction of heave, roll or pitch, the hydrostatic restoring forces as described in chapter 3 provide a counteracting force proportional to the additional displacement in that direction. For most floating structures the hydrostatic restoring coefficient is a function of the water plane area, as it can be assumed that for small changes in either heave, roll or pitch the water plane area remains equal to the rest position. An expression for c in heave direction therefore becomes $c = \rho g A_w$.

Restoring coefficients in the horizontal plane of surge, sway and yaw cannot be generated through hydrostatic restoring forces, as there is no change in displacement when a body is forced in one of these directions. Restoring forces in the horizontal plane should come from a mooring system, and a resulting mooring system stiffness coefficient. In general, the design and development for a feasible mooring system for FOWTs deserves a complete topic on its own. For this hydrodynamic analysis of upscaled FOWTs only free floating structures are considered.

Another important characteristic of the motions of a floating structure in waves is the concept of coupled motions. A motion in one direction may have an induced motion into another direction. Journée and Massie (2008) distinguish two sets of coupled equations of motions for an object with one plane of symmetry. Symmetric coupled motions are composed of surge, heave and pitch, whereas antisymmetric couples motions are in the directions of sway, roll and yaw.

The implication of these couples motions is that an external force acting in direction i may result in movement of the structure in direction j. For each hydrodynamic and hydrostatic parameters discussed earlier, a six-by-six matrix has to be defined to include these coupled motions. The resulting equation of motion for a general direction of j becomes:

$$\sum_{j=1}^{6} \left(m_{i,j} + a_{i,j}(\omega)\right) \ddot{q}_j(\omega, t) + b_{i,j}(\omega)\dot{q}_j(\omega, t) + c_{i,j} q_j = F_i \cdot \cos(\omega t) \tag{4.5}$$

4.1.2. Surface wave exciting forces

Wind induced surface waves are the main topic on the hydrodynamic analysis of upscaled FOWTs. Water particles in waves describe a orbital trajectory as seen in Figure 4.2. It is this orbital motion of the water particles that dynamically interact with a marine structure, and induces the external exciting loads to the floating platform. The water particle kinematics are influenced mainly influenced by the factors wave elevation, water depth and wave period.

Starting with describing the water surface as regular and linear waves, also known as Airy waves, the elevation of a 2D water surface can be expressed as a harmonic function:

$$\eta = \eta_a \cos(kx - \omega t) \tag{4.6}$$

Here the wave amplitude is defined as η_a, wave number as $k = 2\pi/\lambda$ and $\omega = 2\pi/T$ for wave frequency. When waves are not too steep, the harmonic displacements, velocities and accelerations, and harmonic pressure terms are in a linear relation to the wave elevation, an expression for a wave velocity potential potential Φ_w can be derived for any depth of h, given the total water depth of d (Journée and Massie, 2008). A velocity potential of a flow is defined as the when spacial derivative of the potential in the flow equals the velocity of the flow at that point.

$$\Phi_w = \frac{\eta_a g}{\omega} \cdot \frac{\cosh k(d+z)}{\cosh kd} \cdot \sin(kx - \omega t) \tag{4.7}$$

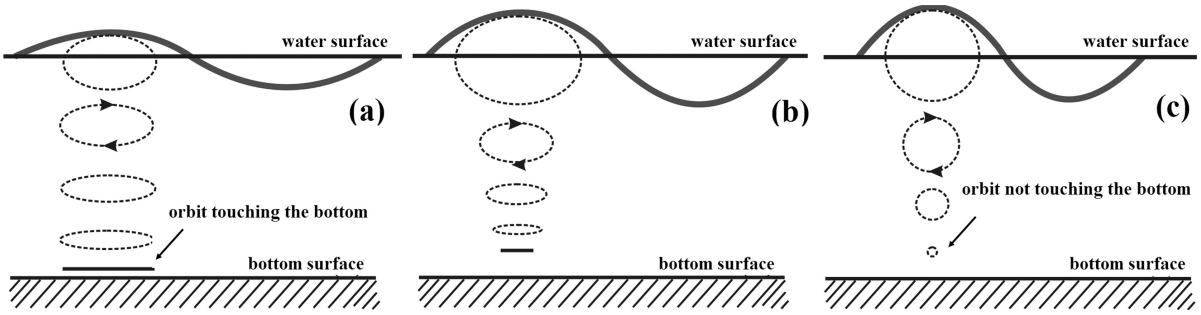

Figure 4.2: Orbital trajectories of water particles in shallow water $d < \lambda/20$ (a), intermediate water depths (b), and deep water $d > \lambda/2$ (c), adapted from Dean and Dalrymple (1991).

Combining this velocity potential and the dispersion relation of $\omega^2 = kg \cdot \tanh kd$, the resulting water particle kinematics for horizontal and vertical velocities and accelerations are derived as:

$$v_x = \frac{\partial \Phi_w}{\partial x} = \eta_a \cdot \omega \cdot \frac{\cosh k(d+z)}{\cosh kd} \cdot \cos(kx - \omega t) \tag{4.8}$$

$$v_z = \frac{\partial \Phi_w}{\partial z} = \eta_a \cdot \omega \cdot \frac{\sinh k(d+z)}{\cosh kd} \cdot \sin(kx - \omega t) \tag{4.9}$$

$$\dot{v}_x = \frac{\partial}{\partial t}\frac{\partial \Phi_w}{\partial x} = \eta_a \cdot \omega^2 \cdot \frac{\cosh k(d+z)}{\sinh kh} \cdot \sin(kx - \omega t) \tag{4.10}$$

$$\dot{v}_z = \frac{\partial}{\partial t}\frac{\partial \Phi_w}{\partial z} = -\eta_a \cdot \omega^2 \cdot \frac{\sinh k(d+z)}{\sinh kd} \cdot \cos(kx - \omega t) \tag{4.11}$$

With these expressions for wave velocity and accelerations the acting force onto a body can be calculated, for example by the equation by Morison et al. (1950) for slender cylinders.

Another way to prescribe the wave force through the wave potential is by the induced pressure of an incoming wave onto a surface of the body. From the linearised Bernoulli equation $\frac{\partial \Phi_w}{\partial t} + \frac{p}{\rho} + gz = 0$, the pressure can be calculated as:

$$p = -\rho g z + \rho g \eta_a \frac{\cosh k(d+z)}{\cosh kd} \cdot \cos(kx - \omega t) \tag{4.12}$$

The forces and moments acting onto the body are then a result that follow from an integration of the pressure over the submerged surface of S:

$$\vec{F} = -\iint_S (p \cdot \vec{n})\, dS \tag{4.13}$$

$$\vec{M} = -\iint_S p\ (\vec{r} \times \vec{n})\, dS \tag{4.14}$$

Here $\vec{n}$ indicates the normal vector of the surface outwards and $\vec{r}$ the position vector of the surface to the point of reference. These last terms for force and moment are the so-called Froude-Krilov forces and are a result of an undisturbed incoming wave.

4.2. Analytic approximation

Given the relative coarse, low-fidelity design concepts generated through the upscaling methodology, and the significant number of unknown factors in the offshore climate, some analytic approximations are made to create a simplified environment to which the upscaled TetraSpar design concepts are evaluated. First the idea of irregular waves and wave spectra based on the theory of linear, regular waves explained earlier, and the assumption of deep water.

4.2.1. Irregular waves

In subsection 4.1.2 the wave and resulting forces are described by a single regular wave with a harmonic component for the wave elevation. However in real life, the sea surface is not made up of regular

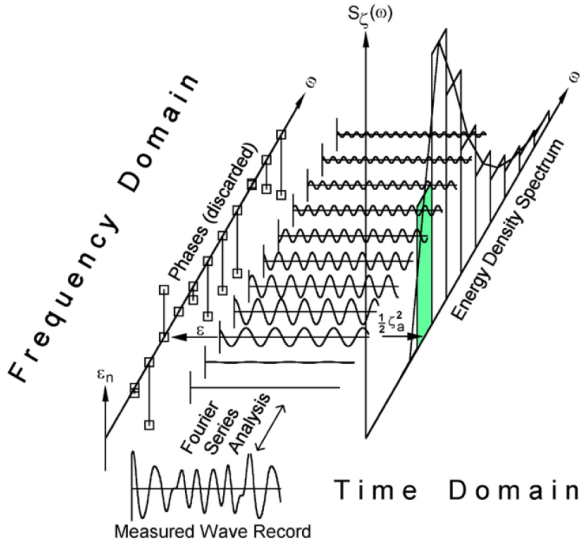

Figure 4.3: Wave record analysis and wave spectrum, by Journée and Massie (2008).

sinusoidal waves with one wave height and one wave period. The sea appears to be a highly erratic and random surface, composed of many different waves travelling in all directions. One way to simplify and approximate this random nature of waves is through wave spectra.

The surface of a sea, especially for wind driven waves, can be expressed as a superposition of many regular waves, all with their own amplitude, length, period and direction. The resulting surface elevation is the sum of all individual wave components, and appears to be erratic and irregular in nature, just like a real sea surface. Through statistics the random surface elevation η_{a_n} per wave period ω_n is captured in an energy density spectrum by:

$$S_\eta(\omega_n) \cdot d\omega = \frac{1}{2}\eta_{a_n}^2 \tag{4.15}$$

To accurately describe a 'real' sea surface, in-situ wave measurements have to be performed. The recorded wave record then is decomposed into a large number of regular sinusoidal waves in superposition, and captured as an energy density spectrum. This process is presented Figure 4.3. Wave energy density spectra are bounded to a location, as the long term wave records that are used to generate a spectrum are highly influenced by the local sea climate.

One well-known wave spectrum is the JONSWAP spectrum by Hasselmann et al. (1973), based on measurements in the North Sea and is described by wind velocity and fetch as input variables. For the case-study in the Metcentre site in the South-West of Norway , the JONSWAP spectrum provides a reasonable representation of the wave climate. A JONSWAP spectrum is expressed by:

$$S_J(\omega) = \frac{\alpha g^2}{\omega^5} \exp\left[-\frac{4}{5}\left(\frac{\omega_p}{\omega}\right)^4\right]\gamma^r \tag{4.16}$$

$$r = \exp\left[-\frac{(\omega-\omega_p)^2}{2\sigma^2\omega_p^2}\right] \qquad \alpha = 0.076\left(\frac{U_{10}^2}{Fg}\right)^{0.22}$$

$$\omega_p = 22\left(\frac{g^2}{U_{10}F}\right)^{1/3} \qquad \gamma = 3.3$$

$$\sigma = \begin{cases} 0.07 & \omega \le \omega_p \\ 0.09 & \omega > \omega_p \end{cases}$$

The resulting spectrum is used to estimate a significant wave height by $H_s = 4\sqrt{m_0}$, a peak spectral period T_p and a maximum wave height $H_{max} \approx 1.86 \cdot H_s$.

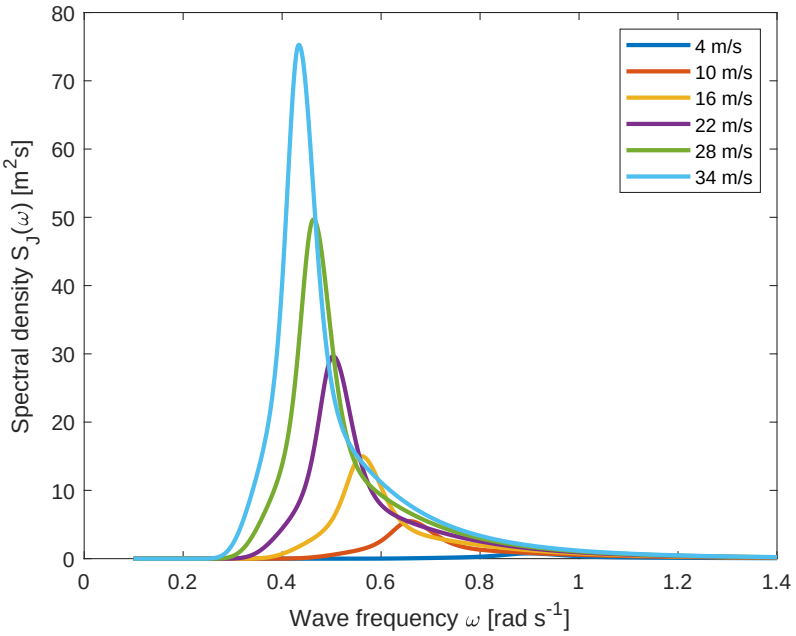

Figure 4.4: JONSWAP spectra for a range of U_{10} wind speeds with a fetch of 400 km.

Table 4.1: Approximated wave conditions by JONSWAP for the Metcentre site.

U_{10}	m s^{-1}	1.0	4.0	7.0	10	13	16	19	22	25	28	31	34
T_p	s	4.4	7.0	8.5	9.5	10.5	11.2	11.9	12.6	13.1	13.7	14.0	14.6
H_s	m	0.5	1.9	3.1	4.3	5.4	6.6	7.7	8.8	9.9	10.9	11.9	13.0
H_{max}	m	0.9	3.5	5.8	8.0	10.1	12.2	14.3	16.3	18.3	20.3	22.2	24.2

Next is to generate spectra that resembles the wind-wave climate of the Norway Metcentre, using the input parameters wind speed and fetch for a JONSWAP spectrum. Starting with the data in Table 2.3 by Onstad et al. (2016) and converting to a U_{10} wind speed by a wind profile power law of $U_z = U_r \left(\frac{z}{z_r}\right)^{0.11}$, a value U_{10} of 34 m s^{-1} is found for a 50-year return period. This wind speed is then used in Equation 4.16 to find a fetch F that resembles the corresponding significant wave height for a 50-year return period. Through an iterative approach, a fetch F of 400 km is found that results a comparable wind-wave climate to the Metcentre site. The last step is to calculate JONSWAP spectra for a range of wind velocities, and resulting wave heights and wave periods. The spectra are plotted in Figure 4.4, the wave conditions are found in Table 4.1.

The JONSWAP wave climate approximations are then applied to define a metocean design condition corresponding to a rated wind speed of wind turbine generators of 11 m s^{-1} at hub height for maximum rotor thrust and wind overturning moment. A value of $U_{10} \approx 8.0$ m s^{-1} is used to account for a lower wind speed at 10 m elevation compared to wind velocities at hub elevation. Combined with a fetch of 400 km, the peak wave period is 9.0 s, a significant wave height of 3.4 m and a maximum wave height of 6.4 m.

4.2.2. Deep water approximation

To simplify the equations for velocity potential (Equation 4.7) and all subsequent derivatives, it is assumed that the encountered waves at the Metcentre site behave as if there is no sea bed influencing the water particle behaviour, an assumption for deep water is made. This assumption is tested by estimating the maximum wave length and wave period at a water depth of 220 m for which deep water

may be assumed, i.e. local water depth equals to halved wave length:

$$d = \frac{1}{2}\lambda, \quad \lambda = \frac{2\pi}{k} \tag{4.17}$$

$$220\,\text{m} = \frac{\pi}{k}, \quad k = \frac{\pi}{220} = 0.0143\,\text{rad}\,\text{m}^{-1} \tag{4.18}$$

$$\omega^2 = kg\tanh kd, \quad \text{Assume } \tanh kd = 1 \text{ for deep water} \tag{4.19}$$

$$\omega = \sqrt{0.0143 \cdot g} = 0.375\,\text{rad}\,\text{s}^{-1}, \quad T = 16.8\,\text{s} \tag{4.20}$$

The wave period for which a deep water approximation is valid, is longer than the estimated peak wave periods obtained by the JONSWAP spectra of Figure 4.4 and Table 4.1. At the highest wind speeds there will be waves with a longer wave period than the limit for deep water approximation. However these waves carry significantly less energy than at peak wave periods, and the effects of this discrepancy are assumed to be negligible for further analysis.

By assuming deep water waves, the hyperbolic terms of the velocity potential Φ_w of Equation 4.7 and its derivatives for velocity, acceleration and pressure are reduced to e^{kz} terms.

4.3. WAMIT modelling

Given the complexity of modelling the dynamic behaviour of floating structures in waves, a numerical analysis is required for all structures except for the most basic designs. For this thesis the modelling of first-order dynamic behaviour of (upscaled) TetraSpar design concepts are performed using WAMIT. First developed in 1987, WaveAnalysisMIT “is a panel program designed to solve the boundary-value problem for interaction of water waves with prescribed bodies in finite- and infinite water depth” (Lee, 1995). The panel method is also known as bounded element method, as each panel describes a element bounded by the edged for which equations are solved.

WAMIT evaluates the hydrodynamic and hydrostatic coefficients of added mass, radiation damping and restoring stiffness, wave exciting forces and moments, RAOs, hydrodynamic pressures and fluid velocities and other quantities. Analysis starts with a prescribed 3D model of the structure, of which its surface is divided into a panel mesh. Then for each panel, WAMIT calculates the total pressure acting on the centre of each panel by Equation 4.12 based on the total velocity potential. The resulting pressure for each panel is integrated over the surface of the panel, to calculate the resulting force and moment by equations 4.13 and 4.14. The key concept for WAMIT is the total velocity potential at the body surface ϕ, given by:

$$\phi = \phi_W + \phi_S + \phi_R = \phi_D + \phi_R \tag{4.21}$$

The total velocity potential at the body surface is the sum of three velocity potential terms, first being velocity potential of the undisturbed incident wave ϕ_W, given by Equation 4.7. The second term is the scattering wave velocity potential ϕ_S, due to the interaction between the incoming wave and the body at at fixed position. The radiation velocity potential ϕ_R is the result of motions of the body itself in still water, which result to waves radiating outwards from the body. The superposition of these three terms is equal to the superposition identified in section 4.1. Often this method is called the diffraction/radiation problem of wave-structure interaction, as the incident and scattering velocity potentials are combined as the diffraction velocity potential ϕ_D. Figure 4.5 depicts the diffraction/radiation problem solved by WAMIT and other bounded element method applications.

These potentials are then solved by boundary conditions at the surface of the body. The velocity of a water particle at the surface of the body is equal to the velocity of the body itself, to ensure a watertight body. For the diffraction potential ϕ_D with fixed body the fluid velocity at the body surface is equal to zero, for the radiation potential the particle velocity at the surface is equal to the velocity of the body.

WAMIT requires as input a mesh of many quadrilateral panels of a 3D body, generated by a computer-aided design (CAD) application. The radiation and diffraction potentials are calculated as a constant value over the whole panel, and integrated over the panel to evaluate the aforementioned hydrodynamic quantities. The panel method requires a body to be discretised into flat, four-sided elements. A finer mesh with more panels might yield better results, as it described the body surface with greater detail. However this does come at the costs of a longer computational time, as the number of equations to be solved increases as well. More on computation time and other considerations on the usage of WAMIT in combination with MultiSurf for the TetraSpar case-study is presented in Appendix B.

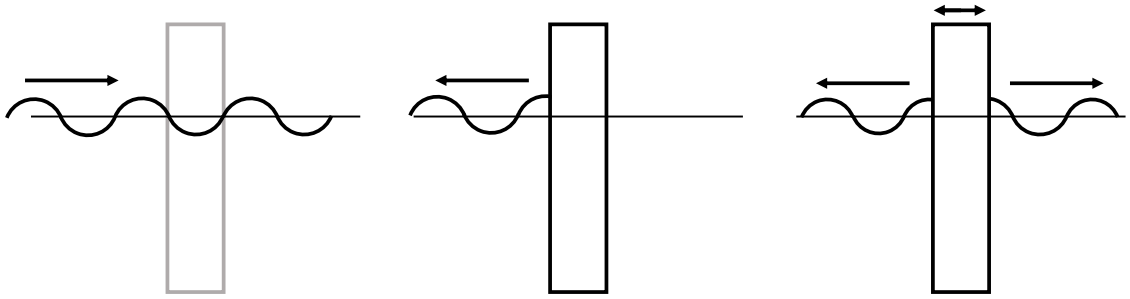

Figure 4.5: Visualisation of total velocity potential ϕ solved in WAMIT. Left an undisturbed incident wave ϕ_W, mid the scattered velocity potential ϕ_S due a disturbed wave by the fixed body, and right the ϕ_R radiation potential as a result of the body's own motions in still water.

WAMIT is a commonly used numeric application in offshore research and industry. One reason WAMIT has been chosen for the numeric modelling of the dynamics of the TetraSpar design concepts is the relative efficiency in computational time. WAMIT computes the output quantities in frequency-domain as function of wave period. Combined with parametric 3D CAD modelling in MultiSurf, TetraSpar panel models and WAMIT are computed in a relatively short amount of time for a large range of wave frequencies, when compared to time-domain modelling like OrcaFlex. This makes WAMIT a suitable tool for assessing initial design concepts and screen for any potential issues early on. For more detailed analyses on the motions and loadings of structures in waves, wind and currents, a time-domain solver is more suitable.

A bounded element method solver is also more effective for studying upscaled marine structure compared to solvers based on the Morison equation. The 3.6 MW TetraSpar demonstrator consists of many slender cylindrical elements. During the development of the demonstrator, much of the hydrodynamic analysis was based on the Morison equation, a semi-empirical equation that describes the force by a fluid acting onto a slender cylinder per length unit as (Morison et al., 1950):

$$dF(t) = C_m \cdot \rho \cdot \frac{\pi}{4} \cdot D^2 \cdot \dot{v}(t) + C_d \cdot \frac{1}{2} \cdot \rho \cdot D \cdot v(t) \cdot |v(t)| \tag{4.22}$$

As said, this equation is a decent approximation for hydrodynamic action on a slender cylinder. The definition of a slender cylinder in context of this equation, is that the cylinder diameter is small relative to the wave length. Journée and Massie (2008) advice a limit to Morison equation up to approximate $D < \frac{1}{10}\lambda$. For diameters larger than this ratio, other phenomena like diffraction start to play a more important role.

As the cylinders of the upscaled TetraSpar design concepts increase in diameter to hold enough weight or buoyancy, the Morison equation might lose its validity for the largest cylinders. Thus a diffraction/radiation solver like WAMIT provides a more robust modelling alternative for structures with increasing diameters than Morison equation based models.

Results computed by WAMIT for the diffraction/radiation problem are based on linear, first order Airy waves. Many of the output values by WAMIT are expressed per wave amplitude. This makes WAMIT a suitable and flexible tool to assess the hydrodynamic performance of structures in waves. When a combination of wave exciting periods and corresponding wave heights are known, similar to data presented in Table 4.1, the first order linear forcing and responses can be calculated with relative ease.

Other reasons for choosing WAMIT over other software packages are the available experience within the organisation, and due to software licensing. Alternatives to WAMIT for panel method numeric modelling are commercial options like WADAM by DNV GL and Aqwa by ANSYS, and the open source code program NEMOH.

4.4. Hydrodynamics of the TetraSpar

After the hydrostatic analysis and upscaling based on overturning moment, the resultant floating foundations are evaluated on the hydrodynamic behaviour by wave-structure interaction. Three topics are

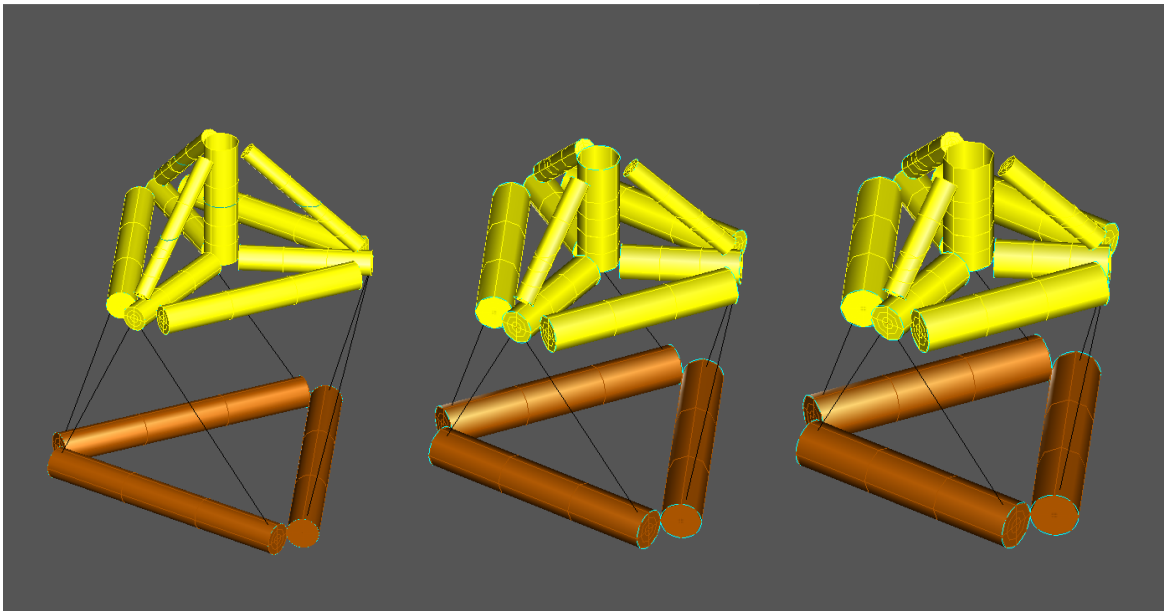

Figure 4.6: MultiSurf CAD models of upscaled TetraSpar design concepts, left 10 MW, middle 15 MW and right 20 MW, as used for WAMIT panel method computations.

evaluated through WAMIT, namely the hydrodynamic coefficients, wave exciting forces and response amplitude operators (RAOs).

Before diving into the dynamics of upscaled TetraSpar substructures, first a number of principles are explained. First of all, the entire structure acts as one rigid body. The floater and keel are connected through the suspension lines as if there is no relative motion between the two bodies.

The study by Pereyra (2018) argues that for TetraSpars fitted with high stiffened suspension lines, in the arrangement of six lines, combined with maximum floater rotations in horizontal plan well below any static heel limit (see Appendix A for definition of static heel limit), the combination of floater and keel is sufficiently stiff that it acts as a single rigid body. From a hydrostatic stability perspective, the keel and floater must act as a rigid body; if the keel may move freely from the floater, the centre of gravity of the floater and payload will no longer be below the centre of buoyancy, and the TetraSpar may lose its spar stability mechanism.

Secondly, the dynamic analysis will only concern wave-structure interaction and loads. Currents are not included, as it is assumed that currents induce loads on a time scale much longer than waves. Furthermore, wind and aerodynamic drag and damping are also omitted. WAMIT is only suitable to calculate hydromechanic and wave loads up to still water level. For a detailed model of upscaled TetraSpars, intricate descriptions of functioning WTGs are required, included wind-superstructure interaction. Other applications than WAMIT are more suitable for these coupled aero-hydro-servo-elastic models, but take significantly more time and effort to accurately implement.

Thirdly, the dynamics of the upscaled TetraSpar design concepts are only evaluated for operational configuration, that is with the keel suspended far below the floater, and the structure is completely ballasted for the still water line to be half way of the centre column. Experience from the 3.6 MW demonstrator shows that the dynamic behaviour of the semi-submersible installation configuration is completely different to the spar configuration which requires a lot of testing and fine tuning to accurately describe the structure as a semi-submersible. The study by Villaespesa et al. (2018) provides an in depth approach and analysis of an older design of the TetraSpar for installation and tow conditions.

Lastly, the dynamics of upscaled floating foundations are analysed without a mooring system, i.e. a free floating structure. The design and development of a functioning and optimised mooring system for each upscaled structure requires a lot of effort, knowledge and many iterations, and it deserves a thesis topic on its own. Given that the mooring system primarily affects the horizontal motions (surge, sway and yaw), the results by WAMIT for these directions are not considered further. For the free floating upscaled TetraSpars, the motions and responses in heave, pitch and roll directions by WAMIT are considerd to be representative and are considered in detail.

3D panel models are generated through MultiSurf based on the resulting dimensions by hydrostatic upscaling, see Figure 4.6 for the 10 MW, 15 MW and 20 MW model renders.

The 3D CAD designs are truncated at the still water line, as WAMIT only evaluates the mean submerged volume of the floating structures. For simplicity and management of resources, the floating wind platforms are evaluated for one wave direction travelling in negative x-direction, for a range of wave periods between 0 s to 60 s. Due to the axis-symmetric design of the TetraSpar, each 60° rotation of wave heading delivers similar results. Expectations are that the wave exciting forces in between the 60° intervals will not deviate significantly.

4.4.1. Hydrodynamic coefficients

The upscaled TetraSpar WAMIT models are evaluated on the hydrodynamic coefficients for added mass $a_{i,j}(\omega)$ and radiation damping $b_{i,j}(\omega)$, and hydrostatic coefficients $c_{i,j}$ as described in Equation 4.1. These hydrodynamic coefficients are obtained as square and symmetric matrices with dimensions equal to the number of degrees of freedom, calculated per wave frequency ω.

The values for added mass are compared to analytic approximations by simplified hand calculations, to check if the results by WAMIT and hand calculations are within the same order of magnitude. According to Haslum (2000), the approximations for added mass for a cylinder in radial or axial directions are:

$$\begin{aligned} a_{radial} &= \rho \cdot \pi \cdot \frac{D^2}{4} \cdot L \\ a_{axial} &= \frac{2}{3} \cdot \rho \cdot \pi \cdot \frac{D^3}{8} \end{aligned} \tag{4.23}$$

For the analytic approximation of added mass, the TetraSpar substructures are resembled as a sum of independent cylinders. To account for the different orientations and projections of the braces in in x-, y-, and z-direction, goniometric relations are added to length L for added mass terms in radial direction. The approximated added mass terms are assumed to be independent of wave frequency.

No radiation damping coefficients are approximated by the simplified hand calculations. These coefficients are highly dependent on wave frequency, and cannot be approximated for a linear system (Haslum, 2000).

Hydrostatic coefficients estimated by WAMIT are those restoring coefficients by the water plane, i.e. for vertical directions in heave, pitch and roll. WAMIT computes the area (moment of inertia) described by structure elements piercing the water line, and combines these in a hydrostatic, frequency independent stiffness matrix. These values for hydrostatic restoring coefficients can be used to cross check with analytic hand calculations.

4.4.2. Wave exciting loads

Wave exciting forces and moments are calculated in WAMIT in two ways. First is the straight forward, direction integration of the diffraction velocity potential ϕ_D of hydrodynamic pressure on each panel:

$$F_j = -i \cdot \omega \cdot \rho \iint_S n_j \cdot \phi_D \, dS \tag{4.24}$$

The second manner is through the so-called Haskind relations, which is defined as:

$$F_j = -i \cdot \omega \cdot \rho \iint_S \left(n_j \cdot \phi_W - \phi_{R,j} \cdot \frac{\partial \phi_W}{\partial n_j} \right) dS \tag{4.25}$$

Which is a relation between the incoming wave field ϕ_W and the radation potentials of ϕ_R in j direction. For the analysis of the (upscaled) structures, both methodologies will be employed to investigate the validity of the WAMIT results. If both integrators deliver similar results without too much deviation, it is assumed that the exciting loads by waves are representative. No further research is conducted on these equations.

4.4.3. Response amplitude operators

Key item used to describe the hydrodynamic behaviour of the floating structures are the response amplitude operators (RAOs). These transfer functions are generated through the aforementioned WAMIT

output parameters, and describe a motion, velocity or acceleration of the structure in a direction as function of wave frequency, per wave period. Starting from Equation 4.1, a RAO is described by:

$$RAO(\omega) = \frac{q_j}{\eta_a}(\omega) = \frac{F_j}{-(M + A(\omega))\omega^2 + iB(\omega)\omega + C} \tag{4.26}$$

Here, q_j is a generalised direction, rewritten as $q_j = q_j \cdot e^{i\omega t}$ and A, B, C and M are the full matrices for added mass, damping, restoring and mass. As the load F_j is a result of a linear, regular wave, the term is direction proportional to the wave amplitude. Hence a RAO is a linear transfer function between a motion and wave amplitude, given a predefined wave frequency.

Another useful feature of RAOs is in conjunction with irregular waves. When the RAO and a wave climate spectrum S_W (like a JONSWAP in Figure 4.4) are known, the two statistics are combined to generate a structure response spectrum by:

$$S_q(\omega) = |RAO_q(\omega)|^2 \cdot S_W(\omega) \tag{4.27}$$

4.4.4. WAMIT model validation

The WAMIT modelling has been carried out for a single direction wave train in surge direction, for wave exciting periods between 0 s to 60 s with an interval of 0.5 s. Even though waves at the Norway Metcentre are expected to have periods up to 20 s, the evaluation range up to 60 s is chosen to evaluate the natural periods of the upscaled design concepts.

All results of this section are based on WAMIT models with 1680 panels, evaluated up to the still water line. Appendix B describes in more detail why these panel models are sufficiently adequate for the evaluation of the upscaled design concepts.

The hydrodynamic coefficients of added mass $a_{i,j}(\omega)$ and radiation damping $b_{i,j}(\omega)$. In Figure 4.7 the values of added mass and radiation damping in surge, sway and heave, due to a motion in these respective directions are presented. The dashed lines indicate the approximated values for added mass by the analytic equations of Equation 4.23.

Evaluating the results for added mass and radiation damping, the thee upscaled design concepts show similar behaviour over the full wave period range, with an almost linear relation between the three models in maximum values. Until a wave period of about 7 s, numeric errors within the WAMIT models dominate the output, especially for radiation damping.

As expected, the results for added mass and damping in the horizontal directions of surge and sway are exactly the same. The projected area of the TetraSpar structures in these directions are equal to each other, which shows in the resulting hydrodynamic coefficients.

A check for the validity of the WAMIT hydrodynamic coefficients is by comparing the results to the analytic approximation values. While the approximated constant values of added mass are either overestimated for surge and sway directions, or underestimated for heave, the relative differences are at a constant offset. In horizontal directions the WAMIT computed added mass values are approximately 25% lower than analytic values, and for vertical direction 12% higher. Even though not perfect, the simplified analytic equations for added mass of Equation 4.23 seem to approximate the tetrahedral substructure of the TetraSpar rather well.

4.5. Results and evaluation TetraSpar wave-structure interaction

The following section continuous on the WAMIT analysis and results, after the models are assessed in previous sections and Appendix B. The results focus on motions and accelerations by waves in surge direction, therefore only the platform motions in surge, heave and pitch are presented. First are the linear and first-order wave action, followed by the response amplitude operators for the upscaled design concepts. To conclude this chapter the results by WAMIT are discussed and evaluated in detail.

4.5.1. Surge, heave and pitch wave action

Next is the linear first order wave action in the symmetric coupled motions of surge, heave and pitch. An overview of the wave exciting forces per wave amplitude are presented in Figure 4.8. All three models show an similar pattern over the full range of wave periods, and both methods by WAMIT to calculate the wave exciting force give comparable results with little differences. In Table 4.2 an overview of wave

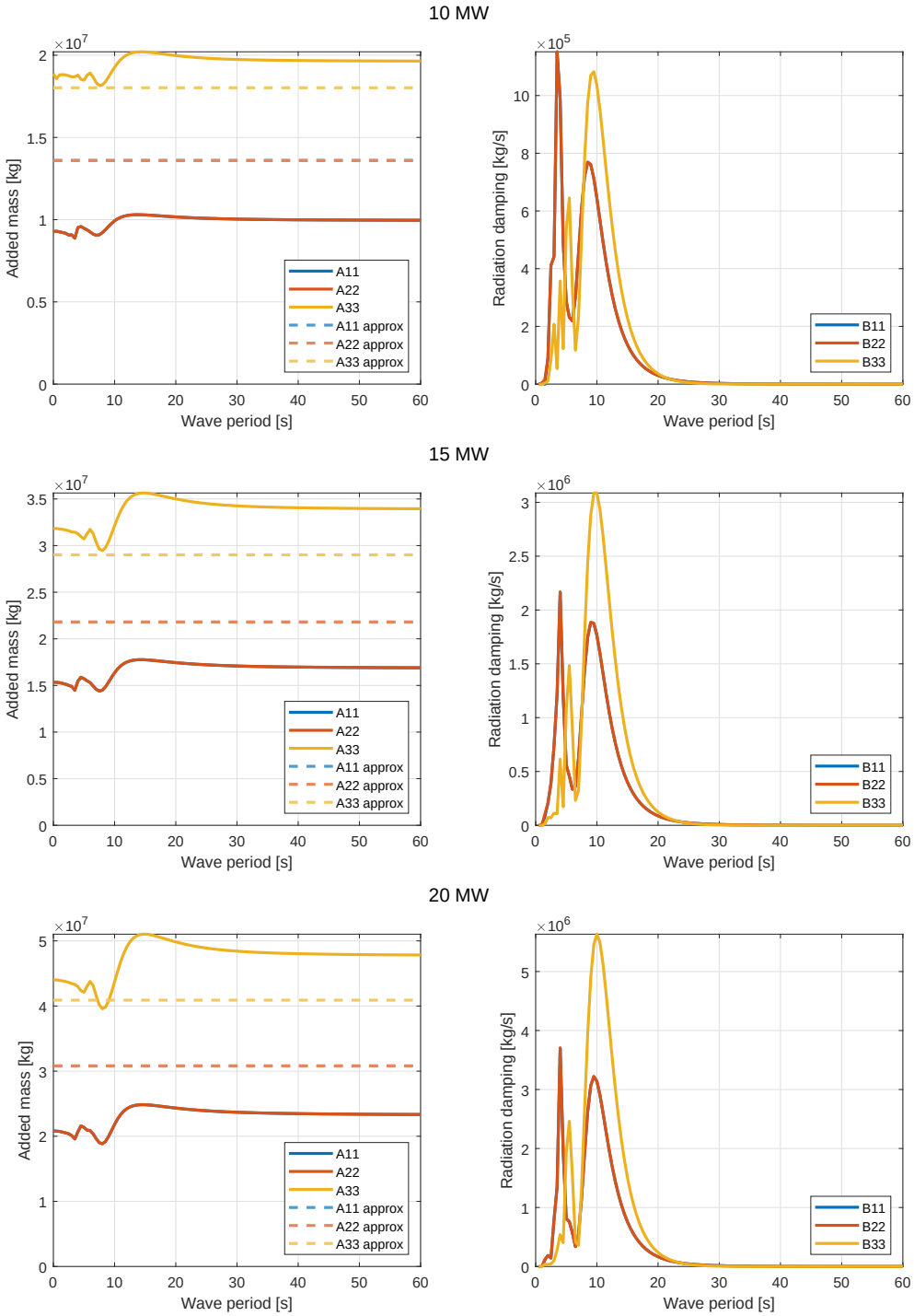

Figure 4.7: Added mass and radiation damping terms for upscaled TetraSpar design concepts.

Table 4.2: Overview of wave loads by WAMIT at design metocean conditions of T_p = 9.0 s, H_{max} = 6.4 m.

Power rating	MW	10	15	20
Surge force over η	N m^{-1}	3.1×10^6	4.7×10^6	7.3×10^6
Heave force over η	N m^{-1}	2.5×10^6	4.2×10^6	5.4×10^6
Pitch moment over η	N m m^{-1}	9.6×10^7	1.8×10^8	2.5×10^8
Surge force H_{max}	N	8.9×10^6	1.5×10^7	2.3×10^7
Heave force H_{max}	N	8.2×10^6	1.3×10^7	1.7×10^7
Pitch moment H_{max}	N m	2.9×10^8	4.1×10^8	5.5×10^8

Table 4.3: Overview of first order hydrodynamic responses by WAMIT at design metocean conditions of T_p = 9.0 s, H_{max} = 6.4 m.

Power rating	MW	10	15	20
Heave displacement	m	0.48	0.46	0.48
Pitch rotation	°	0.63	0.22	0.17
Heave acceleration	m s^{-2}	0.32	0.23	0.24
Pitch angular acceleration	° s^{-2}	0.32	0.11	0.082

loads acting onto the structure for the design wave condition of T_p = 9.0 s and a maximum wave height of H_{max} = 6.4 m is given, under the assumption that wave amplitude is half of wave height.

Interesting results found that for wave periods within the operational range of the wind turbine, that is approximately within 7.0 s to 13 s according to Table 4.1, waves exert the most force per wave period and peaking at approximate 11 s for all design concepts in the three directions analysed.

Furthermore, the wave exciting forces follow an almost linear trend from the 10 MW to the 20 MW model as load over power rating; a doubling in power rating results roughly into a doubling in first order wave exciting force. However, the diameters of all braces only scale by a factor of approximate 1.5 (see Table 3.1).

Reflecting to the Morison equation of Equation 4.3, and combining experience that for large diameter cylinders the wave force onto a cylinder is inertia dominated, this may explain why the force doubles for a smaller increase in diameter. To test the validity of the Morison equation for the upscaled design concepts, an equivalent diameter stick model of the TetraSpar is created, following the approach described by Vugts (2013). This simplified analytic stick model is then used to calculate the wave forcing according to the Morison equation, per wave amplitude.

The graphs for surge force in Figure 4.8 show a third line, representing the analytic Morison approximation according to the equivalent diameter stick model for wave periods up to 15 s. While the dashed lines for the Morison approximation do not align with the results by WAMIT, they do show an similar order of magnitude of meganewtons, and a similar trend of force per wave period, albeit at smaller wave periods. These differences can be explained by discrepancies in the analytic and simplified stick model, or other wave-structure interaction effects not captured by the Morison equation. In all, this comparison does indicate that the Morison equation is able to give an indicative first estimate for wave forcing for (larger) TetraSpar design concepts.

4.5.2. RAOs in heave and pitch

The last WAMIT results to be discussed are the response amplitude operators for the free-floating design concepts,in heave and pitch directions. The RAOs for surge are omitted, the dynamic behaviour of a floater in horizontal direction is largely affected by a mooring system.

Figure 4.9 presents the displacement RAOs for the three upscaled design concepts, as computed by WAMIT by Equation 4.26. Figure 4.10 shows the acceleration RAOs for heave and pitch directions, calculated by $\partial^2 RAO(\omega)/\partial t^2 = |-\omega^2 \cdot RAO(\omega)|$. All RAO plots are capped in the vertical directions, for most responses the peak extends beyond the maximum value of the y-axis. Overall, all design concepts show similar results and behaviour for all WAMIT results.

One item of interest from the RAO plots are the natural periods for the upscaled TetraSpar models. For heave, these are found in the range of 37 s to 39 s for all three models, fairly constant. In pitch

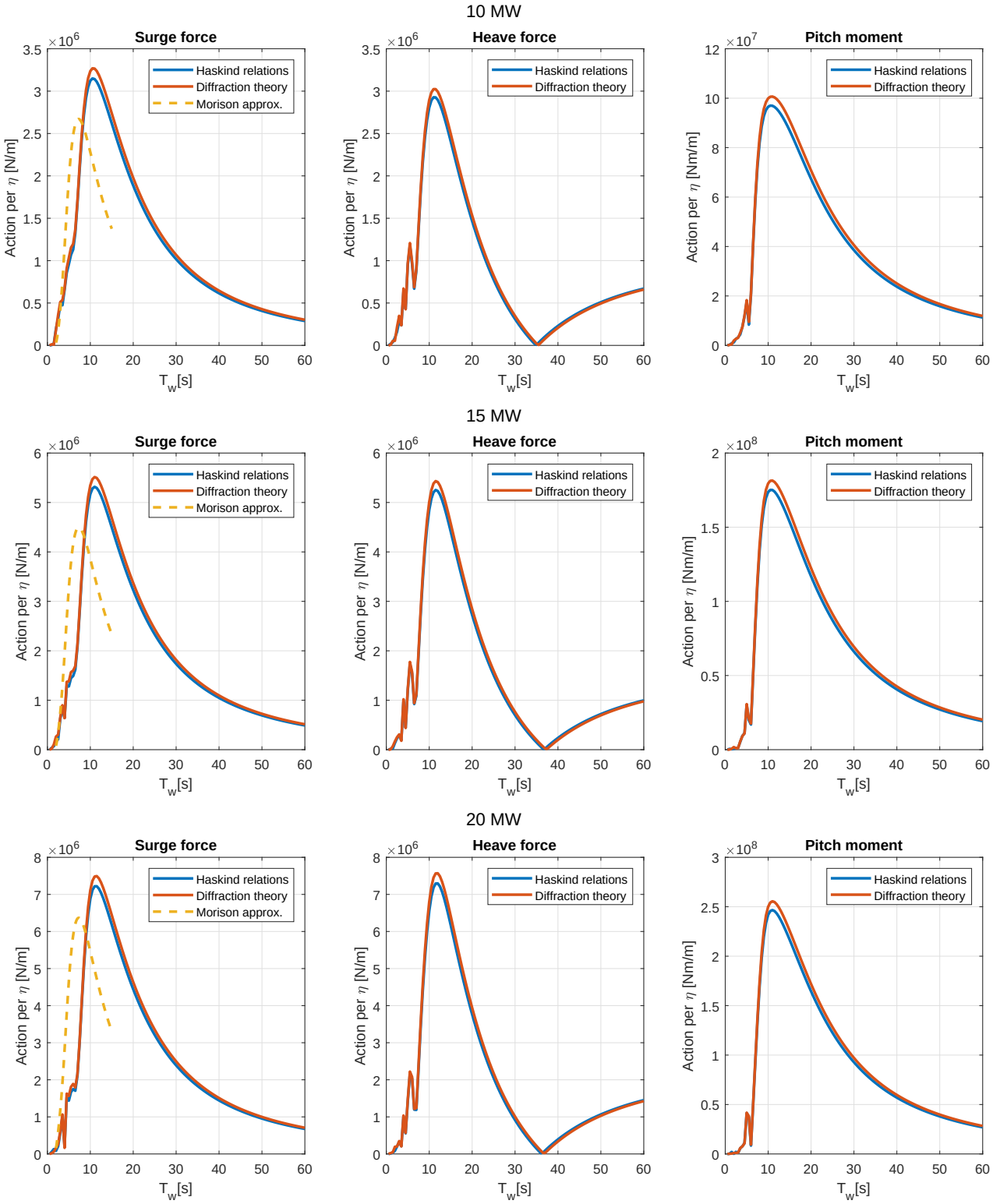

Figure 4.8: First order linear wave action for upscaled TetraSpar design concepts in surge, heave and pitch directions.

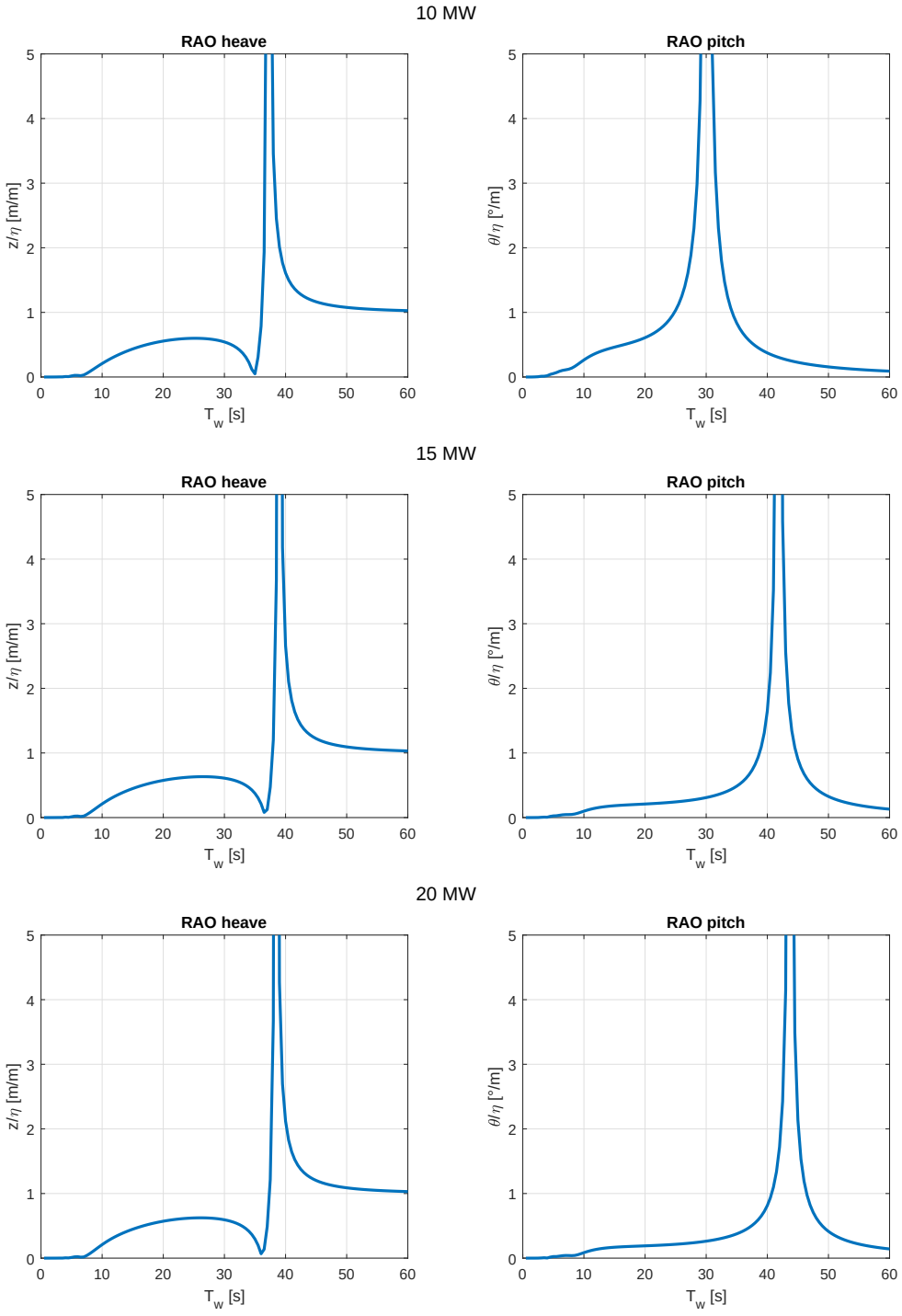

Figure 4.9: Displacement response amplitude operators for upscaled TetraSpar designs in heave and pitch directions.

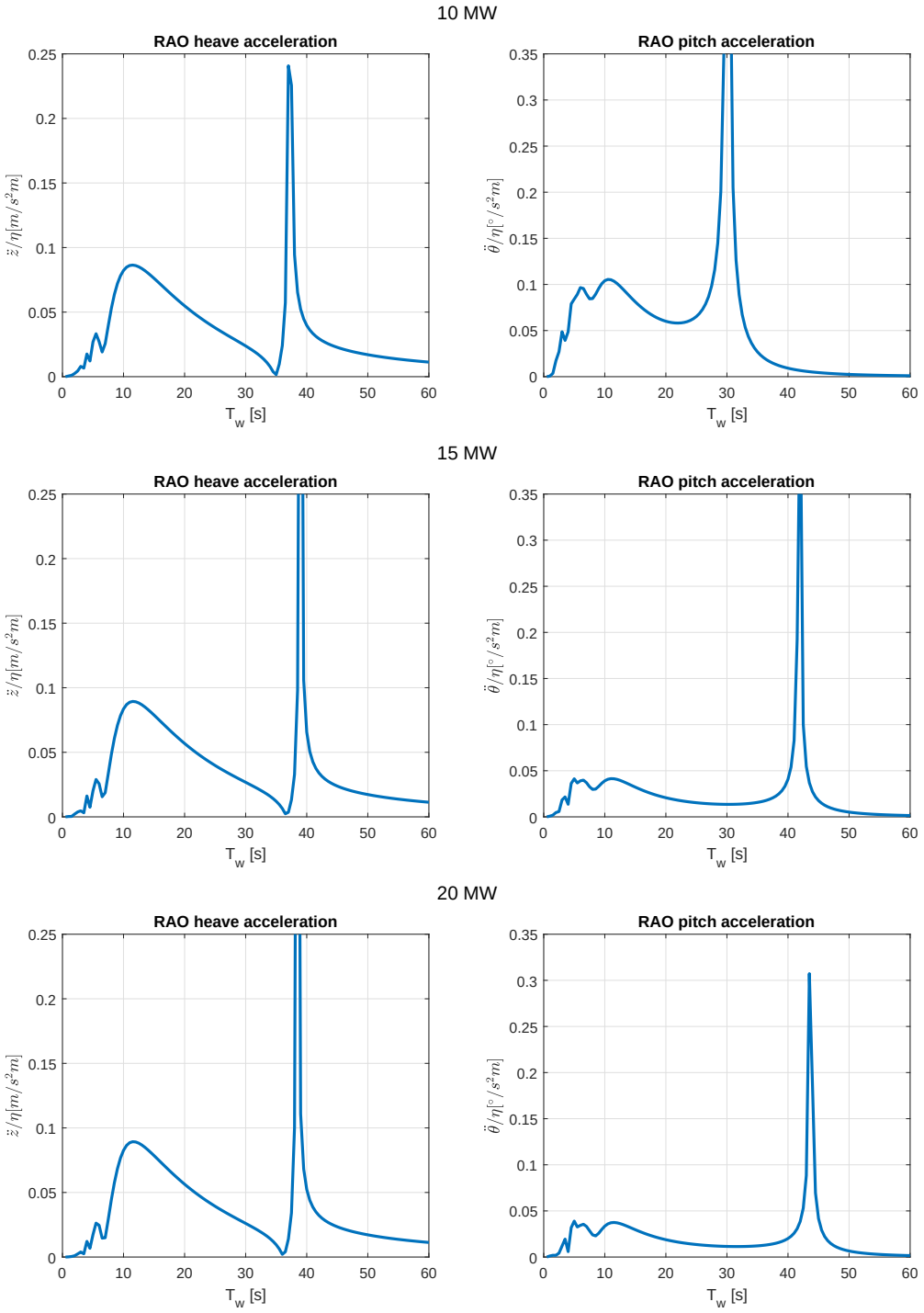

Figure 4.10: Acceleration response amplitude operators for upscaled TetraSpar designs in heave and pitch directions.

direction the spread of natural periods is larger, around 30 s for the 10 MW design concept, while those for larger structures are approximate 41 s to 43 s. The rotational natural periods are sensitive to both stability characteristics and mass moment of inertia of the structure. Both of these parameters are approximated by simplified hand calculated, which can explain the relative differences.

Most importantly in terms of natural periods is that no peaks are within the range of excitation by external forces. Resonance by waves is unlikely for any of the upscaled TetraSpar models. Furthermore, all amplitudes within the wave period range from operational up to a 50-year extreme storm conditions are rather nuanced, no significant amplitudes are observed within the wave period range of 7 s to 15 s.

A relation between the wave action of Figure 4.8 and the structural response can be observed in Figure 4.10 for acceleration RAOs. The local peaks within the operating window in correspond to the peaks in wave forcing. The global peaks in acceleration RAOs are directly related to the natural periods as observed in the displacement RAO figures.

Table 4.3 lists the first order responses of the upscaled TetraSpar design concepts, at the design conditions matching those for wind hub velocity of 11 m s^{-1} offshore Norway.

4.5.3. Discussion of hydrodynamic results

As shown in this section, WAMIT is able to generate a significant amount of results and data on the wave-structure interaction of a marine structure, of which only a small portion is presented by the figures and tables. No anomalies or discrepancies are found in between the numeric models, and the simplified, analytic calculations for added mass and wave force by the Morison equation show similar behaviour and orders of magnitude compared to WAMIT. However, there are some point of discussion on the overall dynamic behaviour of the TetraSpar to be considered in this section, concerning mainly on results of WAMIT itself, coupled dynamics with wind turbine generator, and the omitted mooring system

Even though the WAMIT results and analytic hand calculations show similar orders of magnitude and behaviour, none of these results should be taken as definitive answers. In order for WAMIT to work properly, the 3D CAD models are adjusted such that no braces overlap. For the real TetraSpar design the braces are connected by smooth joints, and the cylinders are tapered to the pinned connection. Expectations are that a detailed design with smoother transitions between the cylindrical braces and cylinder ends will result into lowered and more nuanced values for the presented results.

Furthermore, as show with the convergence study of Appendix B, the presented WAMIT results for models with 1680 panels are up to 10% higher than for WAMIT models with significantly higher panel counts. A larger amount of panels for the WAMIT models gives more accurate results, but a costs of significantly longer computation run times.

Another limitation of WAMIT is that is only calculates one source of damping of radiation, as the application assumes a potential flow. Other types of damping like viscous damping and skin friction are not considered in the calculations, but may have an effect on the total structure motions, as more damping sources absorb the total energy of the system, and further reduce sytems motions and excursions.

Lastly, WAMIT is only suitable to calculate first-order waves and corresponding effects. For a moderate sea state first-order waves are a reasonable approximation for a single wave. However, for increases wave heights or wave steepness, higher-order wave effects become more important. Sharper wave crests and shallower troughs may interact differently with the structure than first-order sinusoidal waves. Other wave-strucutre interaction solvers than WAMIT are advised to calculate the hydrodynamic responses for more extreme metocean conditions

One of the major subsystems omitted from the dynamic analysis is the dynamics of the wind turbine generator itself. For the WAMIT calculations, the WTG is represented as a static structure with mass and inertia. However, the WTG superstructure itself accounts for a significant portion of the action and loads onto the FOWT, is highly dynamic and on a different time-scale than wave hydrodynamics. Comparing wind force and moment to wave action, the horizontal component by wind is approximate one eighth of the wave surge force, while the overturning moments are of comparable magnitudes. For further analysis is it important to not only capture aerodynamic loads in combination with hydrodynamic action, but also investigate a wide range of load cases of different metocean conditions.

For the upscaling design methodology it is assumed that relative to waves, the wind action and subsequent overturning moment is constant. However, superposition of wind forces according to Equation 3.5 and wave forces computed by WAMIT is not recommended. The exciting periods of these two environmental forces are significantly different: first-order wave forces cover relatively short periods up to 20 s, whereas wind forces cover a much longer range of periods, typically in the order of minutes. Simply combining the two environmental force components completely discards the fundamental differences in dynamic action.

Another significant contributor to the dynamic response of a FOWT is the aerodynamic damping by the WTG. A study by Liu et al. (2017) shows that for bottom-fixed WTGs the effects aerodynamic damping in the numeric modelling of the system greatly influences the structural response and decreases structural loads and deflections of the RNA. For floating WTGs the effects of aerodynamic damping are expected to be even more significant, as the complete structure rotates and and translates significantly more than bottom-fixed structures. The aerodynamic damping provides an energy sink to reduce the motions and dynamic behaviour for the structure. For FOWTs, an inclusion of aerodynamic damping is expected to have the greatest effects on rotational motions of pitch and roll, lowering the dynamic behaviour and results for RAOs in these directions. Furthermore, Liu et al. recommend to include aerodynamic damping into account from initial design stages, to restrain vibrations inside the structure and to consider for decreased lifetime fatigue loads of the structure.

The last point of discussion is the omitted mooring system. Mooring lines provide restoring force and moment to limit the offset of the floating structure with respect to its equilibrium position. A maximum offset is required to safeguard the integrity of power export cable, and minimise the risk of collision offshore when two structures are close. According to Henderson et al. (2016), the “maximum offset is determined by combining the mean FOWT excursion from steady loads with the amplitude motion range from the time-varying cyclical loads. Steady loads include the mean rotor thrust force, wind drag from exposed surfaces, current drag, and the mean second-order drift force. Cyclical loading arises from dynamic contributions from wave-induced drag loads, frequency-dependent added mass, atmospheric turbulence, and sum-difference and sum-sum second-order wave loads.”

While some of the contributions are known, like a steady mean rotor thrust force by the WTG rotor size and a dynamic wave-induced drag loads by the first-order calculations by WAMIT, most of these terms are unknown at this point and require specialised computation software to determine the combination of these loads and actions. Only then a viable and representative mooring system can be designed.

Even though a mooring system is excluded in the first-order dynamic response by WAMIT for the free-floating design concepts, some significant effects can be expected when a mooring system is incorporated. Most importantly is the added inertia by the mooring lines to the total structure. This will reduce motions and accelerations of the structure in all degrees of freedom, despite that the mooring system predominantly restrains horizontal motions in surge, sway and yaw. The natural periods observed in the RAOs will become slightly longer for heave, pitch and roll when a mooring system is included because of the additional interia. Furthermore, additional natural periods for the surge, sway and yaw are introduced. Expectations are that natural periods induced by a mooring system will be significantly longer than the vertical motions, as the stiffness of a mooring system is significantly lower than the hydrostatic restoring stiffness coefficients.

5

Structural design

As the upscaled design concepts for FOWTs have been generated by hydrostatic stability and maximum wind overturning moment in chapter 3, and first order dynamics of the resulting design concepts have been modelled in chapter 4, the next step in the upscaling design methodology is the structural design and analysis of the upscaled structure.

The process on the development and detailed analysis on the structural engineering of an offshore structure is a resource extensive, which requires lots of knowledge, experience and specialised software to design a structure that is will survive the harsh offshore climate over its lifespan. For this thesis, a full structural design and analysis of the upscaled design concepts is deemed to be out of scope. The main goal of this chapter is to identify potential obstacles on structural design when the structure is upscaled. This is done by studying the requirements on structural design described in different offshore structure design codes and recommendations, and analytically assess the effect of a larger dimensioned elements to the structural design.

The focus of this chapter will on the strength of tubular braces, a common building block in offshore structures and a first step simplification to the TetraSpar's braces. Furthermore, the effect of increased thicknesses on fatigue damage is analysed, and the possibility of vortex induced oscillations.

5.1. Effects of upscaling in structural engineering

The following section analyses the structural strength of common elements in offshore engineering. This will be a largely qualitative analysis, with the goal to identify possible challenges while upscaling an offshore structure. The main assumption for this analysis is the linear relation for the upscaling of structural elements, similar to the upscaling process described in chapter 3. In other words, for an increase of the diameter of a cylindrical element, the D/t-ratio will remain constant and the inner wall thickness will increase with equal amount.

5.1.1. Strength of tubular members

Base guidelines for the strength of tubular members are listed in ISO (2007) 19902 code. For many different components and actions are requirements given, this section will focus on five primary arrangements for tubular components on actions on tension, compression, bending, shear and hydrostatic as a one-component force. The strength assessment is based largely on yield failure of a cylindrical member, most likely to occur in ULS conditions:

$$F_y = Af_y \tag{5.1}$$

In which A is the cross-sectional area of the member, F_y the theoretical maximum force a member can sustain without yielding, and f_y the yield strength in stress units.

The first case to consider is axial tension, defined as:

$$\sigma_t \leq \frac{f_t}{\gamma_{R,t}} = \frac{f_y}{\gamma_{R,t}} \tag{5.2}$$

Here σ_t is the axial tensile stress due to internal forces, f_t is the representative axial tensile strength, and $\gamma_{R,t}$ a partial resistance factor. The geometry of the tubular member plays a role in the conversion from tensile force F_t to axial tensile strength:

$$f_t = f_y = \frac{F_t}{A} = \frac{F_t}{\frac{\pi}{4}\left(D^2 - (D-2t)^2\right)} \tag{5.3}$$

From this equation it is clear that the axial tensile stress is proportional to tubular diameter squared, $f_t \propto D^2$. A linear increase of diameter is beneficial to the axial strength of the element, as the axial tension force may increase by a power of two for a similar axial tensile stress.

Next is axial compression, at first sight quite similar to axial tension:

$$\sigma_c \leq \frac{f_c}{\gamma_{R,c}} \quad f_c = \frac{F_c}{A} = \frac{F_c}{\frac{\pi}{4}\left(D^2 - (D-2t)^2\right)} \tag{5.4}$$

Axial compression is similar proportional to diameter, $f_c \propto D^2$. However, for compressive axial loads this is not the only expression to consider. The stability of a member may become a problem, as buckling is a common failure mode for slender members under axial compression.

First item to consider is Euler's buckling theory, that is a description of ideal behaviour under axial compressive loading which may lead to column buckling. According to Vugts (2016), the Euler buckling strength is:

$$f_e = \frac{\pi^2 E}{\lambda_s^2}, \quad \lambda_s = \frac{L}{nr}, \quad r = \sqrt{\frac{I}{A}} \tag{5.5}$$

Here λ_s is the slenderness ratio, n denotes the buckling mode, and r the radius of gyration. As the radius of gyration is equal to the square root of moment of inertia over area, $r \propto D$ for cylinders. As length dimensions for the TetraSpar design concepts are fixed, the slenderness ratio is inversely proportional to a diameter. The resultant Euler buckling strength scales proportionally to the diameter squared, $f_e \propto D^2$.

However, pure axial compression or column buckling are not the only failure modes likely to occur by an compressive load. For thin-walled tubular members, local buckling of some sections within the brace might be the first mode of failure. Vugts (2016) state that the occurrence of local buckling is difficult to describe by analytic equations, and is a semi-empirical phenomenon. ISO (2007) does state that the local buckling strength is partially dependent on the representative elastic local buckling strength f_{xe} as:

$$f_{xe} = 2 \cdot C_x \cdot E \cdot \frac{t}{D} \tag{5.6}$$

Without going into detail on all factors in this equation and focussing only on the geometric term, f_{xe} is inversely proportional to the diameter over wall thickness ratio: a relatively thicker wall will provide a higher local buckling strength. As one of the main assumptions of the TetraSpar upscaling methodology is that the D/t-ratio will remain constant for all braces, the local buckling strength does not change for larger diameter braces.

Third failure mechanism to consider is bending:

$$\sigma_b = \frac{M}{Z_e} \leq \frac{f_b}{\gamma_{R,b}}, \quad Z_e = \frac{\pi}{64}\left(D^4 - (D-2t)^4\right)/(D/2) \tag{5.7}$$

The relation between the bending strength and geometry tubular member is expressed in the equation for elastic section modulus Z_e, and is proportional to diameter to a power three, $f_b \propto D^3$. However, it may occur that a large bending moment M may result to a maximum bending stress larger than the yield strength of the member in the outer fibres of the cross-section, and local yielding might occur. This may induce local deformation, but may not lead to failure of the member. According to Vugts (2016), the

maximum bending stress “can exceed the yield strength without undue consequences”. The bending strength then is related to the plastic section modulus Z_p as:

$$\frac{f_b}{f_y} = C \cdot \left(\frac{Z_p}{Z_e}\right), \quad Z_p = \frac{1}{6}\left(D^3 - (D-2t)^3\right) \tag{5.8}$$

Again, the plastic section modulus is proportional to the diameter cubed, but the bending strength for plastic deformation is linearly related to the yield strength multiplied by a factor of C and Z_p/Z_e, the former depending on steel quality properties like yield strength and Young's modulus, and the latter factor depends on the ratio of D/t. One of the leading assumptions for upscaling states a constant value of D/t for all members. Therefore the plastic bending strength of the tubular braces increases by a relation of diameter cubed, equal to elastic bending strength.

The second to last failure mechanism is shear, divided into two distinct cases of beam shear τ_b due to transverse forces, and torsional shear τ_t due to moments.

$$\tau_b = \frac{V}{\frac{1}{2}A} \leq \frac{f_v}{\gamma_{R,v}} \tag{5.9}$$

$$\tau_t = \frac{M_{v,t}}{I_p/(D/2)} \leq \frac{f_v}{\gamma_{R,v}}, \quad I_p = \frac{\pi}{32}\left(D^4 - (D-2t)^4\right) \tag{5.10}$$

In the case of beam shear τ_b, the strength of the brace is proportional by the diameter squared through the area of the brace, similar to pure axial tension or compression.

For torsional shear through an applied shear moment, the strength is proportional to the polar moment of inertia I_p divided by the radius of the brace, hence the torsional strength relation is $\tau_t \propto D^3$. Note that the representative shear strength is significantly less than yield strength by the relation $f_v = f_y/\sqrt{3}$.

The last strength check is for external hydrostatic pressure, expressed by:

$$\sigma_h = \frac{pD}{2t} \leq \frac{f_h}{\gamma_{R,h}}, \quad p = \gamma_{f,G}\rho_w\left(|z| + \frac{1}{2}H_w\right) \tag{5.11}$$

At first sight it seems that the strength on hydrostatic pressure through hoop stress σ_h is only dependent on the ratio of D/t, which is assumed constant for the upscaling procedure.

However, an effect on increasing brace diameter is found in the semi-empirical equations for the determination for representative elastic critical hoop buckling strength $f_{he} = 2C_hEt/D$, where the elastic critical hoop buckling coefficient C_h can be a function of the geometric parameter $\mu = \frac{L_r}{D}\sqrt{\frac{2D}{t}}$. Unfortunately, this geometric parameter is not of importance for all cases, and a fit-for-purpose approach for each member needs to be implemented to assess the hydrostatic strength of the members.

5.1.2. Fatigue in upscaled structural elements

Fatigue is arguably one of the most challenging failure modes in the design of offshore structures, and is by Vugts (2013) defined as “the mechanism whereby local and very small imperfections (flaws) act as crack-like defect in the material that grow due to variable stresses occurring during the lifetime of the structure.” In contrast to designing a structure for strength, by determining the overall (maximum) stresses a structure may experience, design for fatigue is more difficult to determine as the millions of fluctuating stress cycles accumulate damage throughout the structure. During the design of the structure, estimations on the (environmental) loads over the full lifetime of the structure have to be made, which are then translated to stresses inside the structure.

Fatigue failure is most likely to occur at critical locations, so-called stress hot spots. The study by Vaalburg (2019) assesses the fatigue strength of the pinned connections of the TetraSpar, deemed to be the critical locations for fatigue. Vaalburg analyses nine locations of the TetraSpar's joint connections between the lateral and radial braces prone to fatigue damage, either welded connections or geometric features like holes rapid changes in thickness or other notches.

One way to estimate the fatigue lifetime is through SN-curves in Figure 5.1, a graphical representation of the stress variations S and the number of cycles N. SN-curves are obtained from empirical fatigue

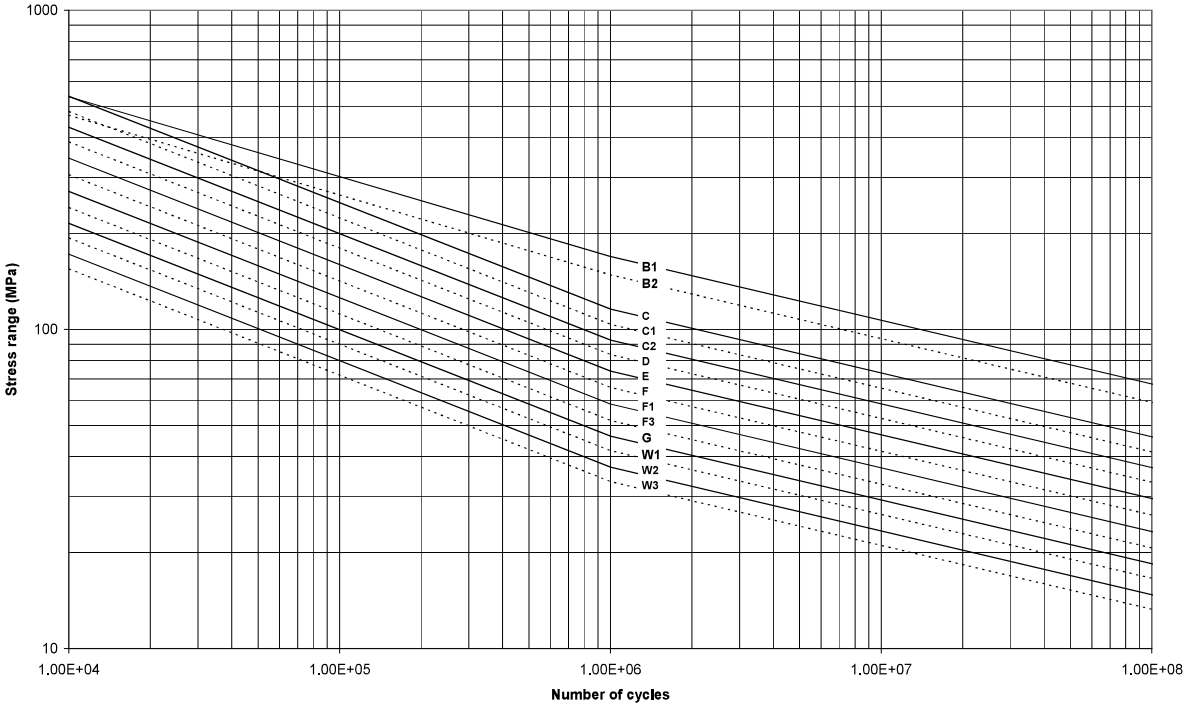

Figure 5.1: SN-curves for welded plates in seawater with cathodic protection for different detail classes (DNV GL, 2014).

tests, by testing small specimens in laboratories on cyclical loading until failure of the specimen when the crack growth through the specimen's thickness.

Assuming a welded joint, the thickness of the plate affects the fatigue strength of the joint in a negative manner. According to DNV GL (2014) this thickness effect "is due to the local geometry of the weld toe in relation of the thickness of the adjoining plates, [and] is also dependent on the stress gradient over the thickness." The thickness effect is accounted for in the equations for design S-N curves by the last term:

$$\log N = \log \overline{a} - m \cdot \log\left(\Delta\sigma \left(\frac{t}{t_{ref}}\right)^k\right) \tag{5.12}$$

The terms $\overline{a}$ and m depend on the detail class of the potential critical location and the amount of load cycles, whereas the thickness exponent k depends on the detail class, a value between 0 and 0.30. This equation shows that a thicker plate reduces the number of cycles by the relation $\log N \propto -m \cdot \log(t/t_{ref})^k$. t_{ref} is either 25 mm for all welded connections other than joints or bolts, or 32 mm for welded tubular joints.

For the TetraSpar design, Vaalburg (2019) states that the critical locations in the pin connections are classified by either C, D or F curves (Figure 5.1), which corresponds to a thickness exponent k of 0.05, 0.20 and 0.25 respectively. For a minimum offshore lifetime of 20 years and a mean wave period of about 10 s, the structure experiences over 60×10^6 load cycles by waves, which corresponds to a factor $m = 5.0$ according to DNV GL (2014).

Figure 5.2 shows the $\log N$ cycle decrease for an increase of the thickness ratio for the parameters relevant to the TetraSpar. As expected, elements with a higher ratio of t/t_{ref} reduces the number of fatigue cycles, but the relative differences decrease for these larger ratios. The effect of detail class and corresponding thickness exponent k may have an bigger effect on the fatigue strength than the increase of material thickness.

5.1.3. Vortex induced oscillations

One challenge specific to structures with slender elements is the phenomenon of vortex induced oscillations, caused by a fluid (either air or water) flowing past a structural component which may cause vortex shedding around that member (DNV GL, 2017). This may lead to oscillations of the element

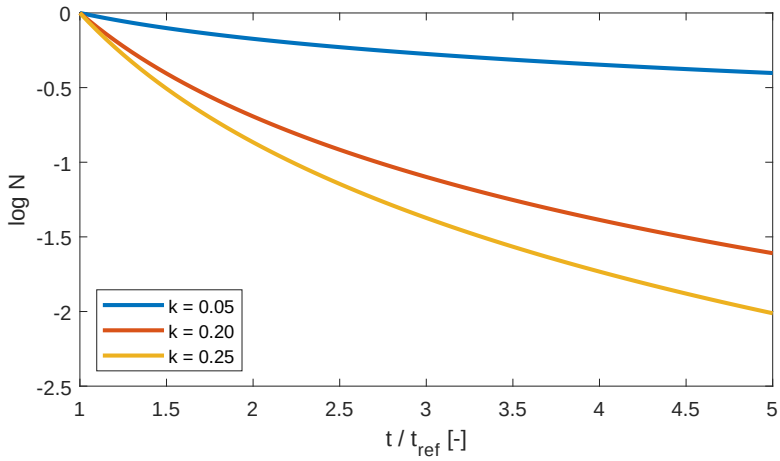

Figure 5.2: Decrease of $\log N$ cycles per increase of material thickness ratio for critical locations identified for TetraSpar.

normal to the longitudinal axis, and may cause significant motions, loads and fatigue damage. Vortex induced oscillations are governed by many different (engineering) parameters including geometry, mass and damping of the structure, Reynolds numbers, reduced velocity and flow characteristics.

While wind and wave dynamics might cause vortex induced oscillations, the focus for this section is to investigate vortex shedding and vibration lock-in caused by currents, and to discuss the effects of increased substructure and brace dimensions on the potential occurrence of vortex induced oscillations.

First to consider is the vortex induced hull motions, likely to occur for cylindrical deep draught floaters like spars. According to DNV GL (2017) these motions are strongly non-linear phenomena and are difficult to determine or predict. Usually model testing is required to determine the responses of vortex induced motions on floating structures. However, the recommended practice does give a guideline when these motions might occur.

Two distinct motions are possible when considering vortex induced motions: oscillations in-line with the current flow, and transverse to the flow. While the former cause small motions and oscillations, and are deemed to not be governing, transverse motions will cause motions and loads increased in magnitude. DNV GL (2017) recommends that for a reduced velocity $V_R > 3 \sim 4$ the hull will start to oscillate transversely. The reduced velocity is a function of hull diameter, current velocity and natural frequencies of the rigid body. As natural frequencies of the rigid body are not exactly defined in the design concept stage of this upscaling method, the equation for reduced velocity is rewritten to natural period by:

$$V_R = \frac{v_c}{f_n \cdot D} \rightarrow T_n = \frac{D \cdot V_R}{v_c} \tag{5.13}$$

To analyse a possibility of transverse oscillating vortex induced motions for the TetraSpar case-study, a simplification of the system is made. Condering a range of current velocities between the mean of $0.3\,\mathrm{m\,s^{-1}}$ and a maximum of $1.4\,\mathrm{m\,s^{-1}}$ for the Metcentre location, and a hull diameter simplified to be equal to the centre column of the (upscaled) TetraSpar, a range of natural periods T_n is calculated for which vortex induced motions might occur. Solving these equations for the lower bound at $V_R = 3$, the resulting natural periods for this simplification are plotted in Figure 5.3.

Another phenomenon that might occur due to vortex shedding around a cylindrical member are vortex induced vibrations. One of the most important implications of vortex induced vibrations is significant fatigue damage on a structural element. When the vortex shedding frequency is close to a natural frequency of that brace, the element can be locked-in the vortex induced vibrations, and start to resonate.

Instead of analysing the occurrence of vortex induced vibrations given the current velocity as with vortex induced oscillations, the following section reviews the relation between brace diameter and vortex induced vibrations. This largely because the natural frequency of all TetraSpar braces will be significantly different, are dependent on many factors and require a more detailed design of each structural element.

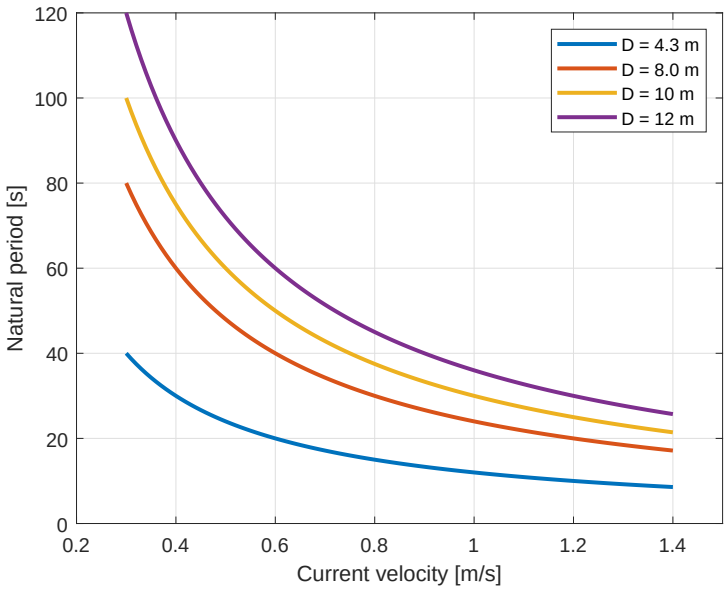

Figure 5.3: Natural period as function of current velocity for vortex induced motions might occur for different diameters of TetraSpar centre columns, assuming a boundary of $V_R = 3$.

Similar to vortex induced oscillations, the vortex induced vibrations can be appoarched by the equation for V_R in Equation 5.1.3. Now only a single structural element, assumed to be a type of beam, is analysed. According to DNV GL (2017), vortex induced vibrations may occur for a range of $1.0 \leq V_R \leq 4.5$ for pute in-line vortex shedding resonance, or $3.0 \leq V_R \leq 16$ for excitation by cross flow vortex shedding. The natural frequency of a single beam is defined as:

$$f_n = C_n \cdot \sqrt{\frac{E \cdot I}{\overline{m} \cdot L^4}} \tag{5.14}$$

For with C_n a constant value is dependent on mode shape and type of supported beam. Analysing only the geometric factors and assuming that the length of each TetraSpar member does not change, the natural frequency is proportional to the square root of the area moment of inertia. Rewritten to a function of cylinder diameter, the proportionality between natural frequency and diameter adheres to $f_n \propto D^2$. With this derivation, it is clear that the reduced velocity for a single beam follows $V_R \propto D^{-3}$, an increase in brace diameter decreases the reduced velocity by a factor cubed.

5.2. Analysis and evaluation

In the previous section, three potential effects of upscaling to the structural design and strength of TetraSpar structures are analysed based on international standards and recommended practices for offshore structures.

First, the TetraSpar's structural elements are simplified to cylindrical braces, and the strength of tubular members is analysed for five types of action and the resulting structural strength. Most types of actions are identified as a function of the tubular diameter, raised to a power. For some types of action, the ratio of diameter over wall thickness was found to be the leading strength indicator.

Comparing the strength relations to, for example the static weight action of the resultant upscaled suspended keels some interesting results are to be found. The ballasted keel weight increases by more than a factor seven from the 3.6 MW to the largest 20 MW concept design, while the diameter of the steel keel cylinders increase by less than three times. Assuming that the primary action on the suspended keel by self weight are either beam shear at the suspension points, or maximum bending moment at the middle, the structural strength of the keel increases by a factor eight for beam shear, or a factor twenty two for bending strength.

Table 5.1: Overview of load types for simple tubular members and leading geometric dependencies on structural strength for upscaling.

Action		Geometric dependence
Tensile		$f_t \propto D^2$
Compressive	Pure compression	$f_c \propto D^2$
	Column buckling	$f_e \propto D^2$
	Local buckling	$f_{xe} \propto D/t$
Bending	Elastic	$f_b \propto D^3$
	Plastic	$f_p \propto D^3$
Shear	Beam	$f_v \propto D^2$
	Torsion	$f_v \propto D^3$
Hydrostatic pressure		$f_h \propto D/t$

Similar analysis for the payload mass and structural strength at the interface between floater and support tower. The payload mass increases up to a factor six from the demonstrator up to 20 MW. Assuming only compression loads, the structural strength increases eight fold due to the non-linear dependence of strength.

These two examples show that there is potential to decrease the size and wall thicknesses of the structural braces than first assumed during the upscaling methodology, which in turn lowers the weight and costs of the primary steel. However, much more research is needed on the actual structural design for upscaled TetraSpar concept designs. Not only must combinations of different actions by weight, aero- and hydrodynamics, buoyancy and other sources be analysed, also the design of the braces itself. For simplicity of this report, the braces are assumed to be simple cylinders. The real TetraSpar braces will be more thin-walled cylinders with strategically placed stiffeners. Given the large diameter, these braces will act more as stiffened shell elements, which are prone to local (skin) buckling and it strength is much more complicated to calculate as function of diameter. In addition, structural elements like the cast joint nodes are not evaluated within the scope of this thesis work, but are essential design details to the TetraSpar.

Next analysed implication of upscaling is the thickness effect on fatigue strength due to larger members. Figure 5.2 shows that the effect of a different detail class, and corresponding factor of k can have as much influence on the decrease in the amount of cycles, than the actual increase of thickness of an element compared to the reference thickness. However, to assess the complete effect of a thicker element, also the stress variations of $\Delta\sigma$ have to be considered. This does require a fully defined, detailed design of all structural elements, and a thorough analysis, like the approach by Vaalburg (2019), of all cyclic loads over the structure's lifetime. It might be possible that a larger structure experiences lower stresses and fatigue damage overall, which offsets the thickness effect.

Another potential source identified for additional fatigue damage is by vortex shedding and the induced oscillations. Figure 5.3 shows the range of current velocities for which vortex induced motions might occur, at the boundary between in-line and cross flow motions. By assuming only the centre diagonal as main hull body, this figure shows that for the higher current velocities present at the Norway location, the natural period corresponding to a reduced velocity $V_R = 3$ are in a range of 30 s to 40 s for the upscaled TetraSpar design concepts. This corresponds to the natural periods in heave and pitch for a free floating structure as derived in chapter 4. Vortex induced motions could pose a structural design challenge during the detailed development of larger TetraSpar floaters, and countermeasures like helical strakes might mitigate additional motions and fatigue damage.

On the other hand, vortex induced vibrations for individual members are less likely when upscaled. As the brace diameters increase, while the length dimensions remain fixed, the structural elements increase in stiffness and natural frequency. Assuming that the 3.6 MW demonstrator does not experience significant vortex induced vibrations caused by current, and the reduced velocity for each brace is $V_R \leq 1.0$, larger substructure braces are less susceptible for fatigue damage due to vortex induced vibrations.

6

Upscaled TetraSpar design

To accommodate larger wind turbine generators, design concepts of the TetraSpar are generated based on hydrostatic stability in vertical and rotational direction, considering the maximum aerodynamic trust and overturning moment by wind to be the key design driver. Then the resulting concepts are analysed on hydrodynamic performance using WAMIT, in which no immediate challenges were found in the motions of the floating foundation. On the structural design aspects, expectations are that the upscaling of individual braces is beneficial to the structural strengths, but that fatigue life could be decreased due to thicker elements and that wide diameters may lead to vortex induced motions.

Overall, the TetraSpar design concepts thus far do not reveal any show stoppers on either of these three topics, and now the resulting structures can be further analysed. First up, the upscaled TetraSpar designs are compared to other large scale FOWTs on different criteria and sizing trends. Secondly, an estimation of the capital expenditure of the upscaled design concepts is made. This is followed by a selection of sensitivity studies are performed on various input parameters and design choices, to indicate where a future detailed TetraSpar design could improve. Lastly, the design concepts are evaluated on the three main topics, and discussed if the resulting structures are feasible for future development.

6.1. Comparison to other upscaled designs

One of the TetraSpar's selling points is the relative lightweight design compared to other designs. This section compares the resulting TetraSpar design concepts by the overturning moment upscaling methodolgy of Table 3.1, to other (upscaled) FOWT concepts. Only a limited amount of data points are presented in this section, as open-access data on displacement and (steel) mass of FOWT designs is scarce.

Figure 6.1 compares the structure displacements as function of power rating for different scaling trends. Displacement is the amount of submerged volume of the substructures, equal to the total (ballasted) weight of the structure and an indicator for total structure size. Even for the limited data set, it is shown that all floating structures are within the same order of magnitude, and clear trends are found in the relation between displacement and power rating.

The analysed upscaling methods show roughly a linear trend in displacement over power rating. The trend lines for mass scaling, power scaling and construction based upscaling are close together, all are based on a (similar) design semi-submersible. The two spar platforms in this figure, the Hywind spar and the TetraSpar based on overturning moment, plot lower displacements figures per power rating; the ballasted masses and underwater structure volumes are smaller than the semi-submersible technologies analysed. As the displacement and mass of the structure is an indicator on relative performance of costs and wave action, the TetraSpar concept shows potential in this respect compared to other technologies.

Another way to assess the upscaled TetraSpar design concepts to other methodologies is by identifying trends for substructure steel. Figure 6.2 shows the primary steel mass for different upscaling methodologies over power rating, and a normalised trend line based on the smallest FOWT design available. While the current 3.6 MW TetraSpar demonstrator still is a relatively lightweight structure in terms of

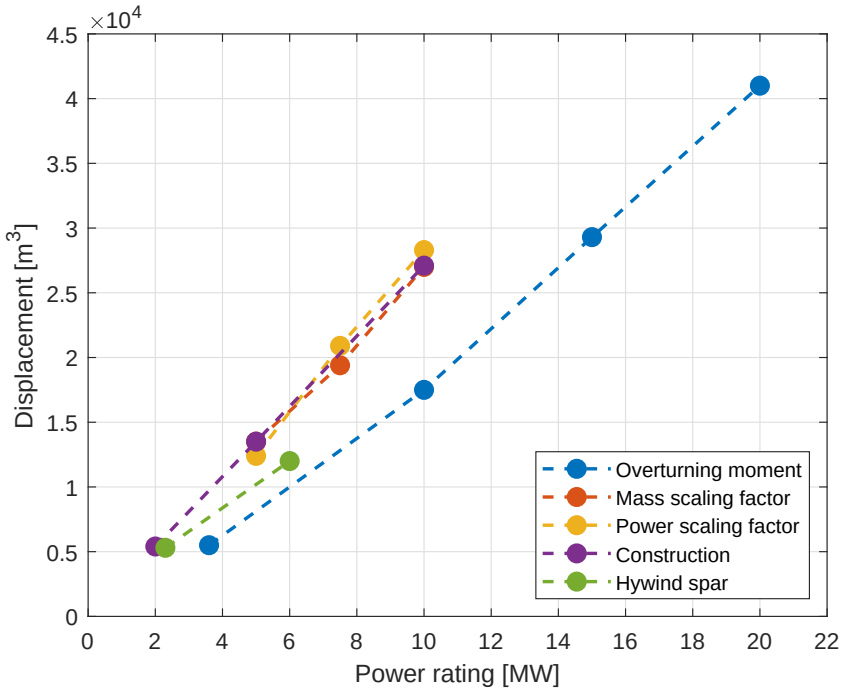

Figure 6.1: Comparison of TetraSpar design concepts (blue) to other upscaling design methodologies by George (2014); Leimeister (2016); Kikuchi and Ishihara (2019) respectively, and the Hywind spar.

primary steel mass compared to other technologies based, the relative advantage diminishes for increased power ratings. The second figure for normalised primary steel mass over power rating, shows that the upscaled TetraSpar substructure design do not follow the general trends by other studies.

The green line by Spearman and Strivens (2020) in Figure 6.2 indicates an averaged trend for a larger set of generic FOWT structures, and sets the trend that for larger wind turbines less structural steel is required, i.e. a larger FOWT structure is more efficient in terms of steel mass. Other academic efforts follow this idea in some way, except for upscaled TetraSpars developed by this thesis work.

Reasons why the TetraSpar does not follow the general trends toward more favourable ratios of steel mass over power rating require more research into detailed designs. However, a couple of explanations can be provided here based on the analysis made thus far. One reason why the TetraSpar's trends deviate from other results is the fundamental difference in substructure classification. All other academic efforts research upscaling of semi-submersible floater designs. Even though spar structures are stabilised by ballast, a comparison between Figure 6.1 and Figure 6.2 shows a larger difference between total ballasted mass (or displacement) and empty steel mass for all semi-submersible platforms in contrast to the TetraSpar design concepts. Even though the semi-submersibles hold more displacement per power rating compared to the TetraSpar designs, much of this additional weight is accounted for by ballast.

Another explanation may be that the initial design of the TetraSpar 3.6 MW demonstrator is a fairly optimised design. Simplifications and assumptions may not be as representable for the large upscaling steps undertaken for in the case-study than previously thought. This in contrast to other academic designs which have not been designed, iterated and optimised like a commercial project would have. Therefore it is likely that the academic FOWTs still have ample room and potential to reduce the steel weight of the structure during upscaling.

A third reason is the assumed constant D/t-ratio during the upscaling of the TetraSpar braces, which results into thicker cylinder walls. In chapter 5 it is found that for larger diameters the structural strength of the braces increases exponentially, likely more than the increase in load. This may allow for a decrease in wall thickness for the cylinder braces, and lower the overall steel mass of the structure, bringing it more in line with other FOWT designs.

The last comparison of the resulting upscaled design concepts is based on the theoretical scaling

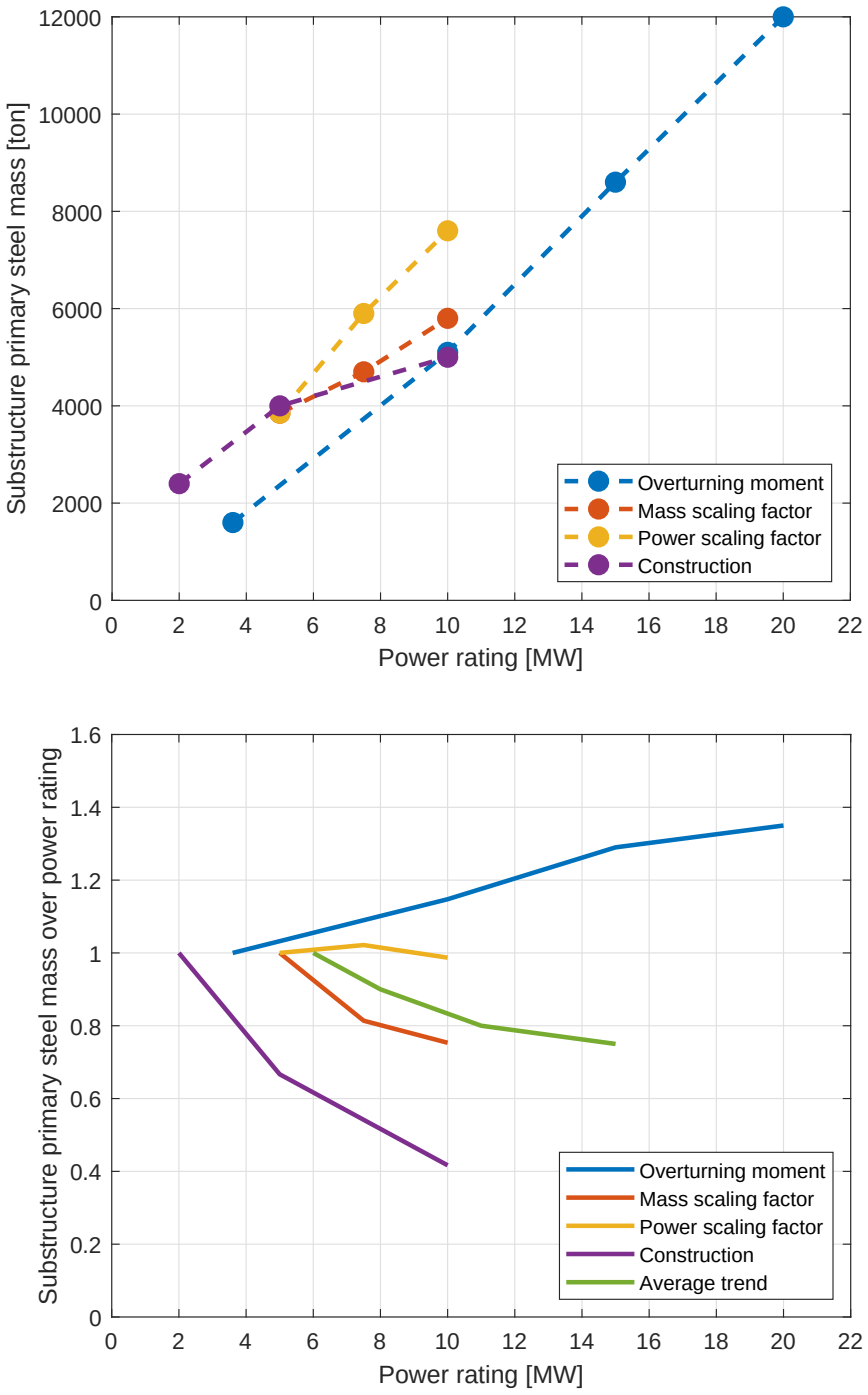

Figure 6.2: Comparison of the substructure primary steel mass over power rating on top, and normalised trends on bottom, for TetraSpar design concepts (blue) and other upscaling design methodologies by George (2014); Leimeister (2016); Kikuchi and Ishihara (2019) respectively. Average trends adapted from Spearman and Strivens (2020).

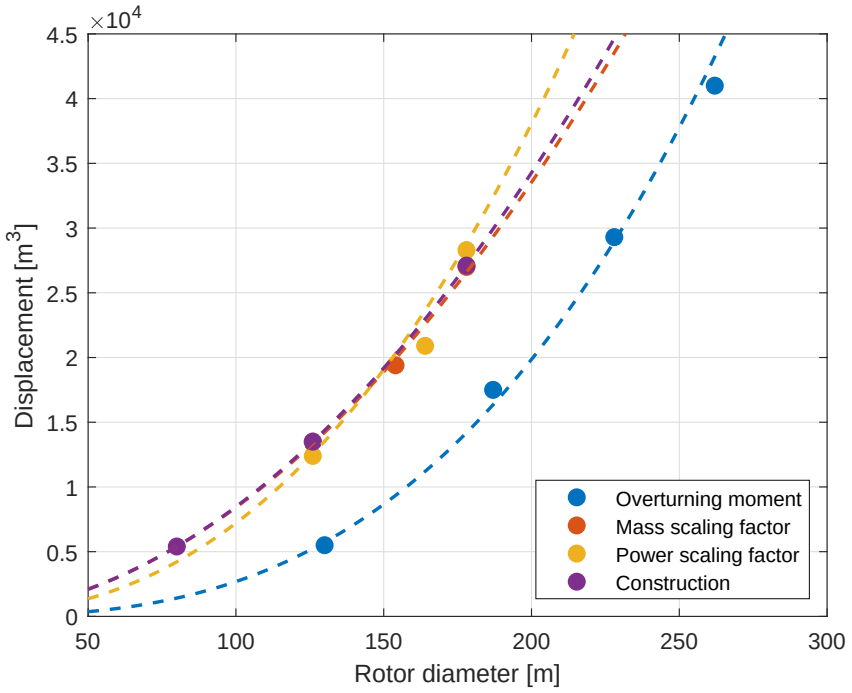

Figure 6.3: Structure displacement over rotor diameter as characteristic length for TetraSpar design concepts (blue) and other upscaling methodologies by George (2014); Leimeister (2016); Kikuchi and Ishihara (2019) respectively, including power law curve fits.

factors (Equation 2.1) and the theory of rational scaling. Figure 6.3 shows the structure displacements over rotor diameter and resulting curve fits. As described by the theory on rational scaling, the curve fits should be described by a power law equations.

For the upscaling strategy for the TetraSpar, the trends are described by $\nabla \propto D_{rotor}^{2.9}$ proportionality. For scaling by a power factor described by Leimeister (2016), the resulting structures are fitted by a trend line of $\nabla \propto D_{rotor}^{2.4}$. Both upscaling methodologies of mass scaling factors and construction based scaling by George (2014) and Kikuchi and Ishihara (2019) respectively show a trend of $\nabla \propto D_{rotor}^{2}$.

None of the upscaling design strategies adhere to the square-cube law, that states a relation of mass proportional to a characteristic length dimension cubed. The trends described by the design methodology based on overturning moment for the TetraSpar, which deliberately discards the square-cube law, follows the $\nabla \propto D_{rotor}^{3}$ proportionality closer than any other upscaling strategy.

6.2. Capital expenditure estimation

The upscaled design concepts of the TetraSpar concept are detailed enough for a first-order cost estimation of the structure, also known as the capital expenditure. This section considered only a single TetraSpar structure i based on assumptions for cost estimation.

The mooring system is dependent on metocean site conditions and chosen design, any cost estimation for mooring is not representative if these factors are not taken into account. Other capital expenditure elements like engineering and development, power and array cables, substations, transportation and installation are dependent on wind farm size and layout, distance to shore and service ports, and other project specifics, are also deemed to be outside the scope of this report.

The capital expenditure estimation considers only a single free-floating TetraSpar structure, based on a few ballpark figures for unit costs. According to Myhr et al. (2014), floating offshore structure costs can be expressed as a product of material costs times a complexity factor. Assuming that the primary cost driver of FOWT substructures is the amount of primary steel required for the substructure, a fair indicator for capital expenditure is steel mass resulting from the upscaled design concepts. An production unit cost of 2.9×10^3 €/ton of steel, adjusted for inflation to 2020, is adapted from Myhr et al. (2014). This includes steel material costs and an averaged production complexity factor for different types of FOWT

Table 6.1: Overview of estimated capital expenditure for free-floating upscaled TetraSpar design concepts.

Power rating		MW	10	15	20
	Unit costs				
Substructure steel	2.9×10^3 €/ton	€	1.5×10^7	2.5×10^7	3.5×10^7
Wind turbine generator	1.0×10^3 €/kW	€	1.0×10^7	1.5×10^7	2.0×10^7
Total capital expenditure		€	2.5×10^7	4.0×10^7	5.5×10^7
Capital expenditure over power		€/MW	2.5×10^6	2.7×10^6	2.8×10^6

substructures.

The second main component for capital expenditure for a single free-floating FOWT is the wind turbine generator. Industry experts advise that currently, large-scale wind turbine generators are listed for approximate 1.0×10^3 €/kW. Combining these two ballpark figures, the capital expenditure costs for the upscaled TetraSpar design concepts are calculated and presented in Table 6.1.

The results show that per unit of power rating, the capital expenditure of the TetraSpar design concepts for WTG and substructure increase. This is expected by Figure 6.2 for normalised trend lines, where the steel mass of the TetraSpar increases relatively to power rating. Based purely on these capital expenditure figures, a 10 MW TetraSpar design concept is economically more attractive than larger wind turbines.

However, there are many more technical and economic aspects involved to decide on the economic feasibility of the design concepts by accounting for items like wind farm size and lay-out, WTG capacity factors, operational expenditures, (metocean) site conditions, energy yield, and many more factors. To generate a more comprehensive economic analysis, including a figure for levelised cost of energy, the upscaled design concepts require a significantly higher level of detail.

6.3. Sensitivity analyses

Thus far, the resulting upscaled TetraSpar substructures of Table 3.1 are based on the 3.6 MW demonstrator design, including all assumptions and design choices. The TetraSpar design and upscaling design methodology offer some flexibility on input values. By varying these data points over a range, an indication of sensitivity to these design choices and assumptions is made. The sensitivity analyses are based only on the hydrostatic upscaling methodology. Further research on the sensitivity for hydrodynamics and structural analysis is recommended.

6.3.1. Keel draught

First sensitivity to be evaluated is keel draught. The TetraSpar's unique suspended counter weight allows the distance of the keel to the floater to be varied without many changes in design. By lowering the keel the structure's centre of gravity drops further below the centre of buoyancy. For an equal structure displacement, this in turn increases the restoring moment and static stability. Assuming a maximum static rotation by wind of 5.0°, the weight of the keel and buoyancy of the floater vary as a result of changing keel draught. Figure 6.4 shows the varying structural mass of the three upscaled designs by the upscaling design methodology as function of keel draught.

This figure shows that there are substantial changes in mass/displacement, and consequently dimensions of the substructure, depending on keel draught. When the distance between floater and keel is limited, e.g. due to shallower water depths, the structure must be adapted to a significantly heavier design to equalise the overturning wind moment. On the other side, a even lower hanging keel offers a lighter structure, with all benefits of less steel, lower hydrodynamic loads and lighter mooring system. The drawback of a lower keel is a reduction in maximum static heel angle; at 100 m draught, the floater may only rotate 10° before a suspension line loses tension, a reduction of more than 30% compared to the base case (see Appendix A).

6.3.2. Heel angle by wind

Next sensitivity discussed is the maximum inclination the structure may experience due to the maximum overturning wind moment. In chapter 2 an explanation is presented on what and why a 5.0° limit for

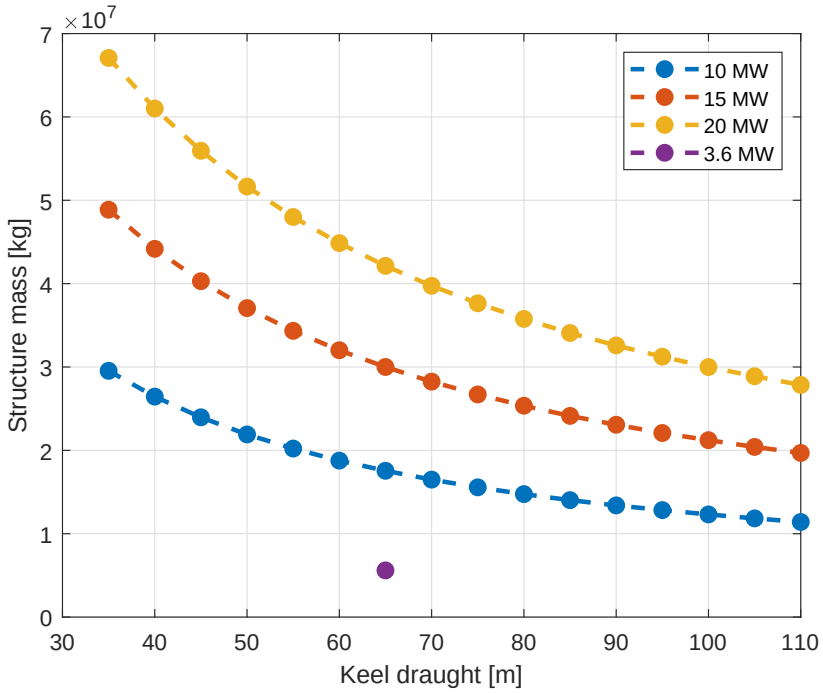

Figure 6.4: Structural mass of upscaled TetraSpar concept designs for varying keel draughts.

the first draft designs is a conservative and reasonable parameter. As this maximum heel is a point of discussion, existing academic literature does not agree on what this number should be, and important assumption to begin with at the start of the upscaling methodology, it is an interesting variable for a sensitivity study.

Figure 6.5 shows the resulting structure mass for the three upscaled design concepts, for a varying maximum inclination angle by wind for a range of 3.0° to 7.0°. Similar trend lines are found as with a variation in keel draught, but with less effect on the total structure mass for an equal amount of change percentage wise.

6.3.3. RNA mass

A third sensitivity study is on the mass of the rotor-nacelle assembly. Figure 2.4 shows that there is a variety in weights for similarly sized turbine generators, and as practice shows, RNA masses may range significantly between multiple OEMs for equal megawatt output figures. This might have a significant impact on the total structure, as the large top mass of the RNA is far away from the structure's centre of gravity.

In Figure 6.6 a relative change in the range of ±20% of the RNA mass, and the resulting structural masses is shown for the three upscaled TetraSpar design concepts. A 20% reduction in top mass results on average a 5% decrease of total structure mass, while a 20% heavier RNA relative to the base case requires approximate 3% of structure mass increase to balance the system. Even though the RNA sits far away from the structure centre of gravity, the comparative small variation of structure mass when adjusting RNA mass is largely due to relatively small RNA mass compared to the full structure mass. Put into ratios, the payload only makes up about 5% of the total mass of the TetraSpar design concepts, of which half is by the RNA.

6.3.4. Hub height

The fourth sensitivity study performed is a variation of hub height, which in turn should change the overturning moment by wind. For the base case upscaled TetraSpar designs, the hub height is calculated as rotor radius plus an offset of a 30 m air gap between still water level and lowest blade tip elevation. This constant offset value is advised by experts to be a reasonable value for bottom fixed WTGs. Air gap figures like this are often mandated by either regulations or OEMs.

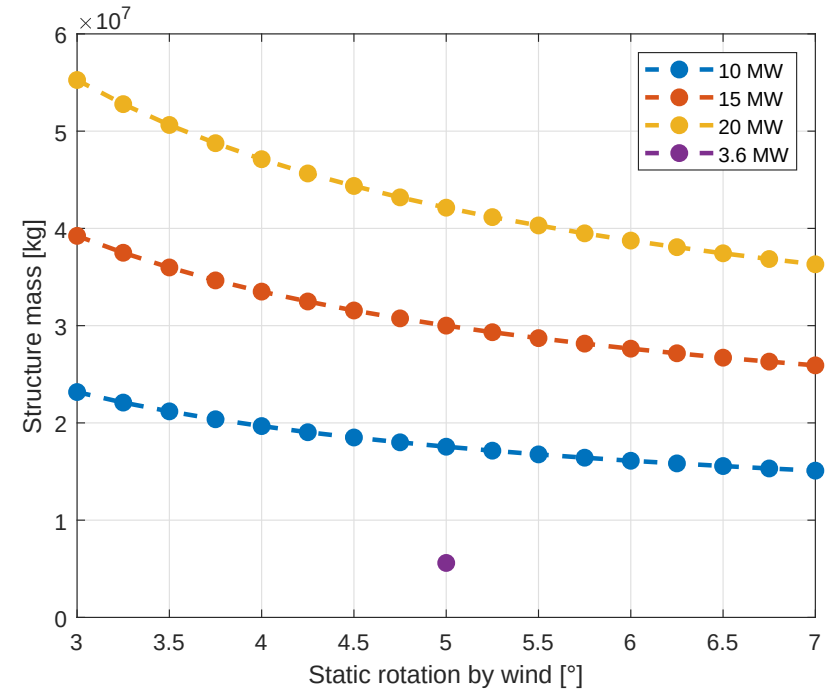

Figure 6.5: Structural mass of upscaled TetraSpar concept designs for varying maxima of static rotation by overturning wind moment.

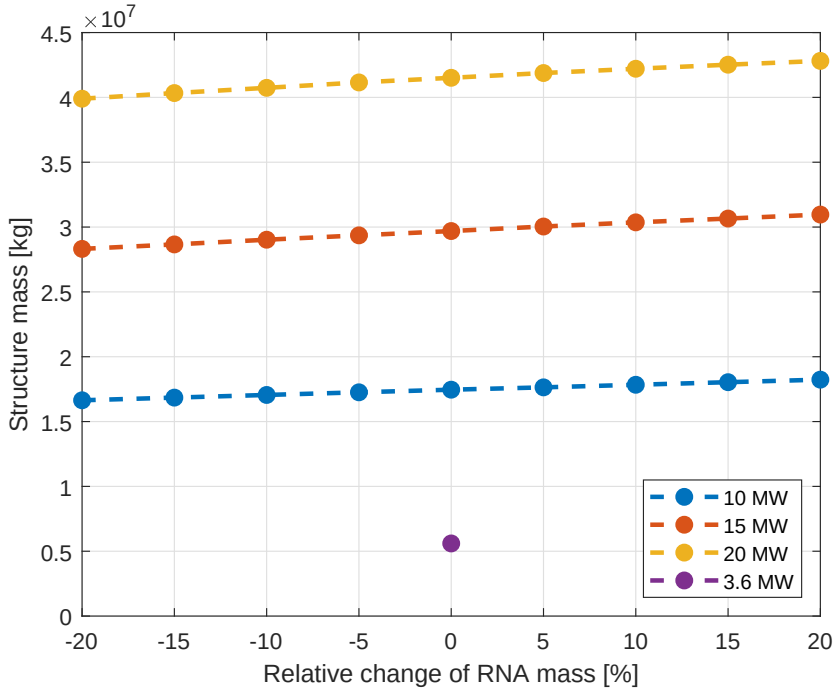

Figure 6.6: Relative change of RNA mass with resulting structural mass.

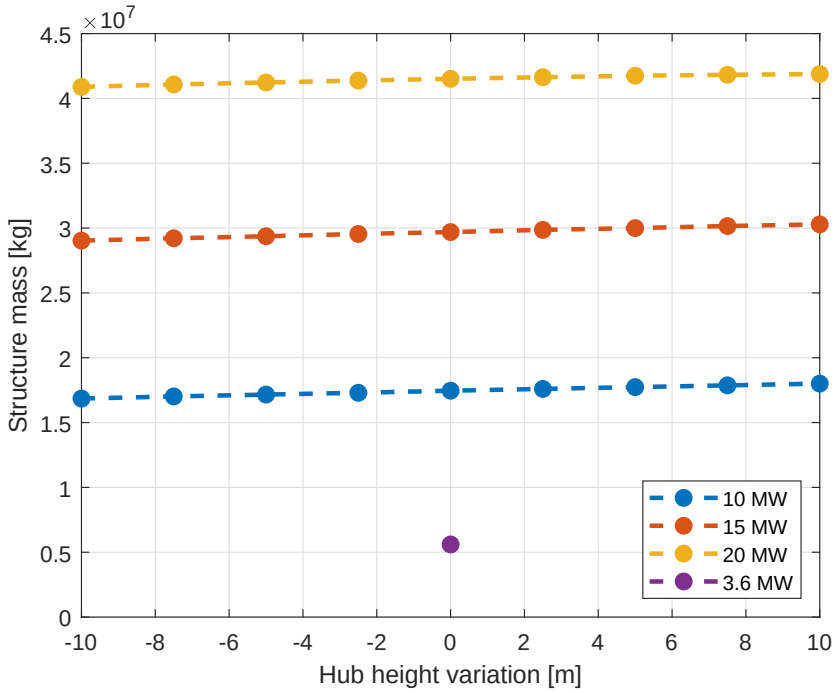

Figure 6.7: Change of hub height and resultant upscaled structures.

In contrast to bottom fixed WTGs, FOWTs can rise and fall with waves, surges and tides and follow the elevation of the water surface. The RAOs for heave show that the TetraSpar concept designs have a reasonable first order amplitude response for more severe weather situations, i.e. for large and long waves, the relative difference between blade tip elevation and highest wave elevation is bigger for FOWTs than for bottom fixed counterparts. This should allow a FOWT to have a relatively smaller air gap requirement than traditionally described. For the 3.6 MW TetraSpar demonstrator this is already the case, the lowest blade tip elevation is at about 20 m above still water level.

Figure 6.7 shows the change of hub height from the base case values as presented in Table 2.6 for a range of ±10 m, and the resultant masses of the upscaled structures. The design concepts in this sensitivity study do not change substantially, partially attributed to the relatively small changes in hub height compared to the absolute lever arm of the rotor to still water level. A 10 m difference on hub height for the generic 20 MW WTG design is only a 6% change in total length of support tower.

The resulting upscaled structures only vary up to 3% in mass comparatively to the base-case designs. This discrepancy can be resolved by taking the fundamental equation for stability and structure's internal restoring moment into account. As stability of the upscaled structures is calculated with the still water line as reference, the lever arms of the buoyant force upwards, and weight force downward is larger than the value for $\overline{GM}$ in between the COB and COG.

The result of this calculation is that the moments by the buoyancy and weight are significantly larger than the wind overturning moment as presented in Table 3.1. As an example, the base case 10 MW TetraSpar is designed for a maximum overturning wind moment of 1.6×10^8 N m. With an COB at approximately 42 m and a COG at 53 m below the still water line, the additional overturning moment by buoyancy is is 6.4×10^8 N m, while the counter rotating moment overturning moment by the structure's weight is 8.0×10^8 N m. The 15 MW and 20 MW design concepts show similar ratios of wind overturning moment to internal structure restoring moments.

6.3.5. Maximum aerodynamic thrust

Shown in the previous section, the effects of alterations in lever arm of the wind overturning moment do not produce significant variations in total structure design. The overturning moment however is calculated by the product of both a lever arm and a force applied. The force of maximum aerodynamic thrust key to the upscaling methodology is calculated by a simplified version of Equation 3.5. Depending

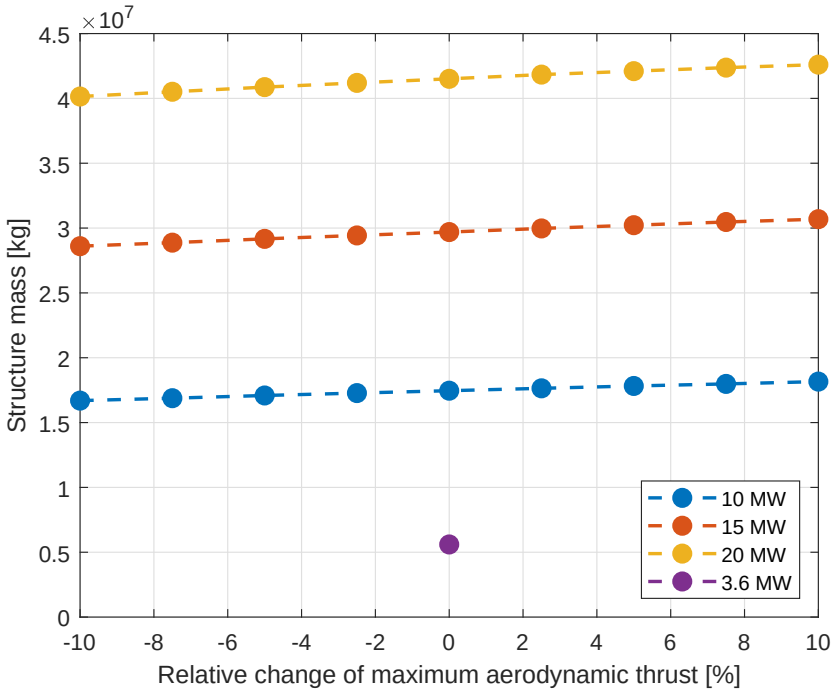

Figure 6.8: Relative change of maximum aerodynamic thrust at rated wind speeds and resultant upscaled structures.

on terms like OEMs, WTG designs and rotor-blade pitch control strategies, the aerodynamic thrust at rated wind speeds may vary between WTG models for similar power output figures.

Figure 6.8 presents the relative change in total structure mass of the design concepts, for variation of wind thrust of ±10% for the three selected power ratings. Similar to differences in lever arm, a relative change in force onto the wind turbine affects the total structure in a limited manner, with variation up to 4% in structural mass for a 10% change in aerodynamic thrust. A similar explanation given for the previous sensitivity study on hub height is applicable; the wind overturning moment is substantially smaller than the structure's internal moments by buoyancy and weight.

6.3.6. Keel density

The fifth sensitivity analysis on the density of the ballasted keel, and in particular the amount of steel in the keel. Up to now, one of the key assumptions for the upscaling design methodology is the constant diameter over wall thickness ratios for all braces of the TetraSpar (as described in Appendix A). As explained in Figure 6.2, this assumption may be particularly disadvantageous for the TetraSpar design as it results to arelatively large steel mass for an increase of structure size compared to other technologies. this also partly explains why scaling trends of the TetraSpar are not in line with other academic scaling trends for primary steel mass, i.e. the substructure primary steel mass to power rating ratio decreases for larger wind turbines (see Figure 1.4).

Critically analysing the resulting upscaled structures in Table 3.1 shows that approximate 40% of the total steel mass of the structure originates from the keel. The suspended keel's primary function is to act as a dead weight, provide enough mass and lower the structure centre of gravity to stabilise the platform. While steel is a significantly denser material than the other ballast materials used for the TetraSpar, it is also a relatively expensive material for dead weight compared to concrete and water. A counter weight designed with a high amount of steel is efficient in terms of required volume, but is expected to be substantially more costly.

To investigate the potential of decreasing the amount of primary steel for the TetraSpar design concepts, a sensitivity analysis is performed by varying the D/t-ratio for the keel braces. The keel braces are still designed and ballasted with enough concrete to achieve neutral buoyancy, and the remaining inner volume of the cylinders is filled with sea water. A higher D/t-ratio indicates a cylinder with thinner walls and less steel, but requires a larger volume of concrete to achieve neutral buoyancy,

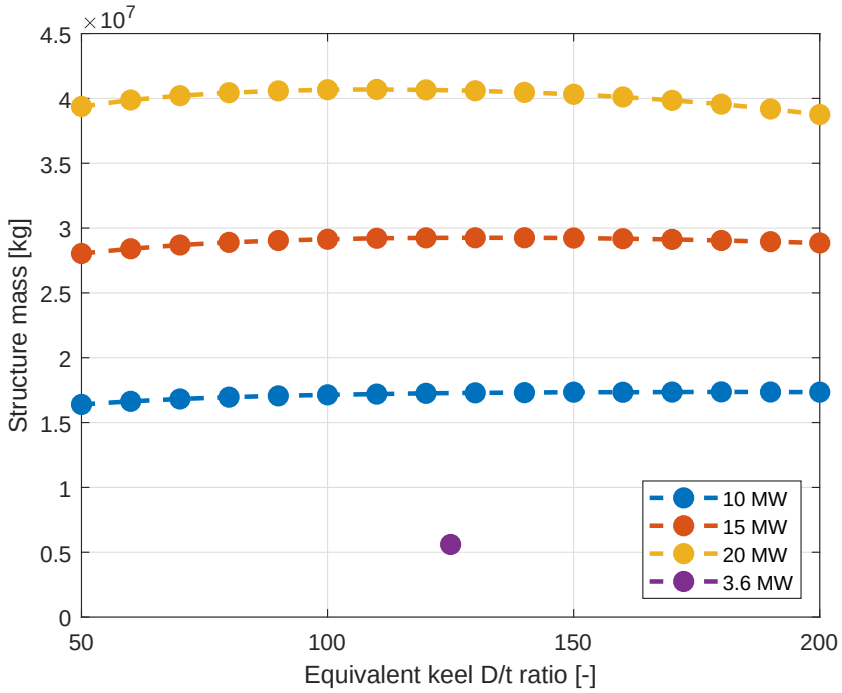

Figure 6.9: Variation in D/t-ratio of the keel braces, and resulting (ballasted) structure mass.

and has a lower total density figure once filled by water.

Figure 6.9 and Figure 6.10 present a change in structure mass and substructure steel mass respectively, for a variation of the D/t-ratio of the keel braces in a range of 50 to 200. Some interesting results arise from this sensitivity study. It is noted that results presented for the 20 MW upscaled model for a D/t-ratio larger than 150 may not be completely representable, since numerical errors in the physical models may cause discrepancies in trends compared to the results for the 10 MW and 15 MW design concepts.

The results presented in Figure 6.9 consider the total ballasted strucutre mass of upscaled design concepts. For keel braces with thicker walls than the base-case, the structure mass decreases by a few percent. This effect is be contributed to the result of a higher D/t-ratio and the subsequent increase of the keel density. As a result, the keel requires less volume to achieve a similar mass. Figure 6.11 shows the variation of keel diameter for a change in D/t-ratio. This reduction in submerged keel volume affects the stability mechanism of the TetraSpar and upscaling methodology. The stability design driver for the design concepts is proportional to the location of the centres of buoyancy and gravity. A denser keel raises the centre of buoyancy, thus increasing of the metacentric height $\overline{GM}$. Therefore a smaller amount of total structure mass is required to create enough restoring moment to counteract the wind overturning moment.

For larger D/t-ratios the effect is not as apparent: the density of the ballasted keel flattens for larger ratios. The keel diameter does not change compared to the base-case of $D/t = 125$, no significant variations in the structure's centre of buoyancy appear thus no changes in total structural mass are found in Figure 6.9.

The other major effects captured by changing the keel density is the reduction in steel mass, shown in Figure 6.10. As stated earlier, approximate 40% of the total steel weight of the base-case design concepts is by the suspended keel. By changing that parameter through the D/t-ratio, the total steel mass may increase by more than 50% at lower D/t-ratio numbers, or may decrease by over 20% for higher D/t-ratio numbers considered in this study. Variation of the up to now assumed constant D/t-ratios for all braces might be a high potential improvement for both economic and technical feasibility of the TetraSpar concept as stated earlier.

As stated earlier for context and explanation on Figure 6.2, the upscaled TetraSpar design concepts

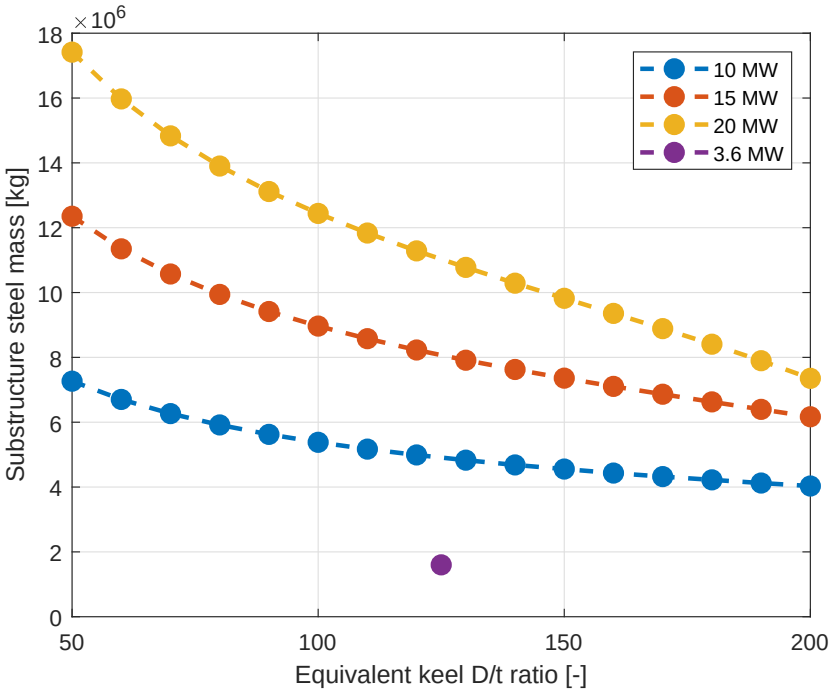

Figure 6.10: Variation in D/t-ratio of the keel braces, and resulting (empty) steel mass of substructures.

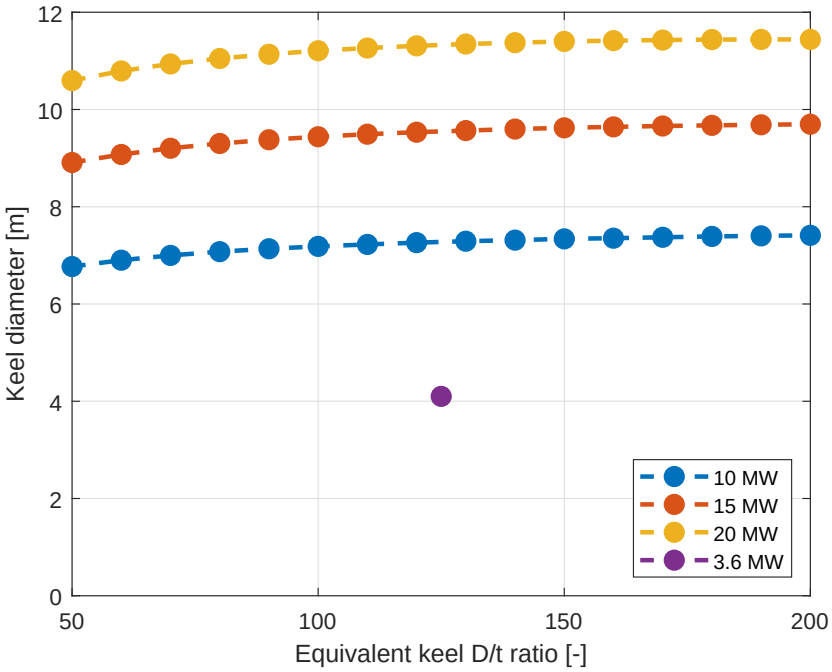

Figure 6.11: Variation of diameter of keel braces as function of D/t-ratio.

thus far lose the relative advantage in steel mass for larger floaters compared to other technologies, and show an increase of steel mass per power rating contrary to the general trends for FOWTs as presented in Figure 1.4 by Spearman and Strivens (2020). Figure 6.2 is reproduced to study how a variation in keel D/t-ratio affects the TetraSpar in contrast to other FOWT technologies.

The shaded areas of Figure 6.12 indicate the range of substructure primary steel in absolute numbers and normalised per per rating for range of keel D/t-ratios between 70 and 180, and the primary steel masses of other FOWT designs. The figures show that the TetraSpar is sensitive to alterations in the amount of steel applied in the structure, and subsequently to the competitiveness of the design in relation to other floaters. The lower bounds of the shaded areas in Figure 6.12 indicate a ratio of $D/t = 180$, a reduction of 30% in wall thickness in the keel compared to the base-case design concepts. This reduction lowers the normalised trend of primary steel mass over power rating for the upscaled design concepts to a value of approximate 1. Contrary to the base-case design concepts, a value of 1 indicates that for a larger structure the amount of primary steel in the floater does not increase relative to power rating, thus a larger structure is not disadvantageous on economic feasibility, opposed to the results of section 6.2.

The wide range of D/t-ratios indicates that the TetraSpar has potential to hold an advantage as a lightweight structure, both in terms of structure mass (see Figure 6.1) and primary steel, but requires a relative decrease in the amount of structural steel required. It is expected that a change of the D/t-ratios for other braces than the keel has similar effects on the primary steel mass, albeit for smaller differences compared to the base-case design concepts, as the keel braces are the largest structural elements. Altering all D/t-ratios could be a solution to further bring down the normalised trend line of Figure 6.12 for the TetraSpar towards the average FOWT trends described by Spearman and Strivens (2020). However, detailed static, dynamic and structural analysis on actions and strengths of upscaled TetraSpar designs are required to utilize the full potential of the structure.

6.4. Discussion

The main points of evaluation and discussion in this upscaling design exercise for the TetraSpar are focused on the research objectives and questions, design considerations and requirements as discussed in the introduction.

This section reflects upon the main design and analysis steps of the upscaling design methodology developed for this thesis work starting from the hydrostatic analysis. The evaluation includes a review on the assumptions, the validity of the results presented and if the overarching objectives are met.

6.4.1. Hydrostatics

In chapter 3 the floating platforms are designed based on hydrostatic equilibria in vertical and rotational direct: the structure stays buoyancy and it will not heel too much at rated wind speeds. Assumed for the TetraSpar, the static stability is defined by the wind thrust and the structure's weight and buoyancy capacity, and neglecting the stability contribution by the water plane area.

The developed algorithm to generate the upscaled design concepts and calculate the stability parameters is compared and tuned with stability calculations for the 3.6 MW demonstrator design. The physical model for this step is created in Matlab based on analytic calculations only. No specialised design software on hydrostatic is used to verify the results, except for a 3.6 MW design concept by the algorithm against the existing demonstrator design. Expectations are that smal deviations may appear for larger structures, given the rather simplistic cylindrical shapes of the TetraSpar braces.

In the TetraSpar upscaling algorithm the stability contribution by the water plane is assumed to be negligible. However, the resulting static stability performance indicator of $\overline{GM}$ during the operational spar configuration is higher than strictly necessary, as the value of $\overline{BM}$ increases enough to be of significance. This is largely due to the assumed increase in diameter for the diagonal braces. If these braces could be reduced in diameter for weight savings and decrease the exposed structure area near the waterline, the difference in scaling by the TetraSpar upscaling algorithm and the resulting $\overline{GM}$ value reduces.

The other static stability indicator of $\overline{GM}$ for installation shows a decreasing trend towards larger substructures, which could indicate that the TetraSpar in semi-submersible configuration becomes less stable for larger wind turbines. Even though the metacentric heights for the upscaled design concepts are positive, these stability parameters are significantly lower than the 3.6 MW design. This outcome is

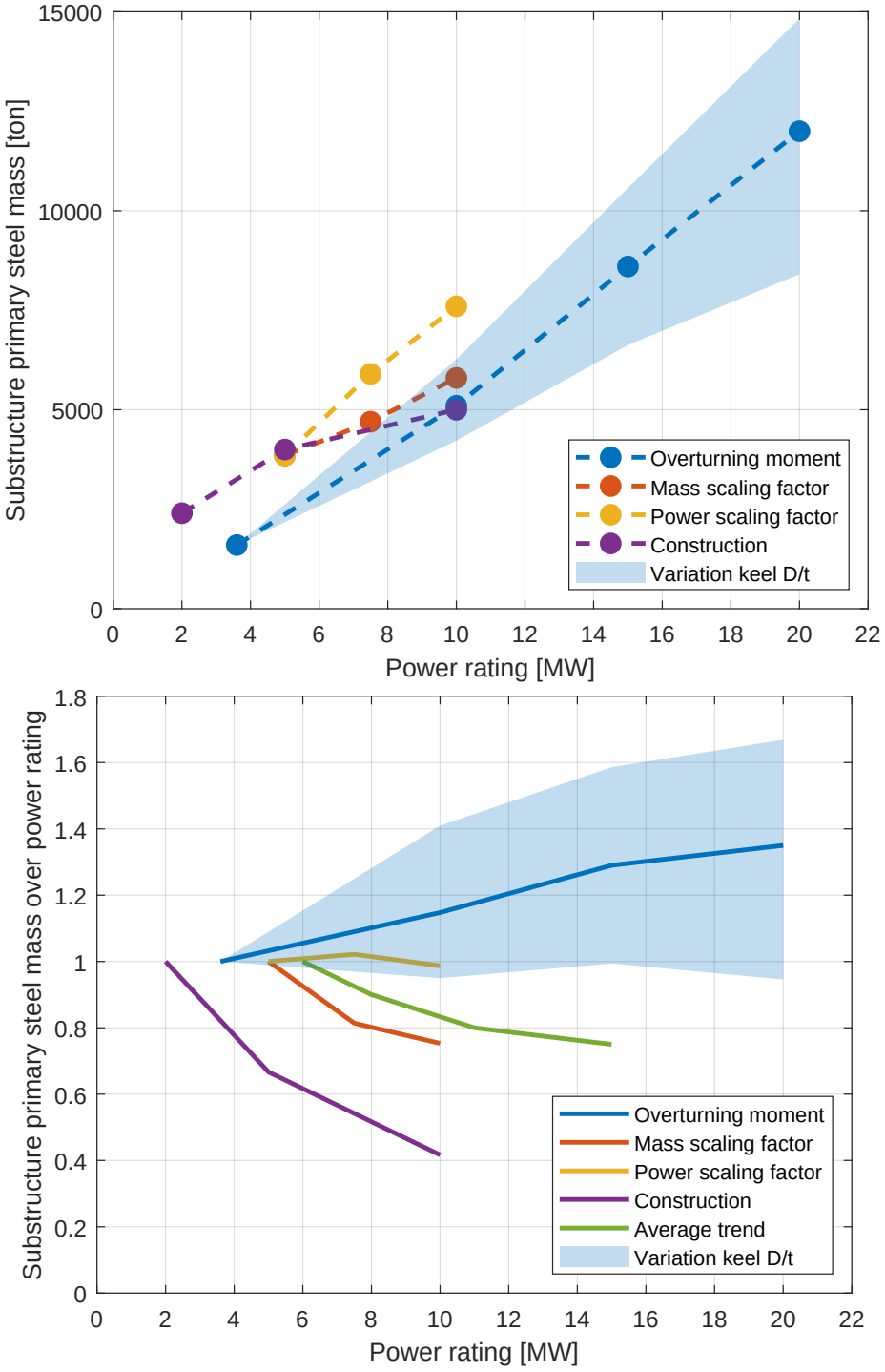

Figure 6.12: Comparison of steel mass for TetraSpar design concepts (in blue) to other upscaling design methodologies, including a shaded area indicating a variation of keel D/t-ratio between 70 and 180.

expected based on subsection 2.4.2: the TetraSpar is upscaled based on the stability mechanism of a spar by varying the centres of gravity and weight of the structure, and does not consider stability in the semi-submersible configuration. As the water plane area moment of inertia remains relatively similar to that of the the demonstrator, the result is that during installation the structure might be less stable.

Strictly speaking, as these values for metacentric height are still positive, the though the values are still positive, these values are significantly lower than the 3.6 MW demonstrator. This might indicate that larger TetraSpar designs may require additional floatation devices to ensure enough stability while the structure is towed to site. However, for semi-submersibles a static stability value of $\overline{GM}$ is not enough, as the stability parameter varies significantly when the structure rotate due to a changing water plane area. For a more detailed analysis a $\overline{GZ}$-curve is required, often analysed by specialised hydrostatics software, to quantitatively determine the stability of the TetraSpar design concepts during tow and installation.

One of the major topic out of scope, but with a substantial effect on the hydrostatics of a floating structure is the mooring system. Many mooring systems function by a heavy line that creates a restoring force when it is lifted from the sea bed. The weight of the suspended part of the mooring line acts as additional ballast to a floater, and increases the structure's draught. If a mooring system is developed for the TetraSpar, another iteration on hydrostatic design is required to account for the addition weight, which in turn affects the size and displacement of the floater.

Lastly on hydrostatics and the upscaling design methodology applied to the TetraSpar, is that the density of each structural element remains constant and are assumed to be straight cylinder, as two of the key assumptions on the upscaled design concepts. This takes into account the structural stiffeners and joint nodes at the ends of all braces for the 3.6 MW demonstrator, but it does not consider any other changes in volume and mass of the braces than purely an increase of diameter. If new joint types, nodes or other structural elements are designed for upscaled concepts, the mass and volume of these braces are affected and will result in different requirements for buoyancy and weight.

6.4.2. Hydrodynamics

The resulting hydrostatic stable designs are evaluated as panel models by WAMIT. Overall, no immediate challenges are observed on dynamic behaviour, and the first order responses at the design conditions are within any extremities. Thus far, the motions and behaviour of the TetraSpar have been discussed only as wave-structure interaction as calculated by WAMIT panel models. The WAMIT free floating analysis approach discards two other major contributors towards the dynamics of the structure: mooring system and wind turbine. Results of the hydrodynamic analysis by WAMIT are reviewed at length in subsection 4.5.3, therefore this section focusses on the other aspects to discuss within the dynamics of the structure.

The results by WAMIT presented for the design point only regard a wave climate corresponding to a hub height wind velocity of $11\,\mathrm{m\,s^{-1}}$ for a JONSWAP spectrum. The functional requirements and design criteria of chapter 2 state that the structure should be able to operate in a range of wind speeds, and survive an metocean enviroment with a 50-year return period. Furthermore, DNV GL (2018) lists a set of design load cases for the full envelope of scenarios a FOWT may experience, including wind-wave misalignment, (partial) failure of subsystems and damaged structures. These cases have not been determined by the WAMIT calculations of this report, as WAMIT considers a more generic situation and only wave-structure interaction.

Even though the RAOs for the upscaled design concepts do not show fundamental challenges in terms of translation and rotation over the entire wave spectrum, a high-fidelity physical model including all aerodynamic, hydrodynamic, higher order effect and (non-)linear structure dynamics is required to evaluate the validity of the structure for the metocean design conditions.

Another topic of discussion within the hydrodynamics of the TetraSpar is during installation and tow-out. This thesis work focused on the upscaling and performance of the structure while it is in the operational spar configuration, not for the installation configuration. It is expected that the hydrodynamic behaviour of the TetraSpar in semi-submersible configuration is vastly different to the spar. Due to the larger water plane area, the stiffness restoring coefficients of the TetraSpar during tow-out are significantly higher. This leads to lower natural periods of the structure, potentially within the wave exciting periods.

Furthermore, numeric analysis and model tests of the 3.6 MW demonstrator show that for the tow-out configuration of the TetraSpar, the motions and dynamic behaviour are not described by a single rigid body but as two bodies of keel and floater plus WTG. As the keel is not yet ballasted, the tensile forces in the suspension lines are low and the keel is not stiffly connected to the floater. It is challenging to model and describe the dynamic behaviour for this situation as a two-body system. This has not been addressed in the hydrodynamic analysis of the upscaled design concepts, but is essential to determine the weather window and installability of the TetraSpar in more detail.

6.4.3. Structural design

The simplified analysis on the structural strength of tubular members shows promising trends for the possibility to shave off some structural steel, and decrease mass and costs when considering (ultimate) strength. This however is only a first rough analysis on structural strength and design, more effort is needed to first develop a detailed design of the primary steel, including the essential TetraSpar nodes to join the elements together, stiffeners of the thin-walled cylinders and the behaviour of shell structures.

Another effect of upscaling, and the inherent increase in dimensions of structural elements is the thickness effect and the relative decrease of fatigue strength. When a high fidelity design of a up-scale TetraSpar concept is developed, additional interest into the fatigue strength of critical members is needed, considering this effect.

Furthermore, an analytic approximation to non-linear and empirical phenomena concerning vortex induced oscillations indicate that larger TetraSpar designs may be more susceptible to vortex induced hull motions as the frequency of vortex shedding is within the range of natural periods of the rigid floating structure. On the other hand, vortex induced vibrations seem to be less likely to occur as braces are stiffer due to an increased dimension.

In all, the first draft structural design analysis does not arise any fundamental issues for upscaling of the TetraSpar structure, but it is the details that matter the most for the structural design. These are not addressed within the scope of the project, and require more research and development.

6.4.4. Upscaled TetraSpar designs

To conclude the discussion, other aspects than the three majors topics are examined that result from the upscaled design concepts. This includes costs, manufacturing, fabrication and installation of the TetraSpar upscaled design concepts.

Reflecting to section 6.2 it shows that the specific costs, that is capital expenditure per power rating, for the base-case upscaled design concepts increases towards larger structures, contrary to the generalised trends argued by literature. However, as indicated by the sensitivity studies, relative small changes and optimisations may lead to favourable specific cost trends for the TetraSpar as well.

Furthermore, the figures for capital expenditure are not complete as many other systems and components are omitted from a functioning FOWT. Based on Myhr et al. (2014), it seems that the wind turbine generator and substructure combined account approximate 75% of the total capital expenditures for spar and semi-submersible platforms, the rest is for components like mooring system, anchoring, installation and export cables. The latter items are specific to location, environment and project size, but overall it is expected that the capital expenditure figures of Table 6.1 are substantially lower than the final costs will be.

In terms of fabrication, no direct challenges of the manufacturing of cylindrical braces are identified. One criterion is that no brace can be larger in diameter than the tower base diameter. This originates from the starting point that the cylindrical braces are to be fabricated by the same processes as support tower sections; if the support tower can be constructed with a certain diameter, than the assumed limit of the process is that maximum diameter. The maximum brace diameter of the TetraSpar upscaled design concepts all are smaller than the assumed tower base diameters, and the criterion is met. However, this approach does not take into consideration of the fabrication of the nodes and joint connections. Expected that these structural element also have to increase in size to fit the upscaled braces, and provide enough strength to withstand the increased loads of the structure.

Another challenge may arise during the assembly of the TetraSpar structure. The design of the floater lends itself to be assembled and erected quayside, then launched into the water. During assembly the floater rests in a yard, often on compacted soil. Compared to the 3.6 MW demonstrator, the

upscaled floaters' mass increase by a factor three to seven. As the total area of the TetraSpar remains relatively constant, the loads acting onto the yard floor will increase by a similar factor.

The last hurdle identified considers the installability of upscaled TetraSpars. Because all braces increase significantly in diameter, the installation method with a lifted keel underneath the floater may become more challenging. Typical water depths in industrial harbours are in a range up to 12 m to 18 m, following size limits for maritime shipping like the (New) Panamax standards.

In semi-submersible configuration with the radial and lateral braces partially submerged, the minimum draught is approximate 14 m for the 15 MW TetraSpar design concept, and over 16 m for the largest 20 MW design. These minimum draughts have significant impact on the number of locations a upscaled TetraSpar can be assembled and completed if the current installation methodology is kept for larger structures. The study by Villaespesa et al. (2018) investigates multiple configurations of floater and keel during tow out, and found that a keel located behind the floater may decrease hydromechanical loads during installation. This could also be an option to reduce the minimal draught of the TetraSpar during installation, but may require complex activities in open waters to secure the keel to the floater for the transformation from semi-submersible to spar.

7

Conclusion and recommendations

The offshore wind industry is advancing to bigger turbines, farther offshore and into deeper waters, and with the next frontier in floating offshore wind turbines these trends will only continue. One promising concept to combine absolute growth of wind turbine generators, and harness the vast potential of deep-water wind energy is the floating TetraSpar platform. This thesis work develops a novel design methodology to upscale the existing 3.6 MW TetraSpar design, in order to accommodate wind turbines generators of 10 MW, 15 MW and 20 MW, and concludes that, within the scope of this research, no fundamental technical showstoppers are identified to upscale the TetraSpar.

Key to the newly developed upscaling design methodology are the fundamental equilibria in vertical and rotational direction: buoyancy is equal to structural weight, and the internal restoring moment is equal to the external overturning moment.

Contrary to previous academic research, generally applying geometric scaling factors derived from the square-cube law for WTGs, the upscaling design methodology in this thesis work is based the primary design driver of maximum aerodynamic thrust at rated wind speeds, and the subsequent maximum overturning moment by wind. Utilising rules-of-thumb, e.g. fixed brace lengths and brace densities, the suspended keel of the TetraSpar is enlarged to counteract increased overturning moments caused by larger WTGs. A developed algorithm for upscaling models the physical interplay between weight, buoyancy and distances between the centres of gravity and buoyancy and searches for a design point. Here, the internal restoring moment of the structure balances the external maximum overturning moment by wind, for a heel angle of 5.0°. Table 7.1 presents a summary of the upscaled design concepts, next to the 3.6 MW demonstrator. An approximate linear relation between structure mass and power rating is identified.

The resulting upscaled design concepts are analysed as free-floating structures on first-order wave-structure hydrodynamics by a diffraction/radiation solver. The computed RAOs show no challenging dynamic behaviour of the TetraSpar in heave and pitch within the operational range of the WTGs, with heave translations in the order of 0.5 m and pitch rotations between 0.2° to 0.6° by waves for the design environment. Free-floating natural periods in these directions are the range of 30 s to 43 s, well outside the wave excitation periods.

Then the effects of upscaling onto the structural design are examined by a literature study on strength and fatigue. While fatigue strength of larger structural elements is decreased through the thickness effect, the increased stiffness of larger diameter braces indicate that the cylindrical structure elements hold ample structural strength for different types of action.

Table 7.1: Summary of masses of TetraSpar design concepts with keel at 65 m draught.

Power rating	MW	3.6	10	15	20
Structure mass	ton	5.6×10^3	18×10^3	30×10^3	42×10^3
Substructure steel mass	ton	1.6×10^3	5.1×10^3	8.6×10^3	12×10^3

Compared to other academic large-scale FOWTs with similar wind turbine generators, a TetraSpar is approximate 30% lighter in terms of ballasted mass. In contrast, the primary steel mass of the upscaled TetraSpar design concepts is similar in magnitude to other FOWT designs. Furthermore, the ratio of steel mass over power rating is disadvantageous for the initial upscaled designs of the TetraSpar. As the amount of steel applied in a marine structure is a reasonable indicator of total capital expenditure, the economic feasibility of upscaled TetraSpar designs decreases for larger structures.

As the structure progresses towards larger WTGs of 15 MW to 20 MW, other challenges arise in aspects which are not directly limiting for the demonstrator project. For example, the minimum draught for these upscaled design concepts is approximate 15 m, about equal to the water depths of typical ports. Also, the physical dimensions of cylindrical braces with diameters larger than 10 m may be problematic during fabrication and assembly. In addition, the stability parameter of the floater decreases significantly for the tow-out configuration of the TetraSpar. This may restrict the weather window for the TetraSpar as semi-submersible to be installed.

Trade-offs and design choices that impact the structure design substantially are, e.g. an increased keel draught, a higher maximum heel limit for rotation by wind, and a reduction of wall thicknesses of structural elements far away from the water line. Variations of aspects like aforementioned will improve both technical and economic feasibility of the TetraSpar for larger floating offshore wind turbines in future iterations, and enhances the competitiveness of the concept.

Recommendations

From the findings in this research, insights gained through experience and conclusions formed by this thesis work, a set of recommendations are formulated. The recommendations are divided into two groups, following the twofold thesis problem statement: for the generalised upscaling design methodology, and the TetraSpar platform concept in particular.

On the upscaling design methodology

- From sizing trends on wind turbine generators, it is found that the square-cube law is not an accurate prediction for future, large-scale wind turbines. Power rating is proportional to the rotor diameter squared, WTG mass is not proportional to rotor diameter cubed due to advancements in WTG technology. It is recommended to apply an upscaling methodology based on other key design drivers than the square-cube law like overturning wind moment. It is expected that this practice delivers more representative and substantiated results.

- Collaborate with OEMs of wind turbine generators to determine maximum allowable heel angles from the perspective of the WTG, based on maximum inclinations, rotations, accelerations and loads for RNA, support tower, rotor blades and other subcomponents. It is shown that the maximum static heel angle by wind overturning moment has significant impact on the total size of the structure, any improvement or increased definition on this regard enhances the potential of FOWTs.

- It would be interesting to evaluate how the upscaling design methodology based on overturning moment can be applied for FOWT concepts with a fundamentally different stability mechanism than the TetraSpar. Which design choices are key to balance the structure, and how does the substructure design adapt to an increased wind overturning moment.

- With limited resources, a diffraction/radiation model of a floating substructure is a fair analysis tool for a first-order estimation on the dynamic behaviour by wave-structure interaction. The physical modelling of a floating structure is rather limited, as it discards any environmental forcing above the mean water line nor incorporates higher-order effects. Especially for more extreme conditions in storms, considering higher-order waves with storm surges and currents, and turbulent winds a first-order radiation/diffraction analysis tool is not sufficient.

  For a more comprehensive model with functioning mooring systems, actively controlled wind turbine generators and flexible structure elements, a coupled aero-hydro-servo-elastic time-domain solver is advised. This approach requires a high-fidelity physical FOWT model, including detailed properties of the structure, a mooring system, export cable and wind turbine generator.

- Contrary to academic expectations, the economic feasibility for larger FOWT structures is not immediately beneficial for increased power ratings. It is advised to generate simplified parametric cost figures for (sub)components of FOWTs to assess the economic feasibility of a new FOWT design early on during project development.

- Research and development into floating offshore wind structures is fast paced, with new findings and insights reported on weekly bases. The relatively high number of recent publications and sources cited in this thesis work is an example of the advancements made in this field. It is important to stay up-to-date with the latest available knowledge and data, as it might provide new insights throughout the project.

To the TetraSpar developers

- Focus in the design, research and development on lightweight structure engineering and search for ways to reduce the primary steel weight. The current 3.6 MW demonstrator is a lightweight structure in terms of steel mass compared to other platforms. This advantage shrinks for upscaled designs. The base-case design concepts show that relative amount of primary steel per power rating increases unfavourably for the TetraSpar, contrary to the general trends for FOWTs.

  One sensitivity study shows that a relative small change in the application of steel in the keel braces, the total steel mass can be reduced significantly. Extensive structural strength studies and analyses are required to determine if and where less steel is sufficient, while maintaining structural integrity.

- Consider a keel draught larger than current design. Given the fundamental stability mechanism of the TetraSpar, a deeper suspended keel and lower centre of gravity shows potential to reduce both total structure displacement and empty steel mass for the substructure. The trade-offs are a lower maximum heel angle in terms of no-slack requirement for the suspension lines, a deeper minimum water depth for deployment, and another configuration of export cable routing.

- Explore the opportunities, limitations and risks of larger structures in the fabrication, assembly and installation phases of the project. A structure with longer braces and a larger footprint may be beneficial to decrease the brace diameter, but could be limited by the maximum width of yards and ports. An overview of maximum dimensions of floating structures for construction yards and ports in regions with a high potential for floating wind is worth to investigate upon.

- For upscaled TetraSpar designs, consider other configurations of floater and keel during the tow-out phase than currently planned. As braces must increase in diameter to generate enough displacement, the minimum water depth for the TetraSpar in tow-out, with keel suspended directly under floater, increases to a point that many conventional ports cannot accommodate the floating structure. Other tow-out configurations may also provide different advantages in hydrodynamic loads and floater behaviour, but may simultaneously induce greater risks for connecting keel and floater while in open waters.

- Study other methods to ballast the keel than the current system of partially solid ballast and partially sea water. An increase of the effective density of a ballasted keel reduces the volumetric dimensions of the keel, therefore reduces the minimum structure draught while in port. An added benefit is that the total displacement of the structure reduces, which is advantageous in terms of hydromechanic forces. If the neutral buoyancy requirement for the keel is discarded, temporary floatation devices during installation phases can provide the required buoyancy.

- Research different configurations of keel suspension lines to account for increased loads, and include redundancy or fail-safe options. The submerged weights of the ballasted keel increase linearly compared to the 3.6 MW demonstrator, and induce significantly higher tension loads in the lines. Assuming a similar configuration of six lines, the static load in one line for the 20 MW design concept is larger than the combined static tensile loads for all six lines of the demonstrator structure.

- Consider the option of temporary floatation devices for upscaled TetraSpar designs during installation. When the outer dimensions of an upscaled floater are kept equal to the demonstrator

structure, the static stability parameter for tow-out reduces drastically, and the semi-submersible configuration may not be stable enough on its own during the transition between port and production site. Temporary floatation devices need to add a substantial amount of water plane area moment of inertia to improve the stability of the structure. The temporary floatation devices should not induce any natural periods of the semi-submersible configuration within the wave exciting period range.

A

TetraSpar upscaling guidelines

The upscaling procedure for the TetraSpar case-study requires a combination of ground rules, assumptions, rules of thumb, criteria and other scaling principles to generate the upscaling design concepts. This appendix summarises all aspects as upscaling guidelines specific for the TetraSpar.

A.1. Wind turbine generator

Starting with the superstructure, the dimensions for the generic WTG designs used for the upscaling procedure are derived on the sizing trends identified in Figure 2.4. From there on, the following steps are taken:

- For a given power rating, the rotor diameter is derived based on the sizing trends of commercial WTG designs, $P \propto D_{rotor}^2$.
- The RNA mass for the generic upscaled wind turbines is defined based on the trends of commercial WTG designs in the historical relation between rotor diameter and RNA mass, $m_{RNA} \propto D_{rotor}^{2.3}$.
- Hub height is defined by the rotor radius, plus a 30 m air gap between mean sea level and lowest blade tip elevation, $z_{hub} = \frac{D_{rotor}}{2} + 30$. This figure is based on the required air gap for bottom-fixed wind turbines as rule of thumb. Floating wind structures may allow for a smaller air gap, as they can follow slowly changing water levels, like tides and storm surges.
- Support tower mass and tower base diameters are based on the academic reference models by Bak et al. (2013) and Gaertner et al. (2020) for the generic 10 MW and 15 MW designs respectively.
- The dimensions for support tower of generic 20 MW WTG are linearly extrapolated based on the aforementioned reference models.
- Centre of gravity for the RNA are located at hub height, for the support towers this location is approximated at an elevation equal to 40% of the length of the tower.

A.2. Floater

The primary function of the floater is to generate enough buoyancy to equalise the (submerged) weight of the complete structure including ballast. To adhere to the idea of geometric-similarity essential to upscaling, the upscaled designs for the floater are guided by the following aspects:

- The tetrahedral shape and outer dimensions will remain equal. The equilateral triagular base of the floater with sides of approximately 60 m in length is deemed to be a soft limit on installability. Expectations are that an increased width will dramatically decrease the number of construction harbours suitable to the TetraSpar.

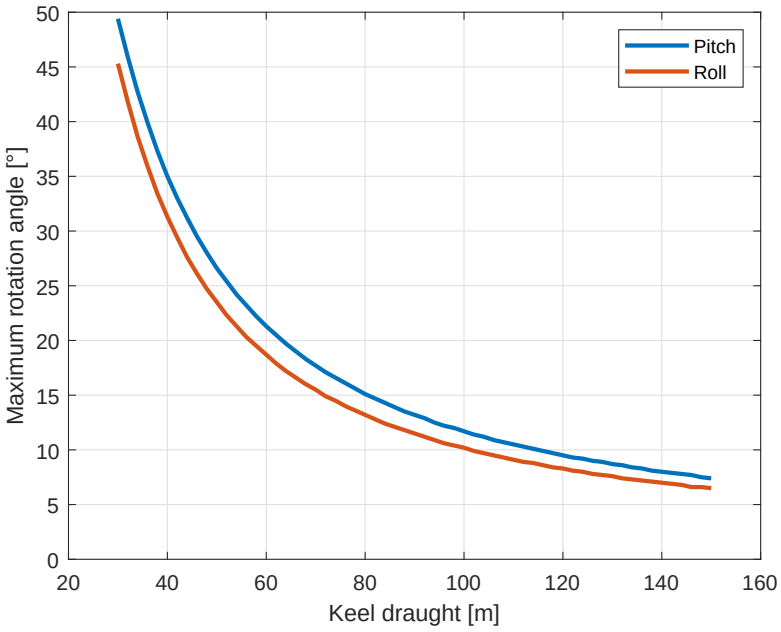

Figure A.1: Relation between keel draught and maximum rotation angle in pitch and roll to account for the no-slack in tension lines requirement.

Table A.1: Specific density and equivalent diameter over wall thickness ratios for unballasted,steel braces for the base-case TetraSpar design.

		Centre column	Diagonal	Radial	Lateral	Keel
Specific density	$kg\,m^{-3}$	365	390	335	215	250
Equivalent D/t ratio	-	85	79	93	144	125

- The length of the centre column stays at approximately 30 m in height, the desired draught for operational configuration of the floater is set at half length of the centre column. This ensures that the interface between support tower and substructure is above any extreme wave elevation, while the horizontal braces are permanently submerged.
- The centre column diameter is equal to the support tower base diameter, to avoid any further complications for the interface between super- and substructure.
- The diameter of diagonal braces is assumed to be half the diameter of the centre column.
- As consequence of the limit on maximum outer dimensions, the length of the radial braces will decrease to allow space for an increased diameter of centre column.
- The diameter of radial braces will remain 87.5% of the lateral brace diameter.
- The specific densities of each element will remain equal, based on the mass and volume of Table 2.2. This is to simplify and to include all stiffening elements, nodes and other primary and secondary steel features. Resulting specific densities and equivalent diameter over wall thickness ratios for slender steel cylinders is presented in Table A.1.

A.3. Keel

The suspended keel allows the TetraSpar to be towed to site as a semi-submersible, and act as counterweight to rotations when lowered and ballasted. The keel has a double function for the stability of the TetraSpar; it holds the majority of the total structural mass required for the internal restoring moment,

and is lowers the centre of gravity of the structure, and thereby increasing the metacentric height. The TetraSpar ability to counteract an overturning moment, the primary design driver for upscaling, is highly dependent on both depth and weight of the keel. The upscaling principles for the keel are:

- The length of the keel braces are constrained, for similar reasons as the floater.
- The keel structure starts as a thin-walled cylinder and is ballasted by concrete with a density of 2400 $\mathrm{kg\,m^{-3}}$, to achieve neutral buoyancy during the installation phases. As the steel weight density of the keel is approximately 250 $\mathrm{kg\,m^{-3}}$, about a third of the internal volume of each keel cylinder must be filled with concrete ballast for a density of 1025 $\mathrm{kg\,m^{-3}}$. When the keel is further ballasted for operations, the remaining two thirds of the internal keel volume is filled with sea water. This results in a ballasted keel density of 1700 $\mathrm{kg\,m^{-3}}$.
- The base-case for keel depth is equal to 65 m draught. The study by Pereyra (2018) shows that static pretension in suspension lines is a function of line geometry, and is dependent on the distance between keel and floater. A high static pretension is beneficial to the no-slack criterion and rigid-body assumption, and allows for larger rotations of the floater relative to the keel before a line loses all tension. Figure A.1 shows the relationship between keel draught and static heel limit for rotation around either the roll or pitch axis of the substructure, and based on the approach described by Pereyra (2018) for static equilibrium in all six degrees of freedom.

B

WAMIT modelling considerations

The usage of WAMIT as tool for linear, frequency domain modelling of wave-structure interaction requires some considerations to be taken into account. Like any other modelling tool, WAMIT does not describe the real world, but is able to describe some engineering parameter and aspects on wave-structure interaction within a limited scope. In addition to the analytic approximations for hydrodynamic modelling in section 4.2, the following appendix describes additional considerations concerning WAMIT (and MultiSurf) as main tool for hydrodynamic analysis on the TetraSpar design.

The main item of interest for WAMIT modelling concerns the modus operandi of the application itself: the panel method and the required discretisation of the body surface. All surfaces are divided into equilateral and flat panels to resemble the underlying body surface within some accuracy. More rectangular panels over a body will describe the surface with a higher accuracy. However, model panels does come at a cost of longer computation time as the number of equations to be solved increases with the number of panels. According to WAMIT (2006), the computation time increases exponentially for an increase in number of panels, and a trade-off between accuracy and speed must be sought for this analysis.

Consulted experts advise that WAMIT produces accurate results when panel sizes in length are approximate 1/8 to 1/10 of the incoming wave length. Below this threshold numerical errors may distort the computed results by WAMIT.

For this thesis, discretisation of the model is done in the CAD application MultiSurf, after which the model is exported to WAMIT. Figure B.1 shows an image in MultiSurf of the discretised centre column, in this case is the circle described the centre column discretised as an octagon. Through iteration it was found that all TetraSpar cylinders discretised into an eight-sided polygon delivers reasonable results at the design point with small numeric errors, while minimising computation time.

One way to visualise numerical errors in WAMIT is by plotting the wave exciting forces, as seen in Figure B.2 for heave of a 10 MW design concept as an example. Here the panel count is raised by increasing the number of rectangular sides for each cylinder. The numeric WAMIT model shows convergence, resulting heave forces for an increase in the amount of panels

The other clear numeric error observed is the erratic behaviour of the lines for wave periods in 0 s to 7 s, or wave lengths up to $\lambda \approx 80$ m according to the dispersion relationship. The results seem to be improve slightly for higher panel counts, but not significant. One reason might be that the size of the largest panel does not decrease significantly for WAMIT models with more panels, compared to the theoretical wave length. For the lowest panel count, the maximum panel diagonal is 21.7 m, while the model with the highest panel count has a maximum diagonal of 10.8 m, 7.18 m and 5.39 m. Following the advise by experts, the last three models should produce accurate results from a wave period of 7 s onwards.

The reason for selecting the model with 1680 panels, with cylinders discretised into an octagon, for all WAMIT modelling calculations is due to computation time. The results for this model are in line and within 10% margin compared to the higher panel count models, but its computation time is much shorter.

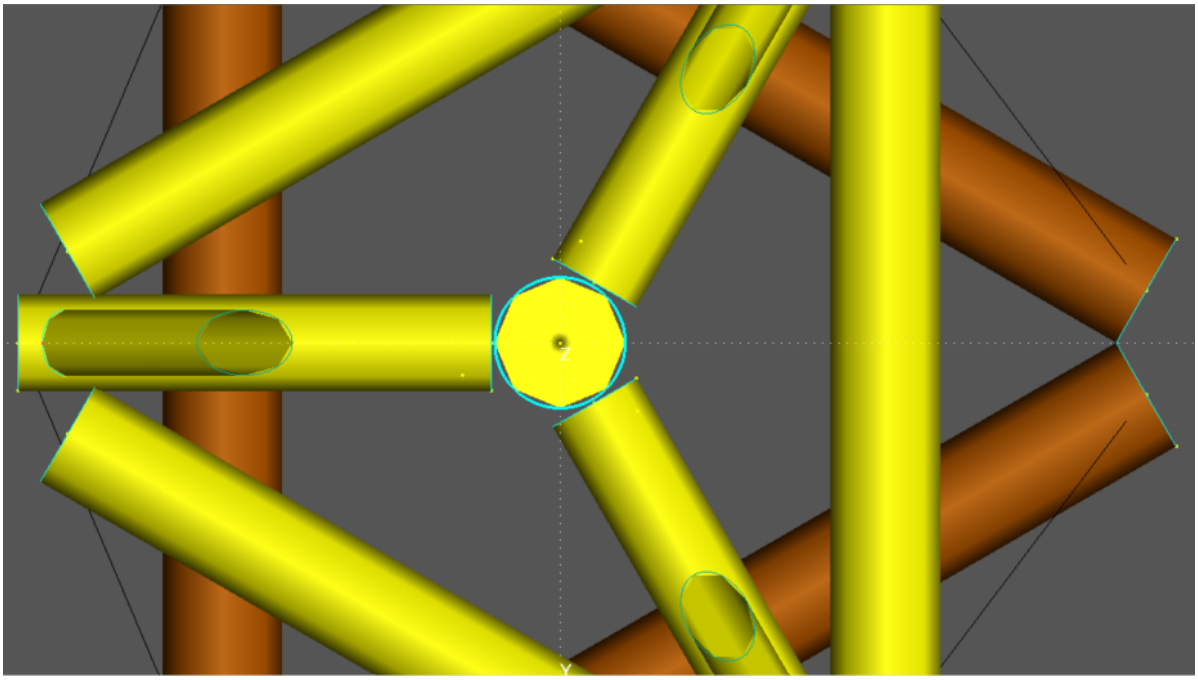

Figure B.1: Top view of MultiSurf model of a TetraSpar design concept. In the the middle the centre column, a cylinder discretised into eight circumferential panels.

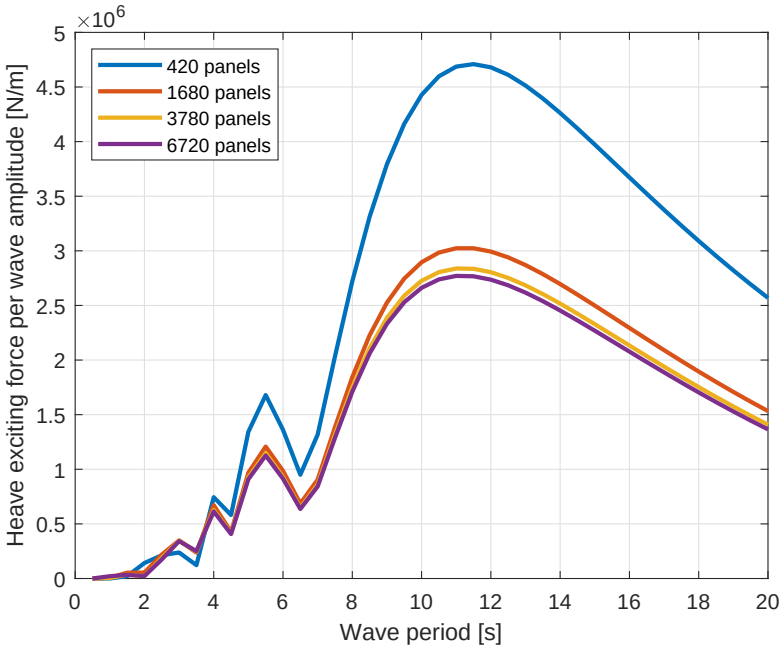

Figure B.2: Convergence study for WAMIT. Shown is the computed heave exciting force for a 10 MW TetraSpar model with increasing number of panels.

The model with the lowest panel count has a computation time of about 0.50 s per wave period, the 1680 panel model takes 5.5 s per wave period, 3780 panel model required on average 28 s of runtime per wave period, and largest model takes more than 90 s per wave period. To compute results like Figure B.2 with 40 time steps requires between 30 s and 1 h for increasing panel counts. Given the limited amount of time available, the second panel model delivers accurate enough results within the margin of error for this thesis, and significantly reduces the computation time.

The erratic behaviour up to 7 s could be smoothed by implementing a smaller time-step than $\delta T = 0.50$ s as displayed in Figure B.2. However, for now the area of most importance to the upscaled design concepts is within wave periods between 8 s to 15 s.

A consequence of the discretisation of all TetraSpar braces is the reduction in surface area of the polygon inscribed within the circle (see Figure B.1), and the decrease amount of volume of the brace. As WAMIT evaluates the volume of the descritised panel model, the diameters of the cylinder in MultiSurf have to be adjusted accordingly, to ensure that the area described by the polygon for WAMIT is equal to the area of the cylinder circle by the analytic upscaling designs. As the length of each cylinder is modelled correctly by MultiSurf, the volume for each brace in WAMIT/MultiSurf is equal to the analytic calculations. The diameters for MultiSurf D_{MS} are converted by:

$$D_{MS} = 2 \cdot \sqrt{\frac{\frac{\pi}{4} D^2}{n \cdot \tan \frac{\pi}{n}}} \cdot \sec \frac{\pi}{n} \tag{B.1}$$

Here, D is the brace diameter according to analytic calculations, and n the amount of edged of the polygon describing the cylinder. For an octagon D_{MS} is about 5.3% larger, while for a dodecagon, D_{MS} is only 2.3% larger than the analytic diameter.

Bibliography

Mairead Atcheson and Andrew Garrad. Looking back. In Joao Crus and Mairead Atcheson, editors, *Floating Offshore Wind Energy: The next generation of wind energy*. Springer, 2016.

Christian Bak, Frederik Zahle, Robert Bitsche, Taeseong Kim, Anders Yde, Lars Christian Henriksen, Morten Hartvig Hansen, Jose Pedro Albergaria Amaral Blasques, Mac Gaunaa, and Anand Natarajan. The DTU 10-MW reference wind turbine. In *Danish Wind Power Research 2013*, 2013.

Josh Bauer. NREL Market Report Finds U.S. Offshore Wind Industry Poised for Multigigawatt Surge, 2017. URL `https://www.nrel.gov/news/program/2017/nrel-market-report-finds-us-offshore-wind-industry-poised-multigigawatt-surge.html`. Online; accessed 20 January 2020.

Laura Cozzi, Brent Wanner, Connor Donovan, Alberto Toril, and Wilfred Yu. Offshore Wind Outlook. Technical report, International Energy Agency, 2019.

Eize de Vries. Haliade-X uncovered: GE aims for 14MW, 2019. URL `https://www.windpowermonthly.com/article/1577816/haliade-x-uncovered-ge-aims-14mw`. Online; accessed 30 November 2019.

Robert G. Dean and Robert A. Dalrymple. *Water wave mechanics for engineers and scientists*, volume 2. World Scientific Publishing Company, 1991.

Cian Desmond, Jimmy Murphy, Lindert Blonk, and Wouter Haans. Description of an 8 MW reference wind turbine. In *Journal of Physics: Conference Series*. IOP Publishing, 2016.

DNV GL. RP-C203: Fatigue design of offshore steel structures, 2014.

DNV GL. ST-0437: Loads and site conditions for wind turbines. 2016.

DNV GL. RP-C205: Environmental conditions and environmental loads, 2017.

DNV GL. ST-0119: Floating wind turbine structures, 2018.

DTU. Wind turbines to venture out into the deep sea, 2019. URL `https://www.dtu.dk/english/news/2019/04/dynamo_wind-turbines-to-venture-out-into-the-deep-sea?id=0875193c-4cf3-4f9f-9b8c-0d882c703d51`. Online; accessed 25 November 2019.

Equinor. Hywind Scotland 5 turbines at Buchan Deep, 2017. URL `https://communicationtoolbox.equinor.com/brandcenter/en/equinorbc/component/default/22936`. Online; accessed 28 March 2020.

Peter Frohboese, Christian Schmuck, and G.L. Garrad Hassan. Thrust coefficients used for estimation of wake effects for fatigue load calculation. In *European Wind Energy Conference*, pages 1–10, 2010.

Evan Gaertner, Jennifer Rinker, Latha Sethuraman, Frederik Zahle, Benjamin Anderson, Garrett E. Barter, Nikhar J. Abbas, Fanzhong Meng, Pietro Bortolotti, Witold Skrzypinski, et al. IEA Wind TCP Task 37: Definition of the IEA 15-Megawatt Offshore Reference Wind Turbine. Technical report, National Renewable Energy Lab.(NREL), Golden, CO (United States), 2020.

Robert Gasch and Jochen Twele. *Wind power plants: fundamentals, design, construction and operation*. Springer Science & Business Media, 2011.

Johannes George. WindFloat design for different turbine sizes. Master's thesis, Universidade de Lisboa, 2014.

Google Maps. [Marine Energy Test Centre location offshore Norway], n.d. URL https://goo.gl/maps/N4wuMJHq1izTzeWJ6. Online; accessed 19 June 2020.

J. Halkyard. Large spar drilling and production platforms for deep water oil and gas. In C.M. Wang and B.T. Wang, editors, *Large floating structures*. Springer, 2015. doi: 10.1007/978-981-287-137-4.

H.A. Haslum. *Simplified methods applied to nonlinear motion of spar platforms.* PhD thesis, Norwegian University of Science and Technology, 2000.

Klaus Hasselmann, T.P. Barnett, E. Bouws, H. Carlson, D.E. Cartwright, K. Enke, J.A. Ewing, H. Gienapp, D.E. Hasselmann, P. Kruseman, et al. Measurements of wind-wave growth and swell decay during the Joint North Sea Wave Project (JONSWAP). *Ergänzungsheft 8-12*, 1973.

Andrew Henderson, Maurizio Collu, and Marco Masciola. Overview of floating offshore wind technologies. In Joao Crus and Mairead Atcheson, editors, *Floating Offshore Wind Energy: The next generation of wind energy*. Springer, 2016.

IEA. World energy outlook 2019. Technical report, International Energy Agency, Paris, 2019. URL https://www.iea.org/reports/world-energy-outlook-2019.

IRENA. Future of wind: deployment, investment, technology, grid integration and socio-economic aspects. Technical report, International Renewable Energy Agency, 2019.

Md Touhidul Islam. Design, Numerical Modelling and Analysis of a Semi-submerisible Floater Supporting the DTU 10MW Wind Turbine. Master's thesis, Norwegian University of Science and Technology, 2016.

ISO. 19902 - petroleum and natural gas industries — fixed steel offshore structures. Technical report, International Organisation for Standardization, Geneva, 2007.

Peter Jamieson and Garrad Hassan. *Innovation in wind turbine design*, volume 2. Wiley Online Library, 2011.

P. H. Jensen, T. Chaviaropoulos, and A. Natarajan. LCOE reduction for the next generation offshore wind turbines. Technical report, INNWIND, 2017.

Jason Jonkman, Sandy Butterfield, Walter Musial, and George Scott. Definition of a 5-MW reference wind turbine for offshore system development. Technical report, National Renewable Energy Lab.(NREL), Golden, CO (United States), 2009.

J. M. J. Journée and W. W. Massie. Offshore hydromechanics. Technical report, Delft University of Technology, 2008. Lecture notes, second edtion.

Yuka Kikuchi and Takeshi Ishihara. Upscaling and levelized cost of energy for offshore wind turbines supported by semi-submersible floating platforms. In *Journal of Physics: Conference Series*, volume 1356, page 012033. IOP Publishing, 2019.

A. Kolios, M. Borg, and D. Hanak. Reliability analysis of complex limit states of floating wind turbines. *Journal of Energy Challenges and Mechanics*, 2(1):6–9, 2015.

Chang-Ho Lee. WAMIT theory manual. Technical report, Massachusettes Institute of Technology, 1995.

Mareike Leimeister. Rational Upscaling and Modelling of a Semi-Submersible Floating Offshore Wind Turbine. Master's thesis, Norwegian University of Science and Technology, 2016.

Mareike Leimeister, Erin E Bachynski, Michael Muskulus, and Philipp Thomas. Rational upscaling of a semi-submersible floating platform supporting a wind turbine. *Energy Procedia*, 100(94):434–442, 2016.

Xiong Liu, Cheng Lu, Gangqiang Li, Ajit Godbole, and Yan Chen. Effects of aerodynamic damping on the tower load of offshore horizontal axis wind turbines. *Applied Energy*, 204:1101–1114, 2017.

Denis Matha, Frank Sandner, Climent Molins, Alexis Campos, and Po Wen Cheng. Efficient preliminary floating offshore wind turbine design and testing methodologies and application to a concrete spar design. *Philosophical Transactions of the Royal Society A: Mathematical, Physical and Engineering Sciences*, 373(2035):20140350, 2015.

Anthony F. Molland. *The maritime engineering reference book: a guide to ship design, construction and operation*. Elsevier, 2011.

J.R. Morison, J.W. Johnson, S.A. Schaaf, et al. The force exerted by surface waves on piles. *Journal of Petroleum Technology*, 2(05):149–154, 1950.

Anders Myhr, Catho Bjerkseter, Anders Ågotnes, and Tor A. Nygaard. Levelised cost of energy for offshore floating wind turbines in a life cycle perspective. *Renewable energy*, 66:714–728, 2014.

Einar Nygaard and Martin Mathiesen. Hywind metocean design basis, MBM-MGE-RA 32. Technical report, Statoil, 2008. Internal report.

Anja Eide Onstad, Marit Stokke, and Lars Sætran. Site assessment of the floating wind turbine hywind demo. *Energy Procedia*, 94:409–416, 2016.

Brandon Thomas Pereyra. Design of a counter weight suspension system for the tetraspar floating offshore wind turbine. Master's thesis, NTNU, 2018.

Mark A. Peterson. Galileo's discovery of scaling laws. *American Journal of Physics*, 70(6):575–580, 2002. ISSN 0002-9505. doi: 10.1119/1.1475329.

Principle Power. WindFloat Pacific OSW Project, 2014. URL https://www.boem.gov/NREL-WindFloat-Pacific-OSW-Project/. Presentation. Online; accessed 14 April 2020.

Principle Power. A photo of the WindFloat Atlantic site with all three turbines in place., 2019. URL http://www.principlepowerinc.com/en/news-press/press-archive/2019/12/30/the-second-platform-of-the-windfloat-atlantic-project-has-set-off-from-the-port-of-ferrol-towards-viana-do-castelo. Online; accessed 28 March 2020.

Principle Power. A photo of the WindFloat Atlantic site with all three turbines in place, 2020. Press release. Online; accessed 5 June 2020.

Ramboll. Floating wind JIP - turbine requirements and foundation scaling. D1: literature review and design basis. Technical report, Ramboll engineering company, 2018. Unpublished and internal document.

Dominique Roddier, Christian Cermelli, Joshua Weinstein, Eirik Byklum, Mairead Atcheson, Tomoaki Utsunomiya, Jørgen Jorde, and Eystein Borgen. State-of-the-art. In Joao Crus and Mairead Atcheson, editors, *Floating Offshore Wind Energy: The next generation of wind energy*. Springer, 2016.

G. Sieros, P. Chaviaropoulos, J. D. Sørensen, B. H. Bulder, and P. Jamieson. Upscaling wind turbines: theoretical and practical aspects and their impact on the cost of energy. *Wind energy*, 15(1):3–17, 2012.

Dan Kyle Spearman and Sam Strivens. Floating Wind Joint Industry Project - Phase 2 summary report. Technical report, The Carbon Thrust, 2020.

Henrik Stiesdal. A floating wind turbine and a method for the installation of such floating wind turbine, 2017. Patent WO2017157399A1.

Henrik Stiesdal. TetraSpar and TetraBase - Industrialized Offshore Wind Turbine Foundations, 2019. URL https://www.stiesdal.com/material/2019/02/Stiesdal-Tetra-01.02.19.pdf. Presentation. Accessed 5 February 2020.

Léon Vaalburg. Fatigue strength assessment of the pin connection in the tetraspar concept. Master's thesis, Delft University of Technology, 2019.

Eduardo Benitez Villaespesa, Cristino Manuel Gonzalez, and Nils G.K. Martin. Transportation and installation of the TetraSpar floating offshore wind turbine. Master's thesis, Aalborg University, 2018.

Jan Vugts. *Handbook of Bottom Founded Offshore Structures: Part 1. General features of offshore structures and theoretical background*. Eburon, 2013.

Jan Vugts. *Handbook of Bottom Founded Offshore Structures: Part 2. Fixed steel structures*. Eburon, 2016.

WAMIT. User manual Version 6.3. Technical report, 2006.